<u>Assessing the Safety and Effectiveness of UV-C Disinfection in Aircraft Cabins:</u>
<u>A Comprehensive Review and Risk-Benefit Analysis</u>

<u>Assessing the Safety and Effectiveness of UV-C Disinfection in Aircraft Cabins:</u>

<u>A Comprehensive Review and Risk-Benefit Analysis</u>

<u>**Executive Summary:**</u> This white paper and its appendix provide **comprehensive evidence that the use of airborne UV-C is a safe and effective method to reduce the transmission and spread of airborne diseases.** In-flight disease transmission has a much larger impact than commonly appreciated, as our analysis shows. For instance, combined <u>**airborne infection rates**</u> **for influenza and COVID-19 are responsible for over 3 million (3,000,000) infections, about 10 thousand (10,000) deaths, and economic costs of over 200 billion dollars annually.**

We found that the addition of far UV-C disinfection in aircraft cabins could have safely r**educed the infections and deaths related to in-flight transmission by 80%.** This applies not only to known airborne diseases such as tuberculosis, measles, and meningitis but also to emerging infectious diseases such as COVID-19, SARS-CoV1, and most likely the next emerging infectious disease outbreak.

Our analysis showed that the addition of far UV-C was equivalent to increasing the air exchange rate of airliners by 2 to 4 times during cruise and about 12 times on the ground. This would reduce residual airborne pathogen concentration by 89% during cruise if ventilation is 15 exchanges per hour and by 96% on the ground if ventilation is 5 exchanges per hour.

Recent research has demonstrated that disinfection with UV-C is safe. The maximum exposure limit for UV-C is much lower than people think, equivalent to **less than five minutes of summer sun exposure.** AeroClenz UV-C system, an ADDMAN Powered Pursuit, uses a combination of safe and effective UV-C levels for occupied spaces and higher levels with triple redundant sensors for intermittently occupied areas.

The findings in this document are supported by peer-reviewed datasets and accepted analytical techniques. The risk versus benefit analysis favors the continuous use of airborne UV-C below exposure limits, and AeroClenz UV-C system disinfection device will significantly reduce the impact of in-flight transmission and translocation of diseases while ensuring high levels of safety.

Authors:

Gary R. Allen, Ph.D., is a physicist with over 90 issued U.S. patents. He worked at GE Lighting and GE Current, a Daintree Company, and currently serves as an independent consultant for disinfection lighting technology and products. He obtained his Ph.D. in Astrophysical Sciences from Princeton University in 1981 and presented a TEDx talk in 2013 on "A Lighting Revolution."

Kris M. Belland, D.O., MPH, MBA, MSS, FAsHFA, FCAMA, FAOCOPM, FAsMA, is the President and CEO of Aerospace Medical Strategic Consultation, PLLC. He has extensive experience in family and aerospace medicine, strategic studies, and public health, and was recognized with numerous awards during his 30+ year career in the US Navy. He graduated from the United States Naval Academy and Philadelphia College of Osteopathic Medicine and is board-certified in Family and Aerospace Medicine and is a past President of the Aerospace Medical Association (2015-16).

Rolf Bergman, Ph.D., is an independent consultant in lighting technology and measurements. He worked at GE Lighting for over twenty-eight years, where he held the position of Chief Scientist, at Lamp Technology. He obtained his Ph.D. in Electrical Engineering from the University of Minnesota in 1972 and currently serves as an assessor of lighting laboratories for accreditation to NVLAP.

Chuck DeJohn, D.O., MPH, MS, FAsMA, FIAASM, is an accomplished aerospace medicine expert with extensive experience in the field. He served as a Navy instructor pilot, a Branch Chief at the Naval Aerospace Medical Research Laboratory, and the lead of the Medical Research Team at the FAA Civil Aerospace Medical Research Institute. He has presented to scientific audiences 97 times and published 39 articles in scientific journals. He currently works as a medical consultant, evaluating the use of direct ultraviolet irradiation to reduce disease transmission aboard aircraft.

Diego M. Garcia, MD, MSHF, Physician-scientist, a specialist in aerospace medicine with a master's in human factors, with over twelve years of working experience in human-systems integration, human performance, aerospace safety, critical care, and clinical aerospace medicine. His expertise as a subject matter expert and educator has led him to collaborate with major aerospace stakeholders and international universities. He is actively working on global health and air transport medicine.

Stephen Glaudel, MBA, has over 45 years of experience in New Product Development (NPD) Management. He held technology leadership positions in various industries and managed global programs. He graduated summa cum laude from Syracuse University with degrees in Electrical-Engineering & Biosystems and obtained an MBA in International Business from St. Joseph's University.

Bill Mills, M.D., Ph.D. (Epidemiology), MPH (Occupational & Environmental Health), MS (Physics), is a licensed physician with over 40 years of experience in primary care, aerospace medicine, and research. He retired from the FAA in 2021 and is an expert in aeromedical epidemiology/biostatistics. He has authored multiple peer-reviewed articles since 2007 and evaluated masks and blocked middle seats for mitigating the inflight transmission of COVID-19 in his last two studies.

TABLE OF CONTENTS:

**Page**

1.   INTRODUCTION

The use of ultraviolet (UV) light to decrease in-flight disease transmission has received attention as a potential measure to reduce the spread of infectious diseases, particularly during the COVID-19 pandemic. This whitepaper is prepared in support of adding UV-C LED lighting aboard aircraft in order to reduce transmission and translocation of airborne diseases. Infectious diseases claim millions of lives globally each year.[10,60,61] The World Health Organization (WHO) addresses this situation as a major global health challenge, especially for low and middle-income countries[60]. Many respiratory pathogens, including Severe Acute Respiratory Syndrome, CoronaVirus-2 (SARS-CoV-2), are transmitted via three principal mechanisms: inhaling infectious airborne droplets (from unshielded coughs or sneezes) before they fall to the floor (within 1 m to 2 m),[1,29,38,40,51] touching contaminated surfaces (fomites) before the pathogen decays, and exposure to infected persons even by simple breathing or talking that can produce aerosols that linger for minutes to hours and can travel much farther than the 1 m to 2 m traveled by droplets.[1,6,7,51] Early in the Covid-19 pandemic, it was recognized that aerosols are a significant route of infection in indoor environments[29]. Because most respiratory pathogens rely on airborne transmission, they are susceptible to UV disinfection.[1] This by no means suggests that UV-C airborne use is the only risk mitigation strategy, but that it supplements other multiple layers including HEPA filters, air flow, outside air ventilation, education, training, engineering design, public health measures and policies, to name a few.[22,34,42,48,51] In the extremely dry air of an aircraft in flight, with typically less than 20% relative humidity, all exhaled droplets smaller than 10 micrometers in diameter will quickly lose their moisture and shrink to a diameter of less than 1 um in less than a second due to evaporation and thereafter remain airborne as aerosols indefinitely. The largest exhaled droplets of up to 100 um, likewise, become aerosolized in less than 10 seconds. [38,51] Because of this uniquely dry environment in flight, the cabin presents an unusual situation where virtually all exhaled virions (particles containing viable virus) remain aloft as aerosols and do not alight onto surfaces due to gravity. Once aerosolized, the only opportunity for mitigation is to disinfect exhaled viruses and inactivate them while airborne (i.e., between passengers), either by continual ventilation or UV disinfection. Surfaces (fomites) are not a primary path for respiratory viral infections for viruses such as Corona and Influenza; therefore, surface disinfection is most likely not effective while in flight, and must be done episodically, prior to the flight.

A limited number of cases of onboard transmission have been reported for a number of respiratory diseases, including tuberculosis, influenza, SARS, measles, and meningococcal disease since the late 1970's.[15,30,36] Following the SARS outbreak of 2003, international air travel stakeholders and other umbrella organizations worked together to develop guidance for cabin crew for the management of a suspected case of communicable disease onboard a commercial aircraft. This guidance is published on the International Air Transport Association (IATA) website and is used by most international airlines.[58] Recent information published during the COVID-19 crisis from aircraft manufacturers on the dynamics of pathogen distribution onboard airliners offered a new perspective on the matter and called for a review of the guidance.[15,21,22,36,42,56]

Aviation Safety Management System (ASMS) is a systematic approach to managing safety in the aviation industry. It focuses on identifying and managing potential safety risks and continuously improving safety performance. SMS encompasses a range of processes, including hazard identification, risk assessment, and continuous monitoring and review. One excellent example of an integrated SMS includes a multilayered risk management process, aligned with the intent of WHO's "Considerations for implementing a risk-based approach to international travel in the context of COVID-19," is considered essential in the context of a public health risk management framework. The objective of the WHO process is to identify the residual risk for unknowingly transporting an infectious passenger or translocating the SARS-CoV-2 virus, considering various risk mitigation

measures in place. This approach is scalable in complexity and considered the baseline for more sophisticated processes (e.g., end-to-end risk assessment models).[17]

Risk mitigation is the most appropriate strategy in the context of pandemic risk management in air transport. In multilayered defense models, the various mitigation measures are depicted as layers (e.g., based on the James Reason Swiss Cheese Model — see **Fig. 1**). Risk-free travel is not possible, but the risk can be reduced through the combined application of these mitigation measures. Currently, scientific peer-reviewed evidence-based efficacy measures for these mitigation strategies are limited; therefore, in some cases the scope of their impact on transforming the inherent risk must be based on expert consensus and available evidence. As a result, much of the risk assessment is qualitative and provides the flexibility to be adopted and integrated into national public health and aviation plans. The risk assessment process will consider the chosen mitigation measures, and regularly re-evaluate how they affect the likelihood and impact of the inherent risk. A State can then determine if the residual risk is within their public health management capacity.[17]
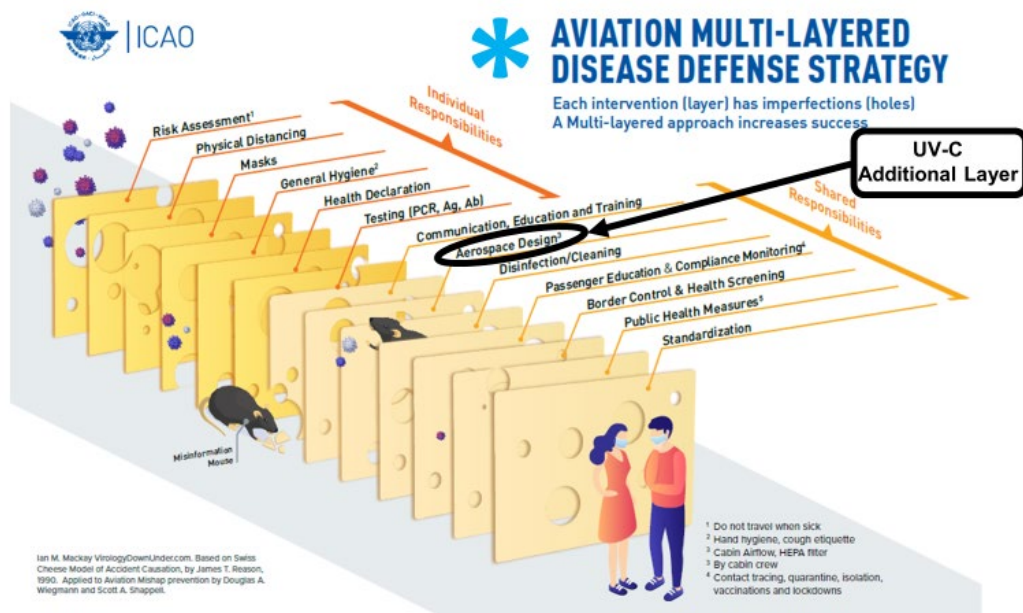

Fig. 1 ICAO Aviation Multi-Layered Disease Defense Strategy (with UV-C sanitization layer added).

Current evidence suggests that utilization of UV-C light in flight can be an additional effective, synergistic risk mitigation strategy that will ultimately reduce transmission of infectious diseases, including existing and emerging airborne infections (viral, bacterial, fungal).[1,8,9,27,31–33]

The appendix of this paper showed that for the period from February 2020 to September 2021, which is around the middle of the US epidemic, there was an estimated 2,645,836 passengers on US air carriers infected with COVID-19, who then transmitted the virus to an additional 2,645,836 people in the general population. This suggests that inflight transmission was responsible for 3.6% of all COVID-19 infections in the US during this 20-month period. Additionally, an estimated 21,800 deaths resulted from inflight transmission, which accounted for 2.4% of all COVID-19 deaths over this period. The societal cost of inflight transmission of seasonal influenza was shown to be about $2.8 billion. These numbers are large even though there was a reduction in the number of flying passengers during this time and masks were mandated.

2.   BACKGROUND.

The Electromagnetic radiation spectrum is shown in **Fig. 2** below. Ultraviolet germicidal irradiation (UVGI) is an established means of disinfection and has been used to prevent the spread of several infectious diseases. UVGI from mercury lamps in the UV-C range (200 – 280 nm) has been used to disinfect air, water, and surfaces, primarily at 254 nm by the disruption of base pair bonds in DNA and RNA so that the strand becomes unavailable for replication **(Fig. 3)**. [12,23,26,31–33]
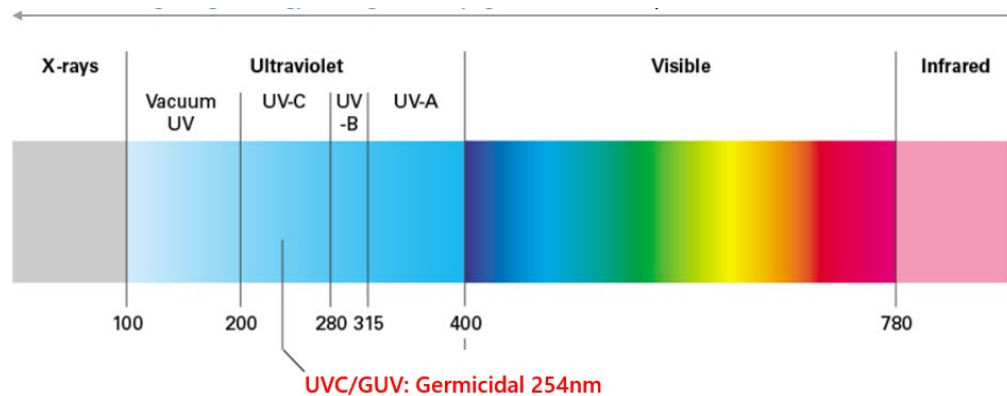
Fig. 2. The Radiation Spectrum.

Earlier methods using ultraviolet (UV) irradiation for decontamination had to rely on high-power (10s of watts) low pressure Mercury lamps which, due to their high output couldn't be used to directly irradiate the air or surfaces in an occupied space without greatly exceeding the published exposure limits (EL) for UV irradiation. Therefore, mercury lamps could only be used in unoccupied spaces, shielded from humans (e.g., at least 7 feet above the floor, or inside the heating ventilation and air conditioning (HVAC) ducts); however, none of these are ideal methods.

In the last decade or so Excimer lamp technology has provided two excimer combinations, krypton with bromine (KrBr*) that emits strongly at 207 nm and krypton with chlorine (KrCl*) that emits at 222 nm. The latter, KrCl* excimer emission at 222 nm, has proven a promising path towards safe and effective disinfection of pathogens with direct exposure of skin and eyes. The reason this region, called Far UV, is of such interest is that the American Conference of Governmental Industrial Hygienists (ACGIH) TLV, or exposure limits (EL) are much higher than at 250 to 280 nm range. The irradiance at 222 nm can be raised at least one, possibly two, orders of magnitude higher than for irradiance between 250 and 280 nm. This increase in irradiance allows much faster disinfection of pathogens, without harming skin or eyes. Much research on the effectiveness of Excimer lamps in disinfection of various pathogens is ongoing, as is research in the short- and long-term safety to skin and eyes from exposure to 222-nm irradiation.

More recently, the emergence of low-power UV-C light emitting diodes (LED)s for inactivation of pathogens, especially airborne pathogens, using UV radiation emitted directly into occupied spaces and exposing occupants to a dose below the accepted actinic ELs have been successfully developed. This method is referred to as direct irradiation below exposure limits, or DIBEL.[1] It has been demonstrated that UV-DIBEL can be an effective component of efforts to combat airborne pathogens such as SARS-CoV-2, Influenza A, the common cold, healthcare-acquired bacterial infections, and others. [1] DIBEL technology can achieve significant levels of pathogen inactivation by providing direct, continuous radiation into the occupied breathing zone while adhering to actinic dose EL. [1] Over the last several decades, photobiological studies have evaluated the sensitivies of a wide array of bacterial, fungal, and viral organisms to UV, particularly UV-C.[1,23,31–33,45]

Unpublished data (Dr. Gary Allen) has shown inactivation rates of aerosolized SARS-CoV-2 and other pathogens have been experimentally measured using 275 nm LEDs emitting UV light below the EL, in a controlled room-sized aerosol chamber, confirming the expected D_{90} dose and the expected inactivation times for aircraft application.

According to the ICAO Aviation Multi-Layered Disease Defense Strategy, multiple, independent methods should ideally be used to disinfect both surfaces and air in the aircraft cabin. UV-C DIBEL is primarily an air disinfection technology with lesser impact on surface pathogens. Regarding surface disinfection, the primary methods are manual wiping with chemical disinfectants and a one-time sweep of the cabin while unoccupied using an intense UV-C source such as a "robot". Both techniques are effective only on surfaces where the manual wiping is done, or where the line-of-sight path from the UV source of the robot can "see" the surface. Both techniques are done when the cabin is unoccupied, and not repeated after the passengers board the cabin. Both techniques likely leave a significant fraction of surfaces that could be touched by passengers uncleaned, (e.g., under armrests or seats, or crevices around buttons or controls) and the application of UV-C LED DIBEL using current UV-C LED technology will likely not remedy those missed sections. If there is no line of sight from the missed sections to the UV source of the robot, then there may also not be line of sight to the UV-C LED in the DIBEL system, either.

However, as soon as the cabin is occupied, any surfaces that had been cleaned manually or by robot while unoccupied can immediately be recontaminated by a contaminated passenger or article introduced into the cabin. Fortunately, transmission of most airborne pathogens (and especially SARS-CoV-2) via contaminated surfaces (called fomites) is not the primary path of transmission between people. Instead, the dominant transmission paths are via (large) airborne droplets, and more typically by (small) aerosolized pathogens. And this transmission would not be due to aerosols left behind by the robot, but rather by aerosols exhaled by infected passengers, starting as soon as boarding commences.

Even after boarding, and the option for broad cabin disinfection with intense "above-EL" UVC doses using robots' becomes unavailable, it is possible for "above-EL" sources to be safely employed, so long as they can automatically and redundantly sense the absence of personnel in generally unoccupied areas of the aircraft such as in the lavatories), thus safely disinfecting those areas in-between passenger visits.

This important, most-likely path of infection transmission for many respiratory pathogens, which is currently missing in the ICAO Aviation Multi-Layered Disease Defense Strategy, is provided by the extra layer of UV-C DIBEL protection.

3.   UV-C ENVIRONMENTAL DISINFECTION

Pathogens may be physically removed from air in an occupied environment by ventilation or filtration of the air. The air is first moved to an unoccupied space, where the pathogens are inactivated and / or mixed with outside air, and then the decontaminated air is returned to the occupied zone.[1] However, since most airborne infectious diseases are either bacteria (or bacterial spores), viruses, or fungi, these pathogens may be inactivated and rendered unable to infect a host by UV radiation in the unoccupied space.[1,23,31,32,53]

High-efficiency particulate absorbing (HEPA) filters are capable of filtering viruses of submicron sizes, including SARS-CoV-2;[47] However, there are shortcomings of this technology. First, there are many cases that lack HEPA filtration (e.g., most smaller private aircraft and most business jets). It should be noted that not all aircraft are equipped with HEPA filtration. For instance, certain private jets and regional airliners, such as the Embraer 145 fleet operated by United and American Airlines, lack HEPA filters, as do all CRJ200 aircraft flown on behalf of United and Delta. Additionally, most regional turboprop aircraft, such as the Dash 8-1/2/3 Series, Embraer 120, and Fokker 50, provide minimal to no filtration of cabin air, as well as the ATR-42/72. Even Gulfstream private jets (all models) do not contain HEPA filters. Second, in order for HEPA filters to function properly, cabin air must flow through the filters, potentially moving air past infectious passengers to susceptible passengers. Unfortunately, airflow patterns created by aircraft ventilation systems can result in uncirculated pockets of air, creating dead zones within the cabin, reducing the effectiveness of the HEPA system, and potentially allowing airborne transmission of disease. Whereas ultraviolet radiation applied in DIBEL mode, while occupied, provides direct inactivation of pathogens in the air between the passengers.[23,26,42,47,56] Most airborne infectious diseases are easily inactivated by UV radiation rendering them unable to infect a host.[1,45]

The UV-C subset of UV radiation between 200 and 280 nm has been employed extensively in germicidal applications.[9,31,32] Extensive scientific literature exists confirming the applicability, efficacy and safety of UV-C environmental irradiation.[24–26,28,31–33,35,37,53] Over the UV-C range, the detrimental effect on pathogens occurs because their intracellular components (RNA, DNA, and proteins) can absorb UV-C photons.[5,23,32,33] Absorbed UV-C photons cause critical damage to the genomic system of microorganisms, preventing them from replicating.[31] Ultraviolet light in the traditional UV-C range has photon energies that are nearly resonant with the absorption bands of deoxyribonucleic acid (DNA) and ribonucleic acid (RNA), enabling very effective inactivation of many types of viruses, bacteria and bacterial spores, as well as fungi and protists.[1,23,26,28,39]

Although viruses have no active metabolic processes that can be interrupted, Ultraviolet-C (UV-C) primarily inactivates pathogens through creation of dimers in adjacent pyrimidine bases of their nucleic acids, interrupting transcription or translation, thus rendering the pathogens inactivated.[1,23,32] Therefore, the effect of UV irradiation on such pathogens is called "inactivation" and not "killing".[32] This process is depicted in **Fig. 3**.

UVC: direct DNA/RNA damage

Before: Incoming UV photon **After:** Forms Pyrimidine Dimers (T/U/C)
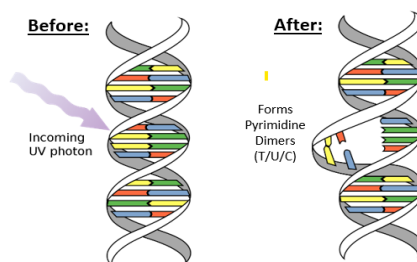
Fig. 3. Inactivation of a virus by UVC light.

UV-C light is significantly attenuated by the human stratum corneum (the outer dead-cell skin layer), the ocular tear layer, and the cytoplasm of individual human cells (**Fig. 4**). Thus, very little UV-C light reaches the living cells in the human skin or the human eye, causing negligible damage compared with the longer wavelengths of UV-A and especially UV-B, which do effectively penetrate these sensitive cells.[9]

Far-UV light (207 to 222 nm), produced by Excimers, has been shown to be as efficacious as conventional germicidal UV light (low pressure mercury emission is primarily at 254 nm) in inactivating microorganisms,[8,9,31,32] with the advantage that shorter wavelengths have shallower penetration into the skin and ocular tear layer compared to the conventional, longer-wavelength germicidal UV light.[9,23,35,37,43]

Some research groups (e.g., Columbia University), manufacturers (e.g., Ushio, Far UV, and Eden Park) and lighting system providers (e.g., Acuity) have endorsed the use of far-UV-C light (222 nm) in occupied public locations, using excimer lamps, as a safe and efficient anti-microbial technology.[9] The approach is based on the biophysical principle that far-UV-C light has a limited ability to penetrate biological materials and can effectively inactivate viruses. However, it cannot penetrate the outer dead-cell layers of human skin or the outer tear layer on the surface of the human eye.[9,43,44]) However, if shorter wavelengths like 222 nm are utilized, the potential dangers of emitted Ozone should be considered. Other limitations of far-UV excimer sources for aircraft applications include the possibility that the system could be too large (the 'bulb' plus its electronic 'ballast', and/or to accommodate optics that may be needed to control the direction of the UV light), the greater expense than UV-C LEDs (ref: Haitz's Law), and the shorter operating lifetime[1], point to the parity of 222 nm excimer sources relative to 265 nm LED sources at the present time for aircraft cabin applications.

Because of the shallower penetration depth of shorter wavelengths of UV-C, the actinic hazard function allows for a higher EL at the shorter wavelengths; for example, 229 J/m^2 at 222 nm vs. 60 J/m^2 at 254 nm, and 37 J/m^2 at 265 nm (a 6.2-fold advantage for 222 nm vs. 265 nm). It is often misstated that this means that far-UV (shorter wavelength) is "safer" than conventional UV-C; however, this is not the case.

Far-UV (shorter wavelength, e.g., 222 nm) is allowed a higher EL (again, Energy = Irradiance-Power x Time) than conventional (longer wavelength, e.g., 254 nm) UV-C, but it is not 'Safer'. If the dose incident onto a person's skin or eyes is below the EL of 37 J/m^2 at 265 nm, that is comparably safe as a dose below the EL of 229 J/m^2 at 222 nm. A 222 nm system will typically be designed to operate with a safe margin below the EL of 229 J/m^2, and a 265 nm system will typically be designed to operate with a safe margin below the EL of 37 J/m^2, so that they are comparably safe.[2] However, as wavelengths become even longer (into UV-B range, above 280 nm), skin-depth penetration rises dramatically. This can be visualized in the graphic below **(Fig. 4, Fig. 5).**
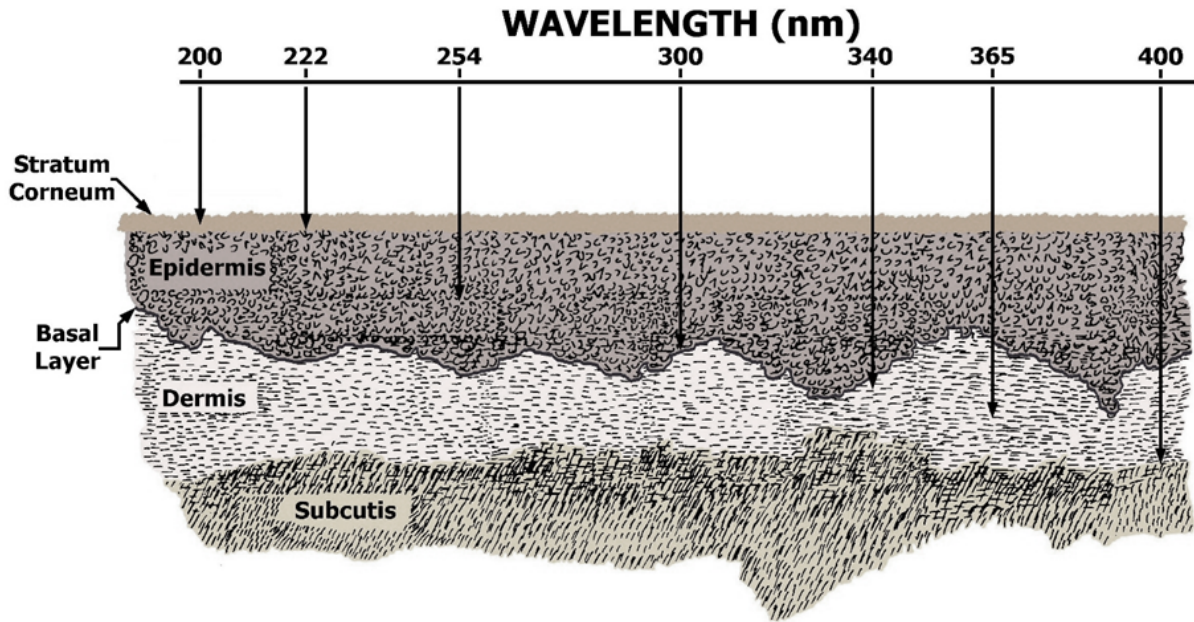
Fig. 4. Penetration of Human Skin by Ultraviolet Energy (David Sliney, PhD 2023)

The information in **Fig. 5** validates that the absorption of UV-C by the skin increases rapidly below 240 nm. Thus, the penetration of the UV irradiance into the basal layer is significantly decreased at 222 nm compared to 265 nm. For simplicity, consider the irradiance levels incident at the mid epidermis for the two wavelengths 222 nm and 265 nm, which are about 10^{-4} mW/m^2 and about 5×10^{-4} mW/m^2 respectively. This indicates that for a given incident irradiance at the surface of the skin, only about ⅕ as much of the incident irradiance at 222 nm vs. 265 nm penetrates the lower layers of the skin.
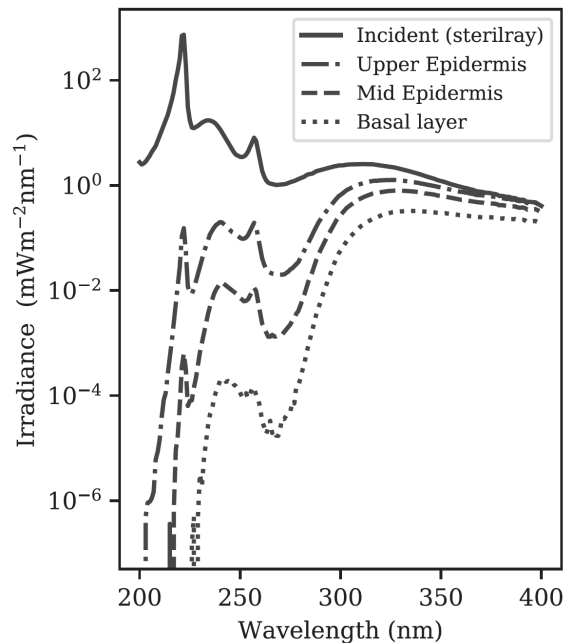

Fig. 5. Irradiance of the far-UVC and MCRT simulated fluence incident on the upper and mid-epidermis and basal layer. [54]

The question then is how efficacious the 222 nm system is operating somewhat below 229 J/m^2 vs. the 265 nm system operating somewhat below 37 J/m^2. At first blush, the answer is that the 222 nm system can be 6.2 times more efficacious, but that is not true. The excimer light source operating at 222 nm is too large (about 30 mm) to accommodate optics to spatially confine the irradiation, while a UV-C LED (about 1 mm) can provide a narrow beam using a lens having only about 10 mm diameter. By contrast, LEDs are small solid-state compound-semiconductor devices, which can be fitted with lenses to direct light as needed, such as in unoccupied spaces.   The optical advantage of a small LED (1 x 1 mm) vs. a much larger excimer lamp (45 x 60 mm) is visualized in **Fig.6** (roughly to scale).
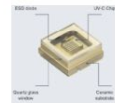
Fig. 6. Scale comparison: Excimer lamp 45 x 60 mm (left) vs. LED package 3.5 x 3.5 mm with 1 x 1 mm light emitting die in the center (right)

A typical application of DIBEL technology in an occupied aircraft cabin is depicted in **Fig. 7** showing the UV-C intensity distribution emitted from a single UV-C Puck mounted in the ceiling above the aisle, midway between opposing rows of seats. Fig. 7 indicates both a narrow "UV-C Spot Cone" and a broad "UV-C Flood Cone". Typically, in this application a linear array of UV-C Pucks is mounted along the center of the ceiling of the aisle, with UV-C Pucks spaced a few feet apart, sufficiently close together that the overlap of the UV-C Flood

Cones provides nearly uniform irradiance throughout the occupied space, not to exceed the maximum allowed EL.[1]

Even though the UV-C Flood Cones provide a dose well below the EL to a seated passenger, if a passenger stands up or raises a hand into close proximity to the LED source, the EL may be exceeded. In fact, the UV-C irradiance (dose) increases with the inverse square of the distance between the UV source and the subject (i.e., "Inverse Square Law), such that a dose that's safe at a distance of 2 feet from the LED will be 4x higher at a distance of only 1 foot from the LED. A pair of redundant Passive Infrared (PIR) detectors determine if a passenger's head or hand enters the zone where the irradiance exceeds the EL, and then turns off the LEDs in that UV-C Puck until the PIR sensors detect the absence of personnel within the EL range.

In contrast, the UV-C Spot Cones have a beam width narrow enough to be limited to the aisle, with negligible (<< EL) UV-C incident onto a passenger seated in a seat adjacent to the aisle. The UV-C dose within the Spot Cone exceeds the EL so that the contaminated air within the aisle may be disinfected at a much higher rate than that provided by the lower-irradiance Flood Cones. To ensure safety, the Spot Cone is monitored by both a pair of redundant Ultrasound sensors and a pair of redundant LIDAR sensors for each UV-C Puck. The sensing range of the sensors is such that if any passenger is standing, kneeling or even lying down in the aisle, the LEDs of that UV-C will be turned off until the zone is again unoccupied. Further, if a passenger's arm is extended more than a few inches beyond the armrest, the sensors are likewise activated to turn off that UV-C Puck.
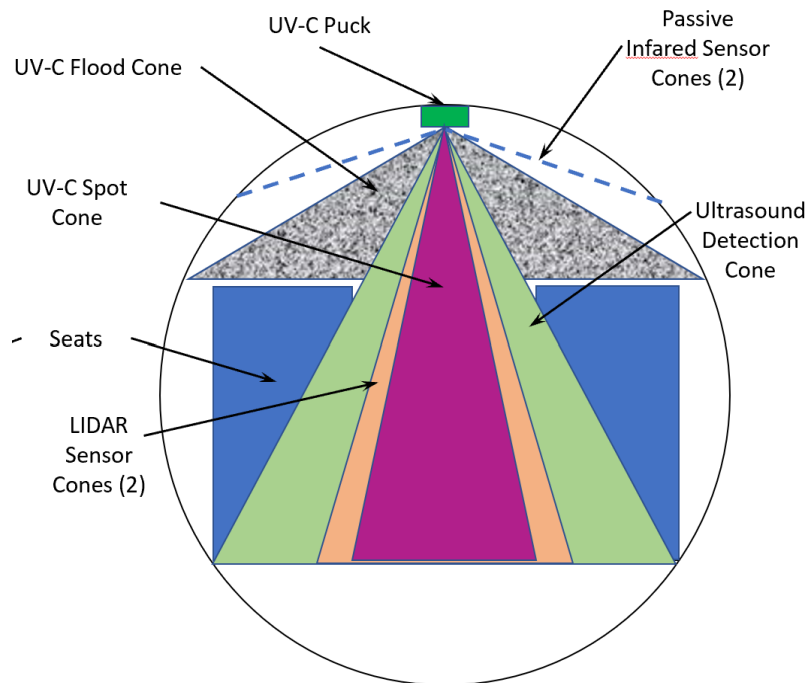
Fig. 7. Typical application of DIBEL technology (used in an array fashion) in an occupied space. The array in this application could be a linear array along the center of the ceiling of the aisle, with UV-C Pucks spaced a few feet apart, for example.

The installation is configured such that within the occupied zone, (the top of which is depicted by the dashed line in **Fig. 7**), the irradiation is within the allowable EL.[1]

4. EFFECTIVENESS

The efficacy of UV irradiation for air disinfection may be quantitatively compared with traditional air disinfection technologies, by a method related to air changes per hour (ACH). A straightforward example of a traditional air cleaning technology used in aircraft is the introduction of outside air, and the filtering of recirculated air by the cabin ventilation system. A common metric used to compare air disinfection technologies is the air-exchange rate (AER) measured in ACH, defined as:

$$ACH = Q/V$$

where Q is the air flow rate (m^3/h), and V is the volume (m^3).[1] The American Society of Heating, Refrigerating and Air Conditioning Engineers (ASHRAE) recommends air exchange rates between approximately 6/h to 8/h for residences, 10/h to 12/h for offices, and 14/h to 18/h for restaurants and public buildings.[20] A typical AER in wide-body aircraft is variously quoted between about 5 ACH on the ground, up to 35 ACH when cruising.[50] When ventilation is used to replace existing, potentially contaminated air, with fresh air the air is not flushed through like a piston, but rather flows and diffuses from the air inlet to the air outlet through the volume of the cabin. When a volume of air equal to the volume of the cabin is introduced, only 63% of the original air exits the cabin, along with 37% of the newly introduced fresh air. With 63% of the existing air replaced by fresh air during each air change, it takes 2.3 air changes to replace 90% of the original air with fresh air. For example, if the AER in the cabin is 15 ACH, then 90% of the cabin air is replaced by fresh air in about 9 minutes. If a susceptible person inhales enough airborne pathogens to become infected in less than about 9 minutes, typical for infection by SARS-CoV-2, then an ACH of 15 is only marginally good enough to mitigate the risk of infection.[14,19,56]

Air disinfection by UV irradiance can be quantitatively compared to air disinfection by ventilation by introducing an equivalent ACH (ACH_{eq}) for UV disinfection that is derived quantitatively in recent scientific efforts[1]

$$ACH_{eq} = 2.30 \; x \; E \, / D_{90}$$

where E is the UV irradiance (J/m^2) averaged throughout the volume of the cabin, and D_{90} (J/m^2s) is the UV dose required to achieve 90% inactivation of a pathogen in or on a solid, liquid or gas medium. For example, D_{90} for SARS-CoV-2 in air is about 6 J/m,[21] the irradiance, E, when operated at the allowable EL for 265 nm is 36 J/m^2, so that the theoretical ACH_{eq} is about 14/h. In practice, an engineering margin of at least 20% below the EL should be used, and the irradiance cannot be perfectly uniform throughout the irradiated volume (assume average is 50% of maximum), so that ACH_{eq} is reduced by a factor of about 0.5 x 0.8 = 0.4, so that the theoretical ACH_{eq} = 14 may be about 5/h in practice. Using sensors, controls, and optics, ACH_{eq} may be enhanced by a factor of about 10 to 50. A practical system using 275 nm LEDs has been demonstrated with ACH_{eq} ~ 40/h.

D_{90} values for UV disinfection in air at 254 nm for various viruses, bacteria, and spores, are shown in **Table 1.** [1,26]

Table 1. D_{90} values for UV-C disinfection in air at 254 nm for various microbes.

Pathogen	Type	D_{90} in Air (J/m^2)	D_{90} Category
SARS-CoV-2	Virus	5[a]	Low
Mycobacterium tuberculosis	Bacteria	5	Low
Staphylococcus aureus (*e.g.*, Methicillin-resistant **Staphylococcus** aureus, MRSA)	Bacteria	5	Low
Coronavirus (some common colds)	Virus	6[b]	Low
Pathogens responsible for pneumonia: *S. aureus* (5), **Klebsiella** *pneumoniae* (7), **Pseudomonas** *aeruginosa* (4), **Streptococcus** *pneumoniae* (~5)	Bacteria	6[c]	Low
Escherichia coli	Bacteria	8	Low
Influenza A	Virus	19	Medium
Adenovirus	Virus	44	High
Candida auris	Fungus	~50[d]	High
Clostridioides difficile	Bacterial spore	~50[d]	High

D_{90} for Influenza A, common colds, pneumonia, TB, measles, etc., are typically about 2-5 times higher than for SARS-CoV-2 in air (i.e., about 10 to 25 J/m^2), so that these other airborne pathogens will be inactivated at lower ACH_{eq} rates up to about 50/h, following the above examples.

Another commonly used designation for dose is D_{99}, which is simply twice the D_{90} dose. That's because the first D_{90} dose inactivates 90% of the pathogens and then another D_{90} dose inactivates 90% of the remaining 10% of pathogens, leaving only 1% of the original pathogens.[19] Similarly a $D_{99.9}$ dose will be three times that of the D_{90} dose. The linearity of this relationship typically holds through 99% to 99.9% inactivation, then begins to saturate at higher doses.[19] This is an enabling feature of providing continuous disinfection whereby the contamination level continuously declines unless additional contamination is added after some initial contamination.

Equivalent Air Exchange Rate (ACH_{eq}) is proportional to the UV irradiance (flux density) and inversely proportional to D_{90}, as shown in the equation above.[1] Therefore, to provide the highest possible ACH_{eq}, a UV disinfection system (e.g., DIBEL and/or Spot) should maximize the UV flux throughout the occupied space without exceeding the EL. For a UV disinfection system that is limited to DIBEL only (without Spot beams that locally exceed the EL), **Table 2** shows ACH_{eq} values for D_{90} for 8 hours of continuous DIBEL for low, medium, and high categories of pathogens in air at 254 nm.[1] The ACH_{eq} values for 275 nm irradiation would be lower by 2-fold, and for 222 nm would be higher by a factor of 3.8.

Table 2. ACH_{eq} values for D_{90} for 8 h of continuous DIBEL.

D_{90} Category in Air (J/m^2)	Example Pathogens	ACH_{eq} (h^{-1})			
		2020 (275 nm)	2021 (275 nm + optics)	2025 (255 nm + optics)	Potential (225 nm + optics)
Low ~ 5	SARS-CoV-2, tuberculosis, pneumonia-causing bacteria, MRSA	1.1	4	8	150
Medium ~ 20	Influenza A	0.3	1.2	2.2	40
High ~ 50	Adenovirus, *C. auris, C. difficile*	0.1	0.4	0.8	15

The DIBEL efficacy estimates in **Table 2** apply only to the flood beam in a flood plus spot system. The present-day values of ACH_{eq} are not hypothetical. They have been confirmed by actual measurements of ACH_{eq}, using a flood beam only, in a room sized aerosol chamber provided with aerosolized SARS-COV-2 virus using the UV-C LED DIBEL technology as presented in this paper. The addition of a spot beam leverages the ability to exceed the EL at locations in the cabin that are not occupied for long periods of time, such as the aisles, galley, or lavatory by sensing occupancy in the region of the spot beam and turning off the spot beam while that zone is occupied. The ACH_{eq} in an aircraft cabin is typically enhanced by up to 10 times by the addition of occupancy-controlled spot beams, such that a typical combined efficacy is 30 to 60 ACH_{eq}, or higher, depending on the spatial control of the spot beam and the amount of UV-C emission available from the today's LEDs, which are rapidly improving year by year.

It is anticipated (although not yet verified) that a Flood-only (DIBEL) system will provide ACH_{eq} in aircraft applications exceeding 100 ACH_{eq} within a few years (see "Potential" column in **Table 2**), which may be further enhanced by adding spot disinfection. This is to be compared with the current typical range of ACH in aircraft of about 5 to 20/h.

Because of the method used to mathematically derive ACH_{eq} for UV disinfection, the ACH values for ventilation and the ACH_{eq} values for UV disinfection are additive. For example, if the aircraft provides 15 ACH of ventilation and the UV disinfection provides 30 ACH_{eq}, then the total ACH in the cabin is 45/h. That means that, whereas the ventilation alone would disinfect 90% of the cabin air in about 9 minutes, the combination of ventilation and UV disinfection would disinfect 90% of the cabin air in about three minutes, or three times faster. [10, 46]

Although dose is not exactly linearly proportional to the risk of infection, the risk of infection will also be significantly reduced, comparable to the three-fold factor. This scale of ACH_{eq} has been demonstrated in prototypes with today's LEDs and optics. With the rapid advent of improved UV-C LEDs and UV-C optics, this three-fold factor is expected to become approximately 30-fold or more within a few years. The three-fold improvement will reduce the time to 90% inactivation from three minutes down to about six seconds. Notably, from **Table 2**, this six second disinfection time applies to SARS-CoV-2, TB, pneumonia and MRSA, while the 90% disinfection time for Influenza A would be about 22 seconds. The eventual capability of UV-C disinfection inside the cabin (90% disinfection of many airborne viruses in six seconds) will be faster than the transit time for aerosols from an infected person's mouth to a susceptible person's mouth a few meters away.

5.   SAFETY

Every wavelength of light, from the UV through the IR, can potentially pose a health risk to humans if the dose exceeds the allowed EL. The EL for actinic hazard as provided in International Electrotechnical Commission (IEC) Standard 62471:2006 is 30 J/m^2 in any eight-hour period.[1,18] This regulation is based on the maximum sensitivity of the human eye, which was found to be at approximately 270 nm, and pertains to the fairest skin and eye phenotypes, but does not apply to individuals with rare drug-induced or genetic hypersensitivity to UV.[9,16,18,35,37]

The known side effects of overexposure to UV-C radiation include transient corneal and conjunctival photo-keratoconjunctivitis and erythema of the skin.[1] Although the National Toxicology Program (NTP) has stated that UV-C radiation is reasonably anticipated to be a human carcinogen, and the International Agency for Research on Cancer (IARC) has reported that UV radiation (including UVA, UVB, and UVC) is carcinogenic to humans.[57]

"Most skin cancers are a result of exposure to the UV rays in sunlight. Both basal cell and squamous cell cancers (the most common types of skin cancer) tend to be found on sun-exposed parts of the body, and their occurrence is typically related to lifetime sun exposure. The risk of melanoma, a more serious but less common type of skin cancer, is also related to sun exposure, although perhaps not as strongly."

Fortunately, radiant energy in the UV-C band has very shallow penetration depths which account for the superficial nature of any injury from excessive exposure. These effects are transient, lasting 24 to 48 hours[1] because only the corneal epithelium and the superficial epidermis are significantly affected and normal cell turnover soon causes the signs and symptoms to resolve.[1,33,43,44,52,54]
Recent studies show no evidence of induced skin cancer or other skin abnormalities after long-term (66 weeks) chronic exposure to 222-nm far-UVC radiation, which underscore that there is little to no anticipated risk associated with inflight germicidal use of far-UV-C. In short, the use of UV-C as a disinfecting tool outweighs safety issues with the standardization of dose.[9,18,35,39,43,44,52,54]

UV is no more hazardous than visible or IR light when the dose is maintained below the appropriate EL. Conversely, when received at a dose exceeding the EL for visible light, visible light is more hazardous than UV light when the UV light is maintained below its respective EL.[1,15] DIBEL protocols can ensure that the dose (irradiance × exposure time) received by individuals in the irradiated space remains below the EL. The limits defined by these protocols represent the conditions to which individuals can be repeatedly exposed for eight hours per day over a working lifetime without the risk of photobiological effects such as skin or eye damage. For perspective, a DIBEL system operating for 8 hours below the allowed EL for UV-C poses less risk than five minutes of sunshine per day.[1] In addition to the superficial short-term risks, the long-term risk from an accumulated daily exposure to 254 nm radiation at the EL received over eight hours for five days a week for 20 years, would increase the risk of non-melanoma skin cancer by a factor of about 0.37 %.[1]

Furthermore, per the well-established photobiological effect of time-weighted averaging (TWA), receiving an irradiance exceeding the EL for a brief, or even extended, time does not create a hazard to the skin or eyes, unless the dose (irradiance x time) exceeds the eight-hour allowed dose per the EL. In other words, a person may receive 10 times the allowed irradiance for a half hour and will have accrued only five eights of the TWA dose that is allowed for eight hours. In addition, the TWA is a time-moving eight-hour average, such that the allowed dose is effectively renewed every eight hours due to the relatively short recovery time of the human skin and eyes to UV-C dose.[46,59]

With the increasing application of UV-C lamps for disinfection, questions regarding the generation of ozone in air have been raised, making Ozone concentration an important design consideration when using UV-C emitting lamps.[12] The Occupational Safety and Health Administration (OSHA) limit for eight-hour exposure to ozone is 0.1 ppm and the Food and Drug Administration (FDA) limit for long-term exposure is 0.05 ppm. The minimum level for a typical person is 0.01 to 0.04 ppm. Fortunately, current DIBEL protocols result in ozone production which is 10^{-3} lower than the FDA long-term limit with a 1 mW UV LED at 254 nm.[49]

6.   CONCLUSIONS

UV devices for disinfection of frequently touched surfaces and circulating air streams are in use in public high traffic spaces settings worldwide including vehicles, hospitals, airports, and shopping malls.[28–30] Although UV irradiation has been used for disinfection for many years, in the past it has mostly been limited to applications where humans are absent or shielded from the UV source. DIBEL

is a method of applying germicidal UV radiation in a way that occupied spaces may be directly disinfected, by limiting UV to doses that are below industry accepted ELs for repeated exposure of humans while simultaneously maintaining doses above those required for acceptable reductions of pathogenic organisms in the space.[1]

The benefits of a DIBEL technology that differentiate it from conventional disinfection technologies include:

   • continuous, direct disinfection while occupied, and
   • no required air movement, so that disinfection occurs in the space between an infected person and susceptible people, providing an effective shield between infectious and susceptible individuals that is proportional to the ACH_{eq} provided by the DIBEL system.[1]

In the event of accidental overexposure, the risks are also well established and demonstrated to be minor relative to the benefits of disease prevention.[1,43,52,54] High-traffic areas with increased risks of aerosolization and dissemination due to aircraft airflow dynamics (such as lavatories) should at a minimum be equipped with UV-C sanitization.[13,22,55]

In summary far-UV-C light is anticipated to have about the same anti-microbial properties as conventional germicidal UV light, but without producing the corresponding health effects. Therefore, far-UV-C light has the potential to be used in occupied public settings to effectively prevent the airborne person-to-person transmission and translocation of pathogens such as coronaviruses.[9,35,37]

Current evidence suggests that utilization of UV-C light in flight can be an additional effective, synergistic risk mitigation strategy that will ultimately reduce transmission of infectious diseases, including existing and emerging airborne infections (viruses, bacteria, fungal).[1,3,4,8,9,14,25,28,31–33,35,40,41]

7.   REFERENCES

1. Allen G, Benner K, Bahnfleth W. Inactivation of Pathogens in Air Using Ultraviolet Direct Irradiation Below Exposure Limits. J Res Natl Inst Stand Technol. 2022; 126
2. Barnard IRM, Eadie E, Wood K. Further evidence that far-UVC for disinfection is unlikely to cause erythema or pre-mutagenic DNA lesions in skin. Photodermatol Photoimmunol Photomed. 2020; 36(6):476–7
3. Bhardwaj SK, Singh H, Deep A, Khatri M, Bhaumik J, Kim K-H, et al. UVC-based photoinactivation as an efficient tool to control the transmission of coronaviruses. Sci Total Environ. 2021; 792:148548
4. Blatchley ER, Brenner DJ, Claus H, Cowan TE, Linden KG, Liu Y, et al. Far UV-C radiation: An emerging tool for pandemic control. Crit Rev Environ Sci Technol. 2023; 53(6):733–53
5. Bolton JR, Cotton CA. The Ultraviolet Disinfection Handbook. American Water Works Association; 2011.
6. Bourouiba L. Turbulent Gas Clouds and Respiratory Pathogen Emissions: Potential Implications for Reducing Transmission of COVID-19. JAMA. 2020; 323(18):1837–8
7. Bourouiba L, Dehandschoewercker E, Bush JWM. Violent expiratory events: on coughing and sneezing. J Fluid Mech. 2014; 745:537–63
8. Buonanno M, Randers-Pehrson G, Bigelow AW, Trivedi S, Lowy FD, Spotnitz HM, et al. 207-nm UV Light - A Promising Tool for Safe Low-Cost Reduction of Surgical Site Infections. I: In Vitro Studies. PLOS ONE. 2013; 8(10):e76968
9. Buonanno M, Welch D, Shuryak I, Brenner DJ. Far-UVC light (222 nm) efficiently and safely inactivates airborne human coronaviruses. Sci Rep. 2020; 10(1):10285
10. Centers for Disease Control and Prevention. Estimated COVID-19 Burden. 2022 Retrieved 17

April 2023 from https://www.cdc.gov/coronavirus/2019-ncov/cases-updates/burden.html

11. Centers for Disease Control and Prevention. Estimated Flu-Related Illnesses, Medical visits, Hospitalizations, and Deaths in the United States — 2019–2020 Flu Season. 2023 Retrieved 17 April 2023 from https://www.cdc.gov/flu/about/burden/2019-2020.html

12. Claus H. Ozone Generation by Ultraviolet Lamps†. Photochem Photobiol. 2021; 97(3):471–6

13. Crimaldi JP, True AC, Linden KG, Hernandez MT, Larson LT, Pauls AK. Commercial toilets emit energetic and rapidly spreading aerosol plumes. Sci Rep. 2022; 12(1):20493

14. Heilingloh CS, Aufderhorst UW, Schipper L, Dittmer U, Witzke O, Yang D, et al. Susceptibility of SARS-CoV-2 to UV irradiation. Am J Infect Control. 2020; 48(10):1273–5

15. Hoehl S, Karaca O, Kohmer N, Westhaus S, Graf J, Goetsch U, et al. Assessment of SARS-CoV-2 Transmission on an International Flight and Among a Tourist Group. JAMA Netw Open. 2020; 3(8):e2018044

16. International Agency for Research on Cancer. IARC Working Group on the Evaluation of Carcinogenic Risks to Humans. Solar and Ultraviolet Radiation. 1992

17. International Civil Aviation Organization. ICAO DOc. 10152. Manual on COVID-19 Cross-border Risk Management. 2021

18. International Electrotechnical Commission. IEC 62471:2006 Photobiological safety of lamps and lamp systems. 2006

19. Jones RM, Brosseau LM. Aerosol Transmission of Infectious Disease. J Occup Environ Med. 2015; 57(5):501–8

20. Kennedy HE. Chapter 62. Ultraviolet Air and Surface Treatment. In: 2019 ASHRAE Handbook—HVAC Applications. Atlanta: American Society of Heating, Refrigerating and Air-conditioning Engineers. ASHRAE; 2019:62.1-62.17.

21. Khanh NC, Thai PQ, Quach H-L, Thi N-AH, Dinh PC, Duong TN, et al. Transmission of SARS-CoV 2 During Long-Haul Flight. Emerg Infect Dis. 2020; 26(11):2617–24

22. Kinahan SM, Silcott DB, Silcott BE, Silcott RM, Silcott PJ, Silcott BJ, et al. Aerosol tracer testing in Boeing 767 and 777 aircraft to simulate exposure potential of infectious aerosol such as SARS-CoV-2. PLOS ONE. 2021; 16(12):e0246916

23. Kowalski W. Ultraviolet Germicidal Irradiation Handbook: UVGI for Air and Surface Disinfection. Berlin, Heidelberg: Springer; 2009.

24. Ma B, Burke-Bevis S, Tiefel L, Rosen J, Feeney B, Linden KG. Reflection of UVC wavelengths from common materials during surface UV disinfection: Assessment of human UV exposure and ozone generation. Sci Total Environ. 2023; 869:161848

25. Ma B, Linden YS, Gundy PM, Gerba CP, Sobsey MD, Linden KG. Inactivation of Coronaviruses and Phage Phi6 from Irradiation across UVC Wavelengths. Environ Sci Technol Lett. 2021; 8(5):425–30

26. Masjoudi M, Mohseni M, Bolton J. Sensitivity of Bacteria, Protozoa, Viruses, and Other Microorganisms to Ultraviolet Radiation. J Res Natl Inst Stand Technol. 2021; 126

27. Memarzadeh F. A Review of Recent Evidence for Utilizing Ultraviolet Irradiation Technology to Disinfect Both Indoor Air and Surfaces. Appl Biosaf. 2021; 26(1):52–6

28. Michelini Z, Mazzei C, Magurano F, Baggieri M, Marchi A, Andreotti M, et al. UltraViolet SANitizing System for Sterilization of Ambulances Fleets and for Real-Time Monitoring of Their Sterilization Level. Int J Environ Res Public Health. 2022; 19(1):331

29. Morawska L, Tang JW, Bahnfleth W, Bluyssen PM, Boerstra A, Buonanno G, et al. How can airborne transmission of COVID-19 indoors be minimised? Environ Int. 2020; 142:105832

30. Moser MR, Bender TR, Margolis HS, Noble GR, Kendal AP, Ritter DG. Moser, M. R., Bender, T. R., Margolis, H. S., Noble, G. R., Kendal, A. P., & Ritter, D. G. (1979). An outbreak of influenza aboard a commercial airliner. Am J Epidemiol. 1979; 110(1):1–6

31. Narita K, Asano K, Naito K, Ohashi H, Sasaki M, Morimoto Y, et al. Ultraviolet C light with wavelength of 222 nm inactivates a wide spectrum of microbial pathogens. J Hosp Infect. 2020; 105(3):459–67

32. Naunovic Z, Lim S, Blatchley ER. Investigation of microbial inactivation efficiency of a UV disinfection system employing an excimer lamp. Water Res. 2008; 42(19):4838–46

33. Oh C, Sun PP, Araud E, Nguyen TH. Mechanism and efficacy of virus inactivation by a microplasma UV lamp generating monochromatic UV irradiation at 222 nm. Water Res. 2020; 186:116386

34. Olsen SJ, Chang H-L, Cheung TY-Y, Tang AF-Y, Fisk TL, Ooi SP-L, et al. Transmission of the Severe Acute Respiratory Syndrome on Aircraft. N Engl J Med. 2003; 349(25):2416–22

35. Raeiszadeh M, Adeli B. A Critical Review on Ultraviolet Disinfection Systems against COVID-19 Outbreak: Applicability, Validation, and Safety Considerations. ACS Photonics. 2020; 7(11):2941–51

36. Rafferty AC, Bofkin K, Hughes W, Souter S, Hosegood I, Hall RN, et al. Does 2x2 airplane passenger contact tracing for infectious respiratory pathogens work? A systematic review of the evidence. PLOS ONE. 2023; 18(2):e0264294

37. Ramos CCR, Roque JLA, Sarmiento DB, Suarez LEG, Sunio JTP, Tabungar KIB, et al. Use of ultraviolet-C in environmental sterilization in hospitals: A systematic review on efficacy and safety. Int J Health Sci. 2020; 14(6):52–65

38. Redrow J, Mao S, Celik I, Posada JA, Feng Z. Modeling the evaporation and dispersion of airborne sputum droplets expelled from a human cough. Build Environ. 2011; 46(10):2042–51

39. Reed NG. The History of Ultraviolet Germicidal Irradiation for Air Disinfection. Public Health Rep. 2010; 125(1):15–27

40. Riley RL, Nardell EA. Clearing the air. The theory and application of ultraviolet air disinfection. Am Rev Respir Dis. 1989; 139(5):1286–94

41. Sellera FP, Sabino CP, Cabral FV, Ribeiro MS. A systematic scoping review of ultraviolet C (UVC) light systems for SARS-CoV-2 inactivation. J Photochem Photobiol. 2021; 8:100068

42. Silcott D, Kinahan SM, Santarpia JL, Silcott B. TRANSCOM/AMC Commercial Aircraft Cabin Aerosol Dispersion Tests. Nebraska: National Strategic Research Institute; 2020.

43. Sliney D. Balancing the Risk of Eye Irritation from UV-C with Infection from Bioaerosols. Photochem Photobiol. 2013; 89(4):770–6

44. Sliney DH, Stuck BE. A Need to Revise Human Exposure Limits for Ultraviolet UV-C Radiation†. Photochem Photobiol. 2021; 97(3):485–92

45. Spicer DB. Methods and Mechanisms of Photonic Disinfection. J Res Natl Inst Stand Technol. 2021; 126:126016

46. Stamatas GN, Nikolovski J, Mack MC, Kollias N. Infant skin physiology and development during the first years of life: a review of recent findings based on in vivo studies. Int J Cosmet Sci. 2011; 33(1):17–24

47. Sze To GN, Wan MP, Chao CYH, Fang L, Melikov A. Experimental Study of Dispersion and Deposition of Expiratory Aerosols in Aircraft Cabins and Impact on Infectious Disease Transmission. Aerosol Sci Technol. 2009; 43(5):466–85

48. Tang JW, Bahnfleth WP, Bluyssen PM, Buonanno G, Jimenez JL, Kurnitski J, et al. Dismantling myths on the airborne transmission of severe acute respiratory syndrome coronavirus-2 (SARS-CoV-2). J Hosp Infect. 2021; 110:89–96

49. US Food and Drugs Administration. Ultraviolet (UV) Radiation. FDA. 2021

50. Walkinshaw DS. A Brief Introduction To Passenger Aircraft Cabin Air Quality: COVID-19 and Beyond. ASHRAE J. 2020; 62(10):12–7

51. Wang CC, Prather KA, Sznitman J, Jimenez JL, Lakdawala SS, Tufekci Z, et al. Airborne transmission of respiratory viruses. Science. 2021; 373(6558):eabd9149

52. Welch D, Kleiman NJ, Arden PC, Kuryla CL, Buonanno M, Ponnaiya B, et al. No Evidence of Induced Skin Cancer or Other Skin Abnormalities after Long-Term (66 week) Chronic Exposure to 222-nm Far-UVC Radiation. Photochem Photobiol. 2023; 99(1):168–75

53. Whalen JJ. Environmental control for tuberculosis: basic upper-room ultraviolet germicidal irradiation guidelines for healthcare settings. 2020

54. Woods JA, Evans A, Forbes PD, Coates PJ, Gardner J, Valentine RM, et al. The effect of 222-nm UVC phototesting on healthy volunteer skin: a pilot study. Photodermatol Photoimmunol Photomed. 2015; 31(3):159–66

55. Xiao F, Sun J, Xu Y, Li F, Huang X, Li H, et al. Infectious SARS-CoV-2 in Feces of Patient with Severe COVID-19. Emerg Infect Dis. 2020; 26(8):1920–2

56. You R, Lin C-H, Wei D, Chen Q. Evaluating the commercial airliner cabin environment with different air distribution systems. Indoor Air. 2019; 29(5):840–53

57. Does UV Radiation Cause Cancer? | American Cancer Society. 2019 Retrieved 1 May 2023 from https://www.cancer.org/healthy/cancer-causes/radiation-exposure/uv-radiation.html

58. Cabin Air & Low Risk of On Board Transmission. Retrieved 1 May 2023 from https://www.iata.org/en/youandiata/travelers/health/low-risk-transmission/

59. TLV/BEI Guidelines. ACGIH. Retrieved 1 May 2023 from https://www.acgih.org/science/tlv-bei-guidelines/

60. WHO reveals leading causes of death and disability worldwide: 2000-2019. Retrieved 31 January 2023 from https://www.who.int/news/item/09-12-2020-who-reveals-leading-causes-of-death-and-disability-worldwide-2000-2019

61. World health statistics 2022: monitoring health for the SDGs, sustainable development goals. Retrieved 31 January 2023 from https://www.who.int/publications-detail-redirect/9789240051157

Appendix - Risk vs Benefit Analysis

Outline

1. Purpose, Conclusions, Introduction, and Recommendations
2. Quantify the unmanaged residual risk from Influenza A and COVID-19 that is not effectively mitigated by ventilation and masks (i.e., residual risk of infection or death)
   2.1. Use a Top-down methodology from CDC and FAA statistics
      2.1.1. Executive Summary
      2.1.2. Residual risk due to Influenza A
         2.1.2.1. Excess number of seasonal influenza infections due to inflight transmission
         2.1.2.2. Excess number of COVID-19 infections due to inflight transmission
      2.1.3. Residual risk due to COVID-19 during the period February 2020 through September 2021
         2.1.3.1. Excess number of COVID-19 infections due to inflight transmission
         2.1.3.2. Excess number of COVID-19 deaths due to inflight transmission
   2.2. Estimate the Economic Impact of Infight Transmission of Seasonal Influenza and Pandemic COVID-19
   2.3. Use a Bottoms-up fundamental Wells-Riley formalism
      2.3.1. Residual risk due to Influenza A
      2.3.2. Residual risk due to SARS-CoV-2
3. Quantify the efficacy of UV-C as applied by the Device
   3.1. Define the disinfection efficacy in air for ventilation in terms of Air Changes per Hour from peer-reviewed references.
   3.2. Provide the equation for disinfection efficacy in air for UV in terms of equivalent Air Changes per Hour, ACH_{eq}, as a function of k and D (below) to compare with ACH for ventilation in the aircraft cabin
   3.3. Provide the UV-C susceptibility constant, k, in air for SARS-CoV-2, Influenza, RSV, TB, pneumonia, measles, etc. from peer-reviewed references
4. Explain the unexpectedly high residual risk of airborne infections in aircraft cabins
5. Quantify the reduction in risk of infection from the Wells-Riley equation due to various elements in an SMS "Swiss cheese" model of risk management
   5.1. Quantify the extent to which the device as installed effectively mitigates the unmanaged residual risk (i.e., % reduction in risk of infection or death)
6. Potential safety risks associated with exposure to the radiating device from peer-review references
   6.1. Erythema
   6.2. Photokeratitis
   6.3. Non-melanoma skin cancer

7. Quantify the extent to which the health and safety benefit provided by the UV-C Device outweighs the potential safety risks associated with exposure to the radiating device

   7.1. Risk reduction due to UV-C
   7.2. Risk associated with exposure to UV-C
   7.3. Quantitatively compare the risk vs. benefit of the UV-C application
8. Evidence of aerosol transmission on aircraft
9. Return on Investment for UV-C in aircraft cabins
10. References

1. **Purpose, Conclusions, Introduction, and Recommendation**

The purpose of this Appendix is to provide all necessary detail and references to accurately quantify the Benefits of using UV-C for air disinfection in aircraft vs. the Risk of overexposure to UV-C for passengers and crew.

Summary of conclusions:

1. There are ~ 10,000 annual deaths due to transmission of SARS-CoV-2 and Influenza A, combined, aboard US commercial aircraft.

    We rigorously cross-checked these results using 2 independent methodologies (shown herein), along with confirmation by an independent epidemiological statistics expert. We're preparing a peer-reviewed publication.

2. The estimated annual economic burden due to transmission of SARS-CoV-2 and Influenza A aboard aircraft during the period Feb'20 through Sep'21 is ~ $200 B.

3. Up to about 80% of the annual deaths and annual economic burden might be saved by supplementing the aircraft ventilation with UV-C air disinfection.

4. The one-time cost of implementing UV-C air disinfection on all US commercial aircraft would be ~ $1 per passenger ticket for one year. That's only ~ 10% of the ongoing annual economic burden, or ~ 1,000% return on investment every year.

5. The installation cost of ~ $1 per passenger ticket for one year, amortized across ~ 10,000 annual deaths over the ~ 20-year life of the UV-C product aircraft, results in about $5,000 cost per life saved.

6. The 0.00003% risk of acute (one-time) overexposure may (or may not) result in a 1 to 2-day skin or eye irritation, with no long-term effects or risks, compared to the 15,000 x greater risk at 0.5% of contracting COVID-19 or Influenza A that persists for several days to weeks, and has a finite risk of hospitalization or death.

7. There seems to be virtually no scenario for any occupant aboard an aircraft equipped with a UV-C designed below the EL to receive a chronic, occupational dose of UV-C sufficient to increase the risk of non-Melanoma Skin Cancer.

8. In a very unlikely scenario that could result in chronic, occupational overexposure to flight attendants, the risk of even one flight attendant in the US contracting NMSC over a 20-year period from UV-C overexposure aboard the aircraft is 0.0016%. That 0.0016% of an NMSC case is highly treatable, at a cost of about $900 per treatment, or <<< $1 considering the probability of the occurrence of SNSC, with virtually no probability of even one death.

9. The ratio of Economic Benefits from avoiding deaths from infectious disease to Risk of Economic Burden from having UV-C onboard is > 10 billion to 1.

10. The ratio of Benefits from avoiding deaths from infectious disease to the Risks of adverse health outcomes or death from use of UV-C is incalculably high.

Introduction

The confusion around transmission of COVID-19 and other airborne diseases aboard aircraft can finally be clarified. We don't need to rely on previous unsubstantiated claims like the ones quoted below, even though they've been provided by trusted authorities.

> *"**It's Almost Impossible to Get COVID-19 on an Airplane**, New Military Study Suggests"[39]*

> SCOTT AIR FORCE BASE, Ill. – *U.S. Transportation Command (USTRANSCOM) released the results from its Commercial Aircraft Cabin Aerosol Dispersion Test showing the overall exposure **risk from aerosolized pathogens, like coronavirus, is very low** on the type of aircraft the command contracts to move Department of Defense personnel and their families.[46]*

> *"Even with these prevention methods, a small number of travelers arrive at their destination testing positive for the virus. There has been **little clear evidence to date** if the infections were contracted while aboard flights."[46]*

We've been historically misled regarding the risk of transmission of airborne pathogens aboard aircraft. Even as recently as the 2021 USTRANSCOM report, scientific data was rigorously measured, then misused to incorrectly assure the safety of air aboard commercial aircraft, in response to (well-founded) public fear of COVID-19 transmission aboard commercial aircraft.

The TRANSCOM report acknowledged that
> *"a small number of travelers arrive at their destination testing positive for the virus".*

But the report deflected the hard evidence that was mentioned in the report with the misleading disclaimer:
> *"There has been little clear evidence to date if the infections were contracted while aboard flights."*

Of course, there's been "little clear evidence" because we don't conduct contact tracing in the US. It has generally not possible to establish the transmission route of airborne disease in the US.

Nonetheless, the TRANSCOM-authored reference article on which the above statements are based provides the following evidence to the contrary:

> *"An ideal case study on an 18-hour Boeing 777 flight was completed in part thanks to the **unique pre-testing, and quarantining** required by New Zealand. During this flight, which included a stop for refueling (with the air system disabled) and in-flight meals, **4 in-flight transmission events occurred** amongst 14 passengers located within 3 rows of an index case."[24]*

The case study cited above is strong evidence of airborne transmission of disease aboard an aircraft. The reliability of the data is enabled by the extraordinary controls in place including 100% pre-testing and post-quarantining of all passengers so that illness prior to and following the flight are reliably determined.

Instead of relying on simulated testing of aerosols aboard the aircraft, as in the USTRANSCOM report, this White Paper Appendix quantitatively and empirically estimates the occurrence of transmission of COVID-19 (and Influenza A) aboard aircraft, using data extracted from a peer-reviewed systematic analysis of all highly reliable epidemiological data displaying transmission of airborne diseases aboard aircraft. Most of this data was available prior to the USTRANSCOM report but was ignored by it.

There is recently emerging, statistically significant analysis of inflight transmission of airborne diseases in the cabin[41] that now displaces the historical claims of lack of evidence that have been the mainstay response of the airline industry.

Below is an excerpt from the Abstract of the peer-reviewed 2023 Rafferty article:[41]

> ***Overall, 43.7% (72/165) of investigations provided evidence for in-flight transmission.*** *H1N1 influenza A virus had the highest reported pooled attack rate per 100 persons (AR = 1.17), followed by SARS-CoV-2 (AR = 0.54) and SARS-CoV (AR = 0.32), Mycobacterium tuberculosis (TB, AR = 0.25), and measles virus (AR = 0.09). There was high heterogeneity in estimates between studies, except for TB. Of the 72 investigations that provided evidence for in-flight transmission, 27 investigations were assessed as having a high level of evidence, 23 as medium, and 22 as low. One third of the investigations that reported on proximity of cases showed transmission occurring beyond the 2x2 seating area.[41]*

It is clear that the well-intended, yet inconclusive, analyses of the past can now be superseded by the power of meta-analysis and standard analytical formalisms using statistically significant datasets in more recent studies of inflight transmission of infectious diseases.

An example of a well-intended but non-committal report from the past, a 2002 National Academies (NRC) study that was a follow-up to their 1986 study, included Conclusions as excerpted here:[34]

> • *A person's risk of acquiring an infection on an aircraft depends on several factors, such as the presence of an infectious person and release of infectious agents by that person, the ventilation rate and mixing of cabin air, the amount of air that is recirculated and how it is treated, proximity to the source person, duration of exposure, and susceptibility to the specific infectious agents. These factors could also increase inhalation exposure to allergens and other potentially hazardous biological materials generated by passengers and activities within aircraft cabins.*
>
> • *The proper design, operation, and maintenance of an **aircraft ventilation** system **can limit but not eliminate the transmission of infectious agents** and exposure to other biological agents on aircraft. Exposure to biological agents is increased when people are confined in an aircraft cabin without adequate ventilation.*

The above Conclusions from the 2002 NRC report regarding transmission of infectious diseases is not nearly as impactful as the 1986 recommendation regarding smoking that in fact resulted in banning smoking aboard US commercial aircraft, as excerpted here from the 2002 NRC report:

> *That [1986] report recommended the elimination of smoking on most domestic airline flights and a number of other actions to address health and safety problems and to obtain better data on cabin air quality. In response to that report, the Federal Aviation Administration (FAA) took several actions, including the **banning of smoking on all domestic flights.**[34]*

In fact, the 2002 report analyzed only 2 flights having statistically significant evidence of onboard transmission of Influenza A. However, the attack rates were extremely high: 38% to 72% on one flight; and 12% to – 53% on the second flight. Analyses of similarly limited numbers of flights were reported for measles, TB, and meningococcal disease.

We can now move beyond the limited and inconclusive studies of the past, such as the 1986 and 2002 NRC reports and the 2021 USTRANSCOM report[45], and instead consider the more recent, powerful

meta-analysis of the 2023 Rafferty publication. We can now quantify, rather than dismiss, the risk of transmission of infectious diseases on board commercial aircraft.

Recommendation

Based on the compelling estimates of illnesses, deaths, and economic burden presented in this document, supported by peer-reviewed datasets and analytical formalisms, it is clear that **the airline industry should move to assertively improve the air quality aboard aircraft to greatly reduce the inflight transmission of infectious diseases** in the same manner as they eliminated the health risks and burdens from smoking aboard aircraft. Quantify the unmanaged residual risk from Influenza A and COVID-19 that is not effectively mitigated by ventilation and masks (i.e., residual risk of infection or death)

1.1. Use a Top-down methodology from CDC and FAA statistics

1.1.1. Executive Summary

The excess burden from inflight transmission of influenza can be estimated in several ways including excess illness, excess deaths, or estimated economic costs. This exercise examines the impact of inflight transmission of infection on U.S. air carriers for routine seasonal influenza for the 10 years from 2010 through 2019 as well as the impact from the severe COVID-19 pandemic from February 2020 through September 2021. The numbers are larger than one might expect due to the extremely high density of passengers per cabin volume, as described in Section 4 of this Appendix.

It was estimated that for a typical year, inflight transmission on U.S. air carriers of seasonal influenza was responsible for infection of 473,800 passengers who would have transmitted the infection to an additional 473,800 people in the general U.S. population for a total of 947,600 infections counting only this first wave of secondary infections. This amounts to 3.2% of all seasonal influenza in the U.S. being due to inflight transmission. Mortality resulting from inflight transmission of seasonal influenza infections would be about 38 deaths of passengers infected inflight plus 599 deaths from the first wave of secondary infections for a total of about 637 deaths. This accounted for 1.7% of all U.S. deaths from seasonal influenza. Independent mechanistic Wells-Riley calculations included in this appendix produced similar results.

The COVID-19 pandemic was devastating for the U.S. as well as the rest of the world. The February 2020 through September 2021 time period covers most of the U.S. Delta wave epidemic. For this 20-month period it appears inflight transmission of COVID-19 on U.S. air carriers resulted in infection of 1,058,330 passengers who would have transmitted the infection to an additional 1,058,330 people in the general population for a total of 2,116,660. This again counts only the first wave of secondary infections. Even this conservative estimate indicates that inflight transmission was responsible for 1.4% of all COVID-19 infections in the U.S. during this 20-month period. Mortality resulting from inflight transmission of pandemic COVID-19 infections was estimated to be about 2,070 deaths of passengers infected inflight plus 6,650 deaths from the first wave of secondary infections for a total of about 8,720 deaths over this 20-month period of the pandemic. This amounts to about 0.9% of all deaths from COVID-19 over this 20-month period being due to inflight transmission. Note that these large numbers were in spite of the facts that the number of flying passengers was greatly reduced during this period and that masks were mandated starting about May 2020.

The total societal cost for inflight transmissions of seasonal influenza is about $1.6 billion or $1,688 each. For a disaster like the COVID-19 pandemic the cost of inflight transmission of COVID-19 could be $204 billion or $96,567 per inflight transmission of COVID-19.

1.1.2. Unmanaged residual risk due to Influenza A - Top-down methodology

1.1.2.1. Excess number of seasonal influenza infections due to inflight transmission.

This calculation requires projecting the CDC seasonal influenza risk for each age group of the general U.S. population onto the age distribution of the flying population. Then multiplication by the size of the flying population should yield the annual number who contract seasonal influenza. That is multiplied by the risk that they will be flying on a day when they are contagious. Then multiplication by the effective reproduction number for inflight transmission will estimate the number of inflight transmissions of seasonal influenza. The number of these inflight transmissions that result in death is accomplished the same way by projecting the CDC seasonal influenza mortality risk to the age distribution of airline passengers. The number of infections and deaths in the general population due to these individuals who were infected inflight is calculated by applying a summary reproduction number for the general population to the group who were infected onboard airliners. In this analysis the infectious passengers are considered as the source of infection, those infected inflight as primary infections, and succeeding infections as secondary infections. For the calculation below, the averages for seasonal influenza over the 10-year period from 2010 through 2019 will be used. The detailed calculations are contained in a companion Excel spreadsheet. The interested reader can change any of the parameters in that file to observe the effect on the results. Data for the size of the U.S. population by year is displayed in **Table 1**.

Table 1. Annual US Population 2010 to 2020[51]

Year	Annual US Population	Mid-year Pop
1/1/2010	309,327,143	310,455,312
1/1/2011	311,583,481	312,730,572
1/1/2012	313,877,662	314,968,805
1/1/2013	316,059,947	317,223,138
1/1/2014	318,386,329	319,562,662
1/1/2015	320,738,994	321,905,375
1/1/2016	323,071,755	324,096,942
1/1/2017	325,122,128	325,980,164
1/1/2018	326,838,199	327,584,076

1/1/2019	328,329,953	329,915,517
1/1/2020	331,501,080	

Average from 2010 - 2019 = 320,442,256

The risk of contracting influenza for each CDC age group by year is displayed in **Table 2**.[10]

Table 2. Estimated rates of symptomatic influenza, per 100,000, by age group.[11]

Year	0-4 yrs	5-17 yrs	18-49 yrs	50-64 yrs	65+ yrs
2010-2011	13,743	8,217	5,468	8,241	4,521
2011-2012	4,697	3,712	2,564	3,181	2,334
2012-2013	17,821	12,419	8,384	12,852	9,712
2013-2014	12,712	7,416	9,590	13,713	3,819
2014-2015	16,136	11,895	6,310	11,626	10,120
2015-2016	11,028	7,705	6,668	10,505	2,946
2016-2017	11,950	12,012	6,786	11,766	7,404
2017-2018	17,086	13,332	9,931	18,385	10,096
2018-2019	15,239	12,359	7,088	11,439	4,287
2019-2020	19,519	13,404	10,432	13,747	13,747
Average	14,021	10,472	7,528	11,913	7,163
Median	15,239	12,012	7,088	11,766	7,404
Med Fraction	0.15	0.12	0.07	0.12	0.07

The number of annual passengers on U.S. Airlines can be obtained from the Bureau of Transportation Statistics[7] and is displayed in **Table 3**.

Table 3. Annual Number of Passengers on US Airlines in Millions[7]

Year	# Passengers
2010	720
2011	731
2012	737
2013	743
2014	763
2015	798
2016	824
2017	849
2018	889
2019	926
Average =	**798**

Estimating the proportion of the flying public in each CDC age group was a challenge. I located passenger age groups for U.S. (1984)[35], UK (1998)[37], and UK (2017)[14]. Extrapolated from the age groups in those data to the CDC age groups.

Table 4. The Proportion of Passengers in Each CDC Age Group

Age Grp	2017 UK	1984 US	1998 UK	Average
0-4 yrs	0.01	0.03	0.02	0.02
5-17 yrs	0.05	0.08	0.08	0.07
18-49 yrs	0.59	0.63	0.61	0.61
50-64 yrs	0.25	0.18	0.23	0.22
65+ yrs	0.10	0.09	0.07	0.09

Now the annual number of passengers in each CDC age group can be calculated by: (average annual passengers) * (proportion in each age group). This gives **Table 5**.

Table 5. Annual Number of Passengers in Millions for Each CDC Age Group

Age Grp	Millions of Passengers
0-4 yrs	15.43
5-17 yrs	54.64
18-49 yrs	487.13
50-64 yrs	175.37
65+ yrs	69.51

Then the number in each group expected to have contracted influenza during the year can be calculated by: (annual passengers in each group) * (incidence in that group.) This is displayed in **Table 6**.

Table 6. Annual Number of Passengers in Millions in Each Age Group Expected to have Influenza

Age Group	Passengers with Influenza
0-4 yrs	2.35
5-17 yrs	6.56
18-49 yrs	34.53
50-64 yrs	20.63
65+ yrs	5.15
Total	**69.22**

So, the estimated annual proportion of airline passengers with influenza = (total passengers with flu) / (total passengers) = 0.09. This is about the same as the average annual proportion of the total US population with influenza for 2010 through 2019.

Now the daily number of airline passengers who are contagious with influenza can be calculated. The number of days influenza is contagious is addressed by the CDC.[11]

A reasonable number for duration (days) influenza is contagious = 5. The proportion of a year = (duration days)/365.25 = 0.014.

Estimate the proportion of these passengers who will fly even though they have symptoms = 0.5. Influenza can certainly make you feel pretty bad, but many passengers will endure a lot to get back home.

The average number of annual trips for the flying public during this time frame is reported by Gallup[28] to be 3.5. Since the influenza season usually lasts about 6 months, assume the average days flown per year = 1.75.

So, the chance that an individual will be infectious on a day they are flying = (flts/yr) * (Duration/365.25) * (% flying with Sx) = 0.012

The daily number of infectious passengers = (Duration/365.25) * (% who fly with Sx) * (# flights/yr) * (# annual passengers with flu) = 473,814.

Calculating the number of inflight transmissions needs the overall effective reproduction number R_e for influenza over the flu season. This has been a challenge to locate, but we know R_e must be greater than one in the first part of the season and less than one towards the end of the season. Note that the epidemic curve for an average flu season is fairly symmetric.[12] The case studies for inflight transmission of influenza in recently published article[41] show a pooled secondary attack rate of .0117 and a crude reproductive number of 2.28. So, with an average of about 100 passengers per flight it seems reasonable to assume the R_e for inflight transmission over the season is about 1.0. Note that the average R for seasonal influenza in the general population is usually about 1.3.[5]

So, the total number of annual inflight transmissions of influenza = R_e * (# infectious) = 473,814.

As above, assume the seasonal R_e for the general U.S. population is also about 1. Assume random mixing of passengers infected inflight with the general U.S. population.

So, the total number of secondary cases due to the inflight infected = (the number infected inflight) * R_e = 473,814.

That gives the estimated total annual number of influenza cases caused by inflight transmission equals (# infected inflight) + (# secondary infections from that group) = 947,629. This includes only the first wave of secondary infections for simplicity but there would be additional waves of infection related to the group infected inflight.

The above estimate indicates that inflight transmission of influenza is responsible for 3.2% of all seasonal influenza in the United States.

1.1.2.2.   Excess <u>influenza mortality</u> due to inflight transmission.

The CDC published the general population mortality burden for 2010 - 2019 and analogous pages for earlier years.[10] The median number of deaths from influenza in the U.S. from 2010 through 2019 = 37,293. The median number of symptomatic influenza cases over this same period = 29,480,259.

So, the number of deaths in the general population related to secondary infection from the inflight infected passengers = (US deaths / US cases) * (cases transmitted inflight) = 599. There would be additional deaths from tertiary infections from this group, but these are also omitted for simplicity and to be conservative.

A number of the passengers who become infected inflight will also die. Calculating this more accurately requires accounting for the age distribution of the flying public since the mortality rate varies between age groups and age distribution of the flying public is different.

An estimate for the proportion of the flying population in each age group is presented above in **Table 4**.

The median mortality rate from 2010 - 2019 from influenza for the CDC age groups is displayed in **Table 7.**[10]

Table 7. Estimated Mortality Rates for influenza, per 100,000, by age group[10]

Year	0-4 yrs	5-17 yrs	18-49 yrs	50-64 yrs	65+ yrs
2010-2011	1	0.3	3.9	10.1	62.4
2011-2012	0	0	0.5	3.8	22.6
2012-2013	1.5	1.6	1.5	6.8	81.5
2013-2014	0.4	0.1	2.5	9.6	63.6
2014-2015	2	0.8	0.7	7.6	96.9
2015-2016	0.9	0.2	1.2	5.2	36.6
2016-2017	0.6	0.2	1	6	66.7
2017-2018	0.5	0.8	1.6	9.2	84.6
2018-2019	1.1	0.3	1.2	7	40.5
2019-2020	1.7	0.3	1.9	9.8	29.4
Average	1	0	2	8	58

	Median	1	0	1	7	63

To obtain the mortality rate per 100,000 for these inflight infected passengers, SUM OVER [(proportion of passengers in each age group) * (median mortality rate/100,000 for the age grp)]. The proportion of the flying population in each age group is displayed in **Table 4.**

This gives the mortality rate per 100,000 inflight infected passengers = 8.

The total number of deaths in this group = (# inflight infected passengers) *(mortality rate per 100,000) / 100,000 = 38. Note that this number is a fraction of the general population deaths due to the much smaller proportion of 65+ year-olds in the flying population and the high mortality in that group.

The estimated total median number of annual deaths related to inflight transmission of influenza from 2010 through 2019 = (deaths of inflight infected passengers) + (deaths in general population who were infected from the infected passengers) = 637.

Overall, it is estimated that the annual impact of inflight transmission of **influenza for the period 2010 – 2019** amounts to 947,629 **infections and 637 deaths**.

So inflight transmission could be responsible for 3.2% of symptomatic influenza cases in the United States and 1.7% of the deaths from influenza.

1.1.3. Unmanaged residual risk due to COVID-19 During the Period February 2020 Through September 2021 - Top-down methodology

1.1.3.1. Excess number of seasonal COVID-19 infections due to inflight transmission.

This calculation is similar to the estimate above for inflight infections of seasonal influenza.

It requires projecting the CDC COVID-19 risk for each age group of the general U.S. population onto the age distribution of the flying population. Then multiplication by the size of the flying population should yield the annual number who contract COVID-19. That is multiplied by the risk that they will be flying on a day when they are contagious. Then multiplication by the effective reproduction number for inflight transmission will estimate the number of inflight transmissions of COVID-19. The number of these inflight transmissions that result in death is accomplished the same way by projecting the CDC COVID-19 mortality risk to the age distribution of airline passengers. The number of infections and deaths in the general population due to these individuals who were infected inflight is calculated by applying a summary reproduction number for the general population to the group who were infected onboard airliners.

The midpoint U.S. population during the February 2020 Through September 2021 period was 331,697,413.[50]

The age specific rates per 100,000 for COVID-19 are shown in **Table 8**.[9]

Table 8. Age Specific Rates of COVID-19 Infection per 100,000 from 2/2020-9/2021.[9]

	0-17 yrs	18-49 yrs	50-64 yrs	65+ yrs	All Ages
Infection Rate	35,490	54,860	43,656	32,363	44,650
Proportion	0.35	0.55	0.44	0.32	0.45

The number of passengers on U.S. airlines in millions was 369 in 2020 and 674 in 2021.[7] From Feb 2020 through Sept 2021 there were an extrapolated 844 million passengers.

From Table 4 above, the proportion of passengers in these CDC age groups are:

5-17 yrs (0.07), 18-49 yrs (0.61), 50-64 yrs (0.22), and 65+ yrs (0.09).

The total number of passengers in millions for each age group from Feb 2020 through Sept 2021 is total passengers * proportion in each age group as displayed in **Table 9.**

Table 9. Passengers in Each Age Group

Age Grp	Millions of Passengers
5-17 yrs	57.77
18-49 yrs	515.07
50-64 yrs	185.44
65+ yrs	73.49

The number of passengers in each age group expected to have COVID-19 from Feb 2020 through Sept 2021 is the passengers in each group * incidence in that group as displayed in **Table 10**.

Table 10. Passengers in Each Age Group Expected to Have COVID-19

Age Group	Millions with COVID-19
5-17 yrs	20.50
18-49 yrs	282.57
50-64 yrs	80.95
65+ yrs	23.78

So, of the 844 million passengers flying from Feb 2020 through Sept 2021, $407.81 million of them will have been expected to have COVID-19 at some time from Feb 2020 through Sept 2021.

The proportion of these airline passengers with COVID-19 is 0.48 (407.81/844) compared to 0.45 for the U.S. population.

The chance of any of these passengers flying on a day when they are contagious depends on their duration of infectivity, the proportion who will fly when they may not be feeling well, and the number of days during this period that they fly.

The duration of infectivity for COVID-19 is about 5 days.[8] The proportion of this 20-month period would be duration/578 = 0.009.

Assume that a conservative proportion, 0.5, will fly when they are infectious. A modeling study estimated that 59% of the COVID-19 infectious are from asymptomatic transmission.[23]

Conservatively assume number of flying days during this period averages 3 days. Airline traffic during this period was about 2/3 of pre-pandemic. Pre-pandemic flights per year were about 3.5.[28] So for 20 months' estimate = (20/12) * (2/3) * 3.5 = 3.9.

The chances that one of these passengers will be infectious on a day they are flying = (flts/yr) * (Duration/578) * (% flying with symptoms) = 0.005.

So, the estimated number of infectious passengers flying = (proportion flying infectious) * (passengers with COVID during the 20 mo) = 2,116,668.

A systematic review on contract tracing systems for airlines[41] reports the inflight secondary attack rate for COVID-19 was 0.54.% which assuming about 100 passengers per aircraft translates roughly into an effective reproduction number of about 0.5. Note that mask use was mandatory for most of this time period.

So, the number of COVID-19 infections transmitted inflight = R_e * (# contagious) = 1,058,334.

This group will result in additional infections as they mix with the general U.S. population. The number of direct secondary infection is the 1,058,334 * R_e.

Choosing a summary R_e for these 20 months is challenging. However, we know that as the pandemic is expanding that R_e >1 and when it is contracting R_e <1. Many expect that COVID will become endemic in the U.S., and in this case R_e would be about 1. The epidemic curve over these 20 months covers most of the Delta wave and is relatively symmetric[31,36] so choose an overall R_e = 1. Note that this 20-month period ends just before the much larger Omicron wave which would have produced higher counts of inflight transmission.

So, the number of secondary infections in this first wave = 1,058,334.

This would make the total number of infectious due to inflight transmissions 2,116,668 at this stage. The number infected from 2/2020 to 9/2021 in the US population was 146,585,169 so the percent of all U.S. COVID-19 infections from inflight transmission = 1.4%.

The annualized total number of infections = (total over 20 mo) * (12/20) = 1,270,001.

1.1.3.2. <u>COVID-19 Mortality</u> from February 2020 to September 2021 Due to Inflight Transmission

The general population COVID-19 mortality burden from February 2020-September 2021 was 921,371 and the overall number of cases was 146,585,169 for a case fatality proportion of 0.01.[9]

So, the number of deaths in the general population over this 20-month period related to secondary infection from the inflight infected passengers = (US deaths / US cases) * (cases transmitted inflight) = 6,652.

A number of the passengers who become infected inflight will also die. As for influenza, calculating this more requires accounting for the age distribution of the flying public since the mortality rate varies between age groups and age distribution of the flying public is different.

The median mortality rate from 2010 - 2019 from COVID-19 for the CDC age groups is displayed in **Table 11**.[9]

<p align="center">Table 11. Mortality Rates for COVID-19, per 100,000, by age group[9]</p>

Year	0-17 yrs	18-49 yrs	50-64 yrs	65+ yrs	All Ages
2020-2021	0.9	43.7	253.5	1296.5	280.7
Proportion	0.0000	0.0004	0.0025	0.0130	0.0028

To obtain the mortality rate per 100,000 for these inflight infected passengers, SUM OVER [(proportion of passengers in each age group) * (median mortality rate/100,000 for the age grp)]. The proportion of the flying population in each age group is displayed in Table 4. This gives 0.06 for 0-17 yrs; 26.68 for 18-49 yrs; 55.71 for 50-64 yrs, and 112.93 for 65+ years. So total passenger deaths/100,000 is 195.37.

This gives total deaths of the inflight infected passengers = (deaths per 100,000) * (# inflight infected passengers) / 100000) = 2,068. Note that this number is a fraction of the general population deaths due to the much smaller proportion of 65+ year-olds in the flying population and the very high mortality in that group.

This brings the estimate for total deaths attributed to inflight transmission of COVID-19 to be **8,720**.

The **annualized** total number of **deaths** = (total over 20 mo) * (12/20) = **5,232**.

The total number of COVID deaths in the general population over 20 mo = 921,371.

So, the percent of COVID-19 deaths due to inflight transmission is 0.9%.

Note that this counts only the secondary infections from the inflight infected passengers. There would be additional waves of infection from this group that to be conservative are not counted here. Also note that this large number was in spite of the fact that the number of flying passengers was greatly reduced during this period and that masks were mandated starting about May 2020.

2.2. Economic Impact of Infight Transmission of Seasonal Influenza and Pandemic COVID-19

<u>Cost of Inflight Transmission of Seasonal Influenza</u>

There are a number of studies exploring the economic cost of seasonal influenza. Research efforts from 2007 appears to be the most cited, likely because it answers the question most clearly.[33] Other newer studies are unhelpful because they focus on sub segments of the population.[15,44] The Molinari paper reports $10.4billion ($4.1 - $22.2) in direct medical costs with a total economic burden of $87.1billion ($47.2 - $149.5). A 2018 paper by Putri et al.[40] estimated direct medical costs at $3.2 billion ($1.5-$11.7) and lost work time at $8.0 billion ($4.8–$13.6 billion) for total economic cost $11.2 billion ($6.3-$25.3). All of his measures are smaller than the actual CDC reports. Most notably he estimated 4.4 million outpatient visits compared to median CDC reported 13.5 million annual visits for the 2010-2019 time frame. Molinari overestimated medical visits at 31.4 million and included projected statistical life values in the overall societal cost. An estimate that includes all societal costs could be direct medical costs of $10 billion and total cost of $50 billion. The interested reader can substitute other estimates in the calculations below, but the results should be in the same ballpark.

So, estimate direct medical costs at $10 billion and total societal cost at $50 billion.

From above, the percent of all influenza cases resulting from inflight transmission is 3.2%.

So, estimate the direct medical cost from inflight transmission at $320,000,000, and total societal cost from inflight transmission at $1.6 billion.

The total cost per each inflight transmission of flu would be $1,688.

Cost of Inflight Transmission of Pandemic COVID-19

Estimation of the economic impact on the U.S. from the COVID-19 pandemic is very difficult because of its enormous scale. One article suggests an economic impact of $16 trillion.[16] This includes the economic cost of premature deaths at 4.4 trillion, economic cost of long-term complications at 2.6 trillion, mental health impairment in the general population at 1.6 trillion, and lost productivity of 7.6 trillion. Not counting the mental health category gives a total of 14.6 trillion. So, the 1.4% of COVID-19 infections due to inflight transmission accounts for about $204 billion or about $96,567 per inflight transmission of COVID-19.

For direct medical expenses alone, the cost per symptomatic patient has been modeled at $3037 to $3994.[3,42] For our 20-month time period the CDC estimated 123,979,337 (111,032,406 – 139,954,539) cases of symptomatic COVID-19.[9] Assuming about $3500 per symptomatic patient predicts a direct medical cost of $6.1 billion.

2.3. Residual risk that is not effectively mitigated by ventilation and masks (i.e., residual risk of infection or death) using a <u>Bottoms-up fundamental Wells-Riley formalism</u>

A typical approach in quantifying the risk of airborne transmission of disease in an indoor environment is presented in two independent research papers.[6,39] A thorough description of the Wells-Riley formalism as applied to airborne transmission of SARS-COV-2 is provided in , starting with the rate equation for the (assumed uniform) concentration of pathogen quanta in the space (a quantum is defined as the dose of airborne droplet nuclei required to cause infection in 63% of susceptible persons):

$$\frac{dc}{dt} = \frac{E_p \times f_e}{V} - \left(\lambda_0 + \lambda_{dec} + \lambda_{dep} + \lambda_{cle} \right) \times c \qquad (A1)$$

where:

E_p is the emission rate of quanta into the indoor air from an infected person in the space (quanta/h);

f_e is the penetration efficiency of virus-carrying particles through masks or face coverings for exhalation;

V is the volume of the space (m^3);

λ_0 is the removal rate (/h) of quanta by **ventilation with outdoor or filtered air, e.g., HVAC**;

λ_{cle} is the removal rate (/h) of quanta by air cleaning devices
(e.g., recirculated air with filtering, **germicidal UV**, portable air cleaners, etc.);

λ_{dec} is the infectivity decay rate (/h) of the virus;

λ_{dep} is the deposition rate (/h) of airborne virus-containing particles onto surfaces.

In the regimes of interest for air disinfection inside aircraft cabins, the rates λ_0 (outdoor air) and λ_{cle} (due to germicidal UV) dominate all the other removal rates ($\lambda_{dec} \sim \lambda_{dep} \sim 1$/h) [2022 Peng]. Further, without mask wearing, $f_e = 1$, so that Eq. (A1) simplifies to:

$$\frac{dc}{dt} = \frac{E_p}{V} - (ACH_{vent} + ACH_{UV}) \times c \qquad (A2)$$

The risk reduction due to the effects of ACH_{vent} and ACH_{UV} are most easily recognized when considering the steady state situation which would obtain inside an aircraft cabin after all of the emission and removal rates equilibrated (emission rate of quanta by an infected passenger as well as removal of quanta by ventilation and UV). In steady state, the left side of Eq. (A2) equals zero and the steady-state concentration is given by:

$$c_{ss} = \frac{E_p}{V \times (ACH_{vent} + ACH_{UV})} \qquad (A3)$$

In the baseline case with aircraft ventilation, but no UV disinfection, this reduces to:

$$c_{ssVent} = \frac{E_p}{V \times ACH_{vent}} \qquad (A4)$$

Then, when UV disinfection is added to the aircraft ventilation, the steady state concentration of airborne pathogens is reduced by the factor, R:

$$R \equiv \frac{c_{ss}}{c_{ssVent}} = \frac{\left(\frac{E_p}{V \times (ACH_{vent} + ACH_{UV})}\right)}{\left(\frac{E_p}{V \times ACH_{vent}}\right)} = \frac{ACH_{vent}}{ACH_{vent} + ACH_{UV}} \qquad (A5)$$

Exemplary results of Eq. (A5) are presented in **Table 12**. The ACH_{vent} values of 15 and 30 represent a typical range while cruising, and five represents an approximate ACH_{vent} while on the ground. The ACH_{UV} values are all attainable with present technology, depending on the wavelength of UV and the spacing of the UV emitters throughout the cabin.

Table 12. R, the Ratio of the steady state concentration of airborne pathogens with vs. without UV-C disinfection.

Ratio of c_{ss}		ACH$_{UV}$			
		15	30	60	120
ACH$_{vent}$	5	0.25	0.14	0.08	0.04
	15	0.50	0.33	0.20	0.11
	30	0.67	0.50	0.33	0.20

Table 12 indicates that the reduction of residual airborne pathogen concentration left over following removal by the aircraft ventilations system may be reduced by anywhere from 33% to 89% while cruising, and by up to 96% while grounded.

A conservative value of R, while cruising might be R = 0.33 (a 67% reduction in airborne pathogen concentration), corresponding to ACH$_{vent}$ = 30 and ACH$_{UV}$ = 60. Present technology makes possible an ACH$_{UV}$ of 120 whereby R = 0.20 (an 80% reduction in airborne pathogen concentration). The relative risk of infection will be shown later to be approximately proportional to R.

Now that the dose reduction accrued with UV has been estimated at R ~ 0.20 - 0.33, we can evaluate the dose of quanta received by an exposed susceptible subject; and estimate the probability of infection on the basis of a dose–response model.

The dose-response model used in generally used throughout the literature of infection modeling is the Wells-Riley model.[39,41,43] whereby the probability that any susceptible individual will be infected, P$_{indiv}$, is given by:

$$P_{indiv} = 1 - e^{-n} \qquad (A6)$$

where n, the infectious dose inhaled by a susceptible person in the space, is expressed in units of quanta. Accordingly, the risk of secondary infections increases linearly with n at lower values and nonlinearly at higher values, approaching 100% probability at extremely high concentrations, as demonstrated in **Fig. 1** below.
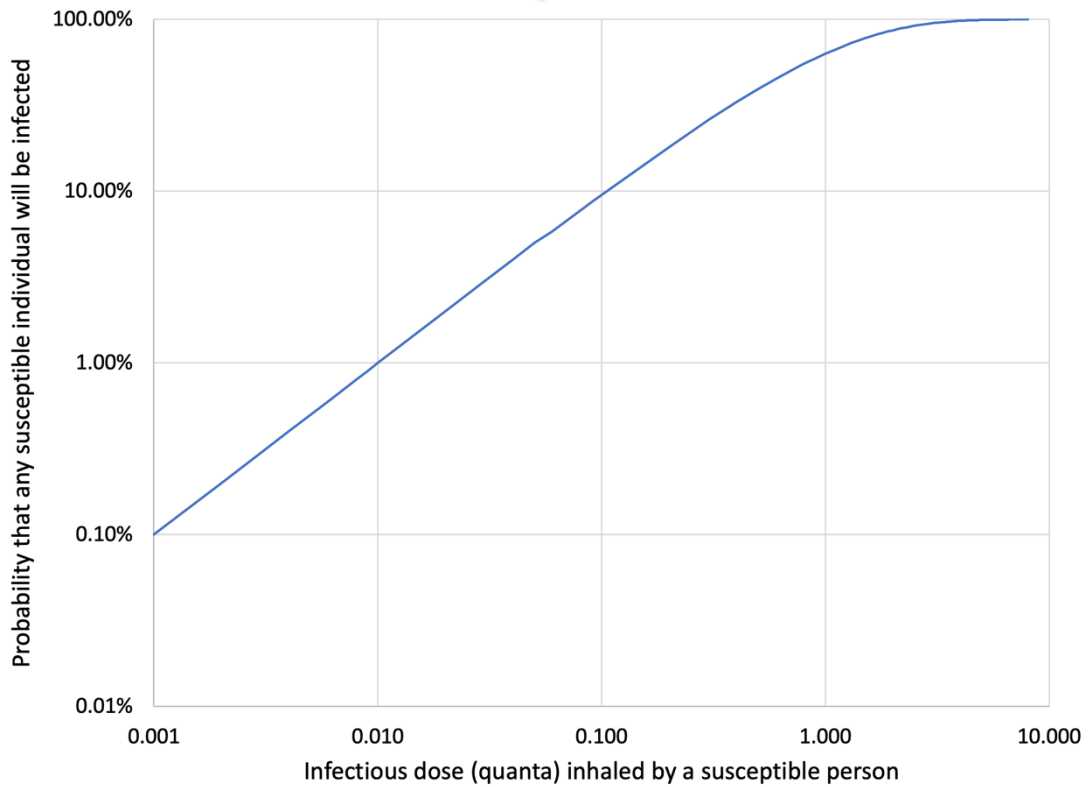
Fig. 1. The probability that any susceptible individual will be infected, from Eq. (A6)

To interpret **Fig. 1**, when the inhaled quanta, n, is 0, the risk of infection, P_{indiv}, is 0.
For a "subcritical" inhaled dose of n = 0.1, the risk of infection is linearly proportional to n, $P_{indiv} \cong$ 10%. By the definition of "quanta" when n = 1, the risk of infection, $P_{indiv} \cong$ 63%, and the response has become non-linear. As n increases beyond 1, the risk of infection increases more non-linearly, so that for n = 2, $P_{indiv} \cong$ 86%, and for n = 3, P_{indiv} approaches the saturation value of 100%, with $P_{indiv} \cong$ 95%.

An important insight from **Fig. 1** is that when n is extremely low, e.g., n ~ 0.001, and the risk of infection is extremely low, e.g., P_{indiv} ~ 0.1%, then taking auxiliary measures to further reduce the risk, such as using UV to reduce n by ~ 2 – 10 times provides a diminishing return. At the other extreme, when the pathogen concentration is so high, e.g., n > 10 that $P_{indiv} \cong$ 100%, then taking auxiliary measures such as using UV to reduce n by ~ 2 – 10 times will reduce P by only a fraction of 1%, again providing diminishing returns.

To express this insight in intuitive terms, if n and P_{indiv} are extremely low, then we'd have no evidence of passengers getting sick on airplanes – this is not the case. And, at the other extreme, if n >> 1 and P_{indiv} ~ 100% then virtually everyone gets sick on every flight, and it's obvious that the risk must be severely reduced – this is also not the case.

So, intuitively the risk of infection aboard aircraft is a finite, non-zero risk and that reducing n by approximately 2 - 10 times might be expected to significantly reduce the risk of infection and the resulting deaths and economic burdens. In the regime where some, but not most, of the susceptible individuals in the space become infected, then the linear approximation of Eq. (A21) is valid, as below.

In the linear (low risk) regime, where n <<1, a Taylor Series expansion simplifies Eq. (A6) to:

$$P_{indiv} \cong n \qquad (A7)$$

The probability, P_{indiv} = n, that any susceptible individual will be infected, given that one of the passengers is infectious, is quantified by Peng (2022) by defining the 3 parameters appearing in the following equation:

$$P_{indiv} = 1 - e^{-n} \cong n = E_{p0} \times B_o \times H_r \qquad (A8)$$

Where E_{p0}, the quanta shedding rate of an infectious person at rest and only orally breathing (no vocalization), and B_0, the average volumetric breathing rate (m^3/h) of a sedentary susceptible person.

The fixed parameters, E_{p0} and B_0, are intrinsic to all infectious and susceptible individuals, while the factor H_r contains all of the variable parameters in any specific situation, e.g., in the aircraft cabin. Since Eq. (A8) was derived for the probability that any susceptible individual will be infected assuming that 1 passenger was infectious, then the probability, $P_{PAX,inf}$, that any susceptible passenger will become infected, considering the probability, $P_{PAX,ill}$, of an infectious passenger boarding a given flight, is given by:

$$P_{PAX,inf} = P_{PAX,ill} \times P_{indiv} = P_{PAX,ill} \times E_{p0} \times B_o \times H_r \qquad (A9)$$

The probability of a of an infectious passenger boarding a given flight is

$$P_{PAX,ill} = N_{PAX} \times \%_{PAX,ill} \qquad (A10)$$

The $\%_{PAX,ill}$ is the % of passengers who are infectious the day of the flight and choose to fly while infected, which is a subset, $\%_{fly}$, who choose fly, of the total infectious passengers ticketed for the flight that day:

$$\%_{PAX,ill} = \%_{Pop,ill,day} \times \%_{fly} \qquad (A11)$$

Combining Equations A9 – A11 above provides the probability, $P_{PAX,inf}$, that any susceptible passenger will become infected, considering the probability, $P_{PAX,ill}$, of an infectious passenger boarding a given flight, is given by:

$$P_{PAX,inf} = N_{PAX} \times \%_{Pop,ill,day} \times \%_{fly} \times E_{p0} \times B_o \times H_r \qquad (A12)$$

The number of passengers who will probably be infected on any given flight, PAX_{Flight,Inf}, is then the probability, $P_{PAX,inf}$, that any susceptible passenger will become infected, times the number of passengers on the flight, N_{PAX}:

$$P_{PAX,inf} \times N_{PAX} =$$

$$N_{PAX} \times N_{PAX} \times \%_{Pop,ill,day} \times \%_{fly} \times E_{p0} \times B_o \times H_r \qquad (A13)$$

The variable parameters in any specific situation are bundled into the "relative risk factor", H_r, which has units of h^2/m^3, where:

$$H_r \equiv \frac{r_{ss} \times r_E \times r_B \times f_e \times f_i \times D}{V \times ACH_{tot}} \tag{A14}$$

The variable parameters in H_r in Eq. (A10) include:

r_{ss} = 1 in steady state equilibrium;

r_E is the shedding rate enhancement factor relative to E_{p0} for an activity with a certain degree of vocalization and physical intensity;

r_B is the relative breathing rate enhancement factor (vs B_0) for the activity of a susceptible person with a certain physical intensity and for a certain age group;

f_e and f_i are the penetration efficiency of virus-carrying particles through masks or face coverings for exhalation and inhalation, respectively;

D is the duration of the exposure in (h);

V is the volume of the space (m^3);

ACH_{tot} is the total removal rate of airborne pathogens including ACH_{vent} and ACH_{UV}.

Substituting Eq. A14 for Hr into Eq. A13:

$PAX_{Flight,inf} =$

$$N_{PAX}{}^2 \times \%_{Pop,ill,day} \times \%_{fly} \times E_{p0} \times B_o \times \frac{r_{ss} \times r_E \times r_B \times f_e \times f_i \times D}{V \times ACH_{tot}} \tag{A15}$$

The shedding and breathing rate enhancement factors, r_B and r_E, quantify the higher rates of shedding and inhaling for infected and susceptible individuals based on their level of vocalization and physical activity.

The enhancement factors, r_B and r_E, are excerpted in Tables **13** and **14**, respectively, below from Peng, et al.[39], and the references therein.

Table 13. Relative breathing rate enhancement factor, r_B.

(a)

Activity		Relative quanta emission rate factor
Physical intensity	Vocalization	
Resting	Oral breathing	1
	Speaking	4.7
	Loudly speaking	30.3
Standing	Oral breathing	1.2
	Speaking	5.7
	Loudly speaking	32.6
Light exercise	Oral breathing	2.8
	Speaking	13.2
	Loudly speaking	85
Moderate exercise	Oral breathing	4.3
	Speaking	20.4
	Loudly speaking	132
Heavy exercise	Oral breathing	6.8
	Speaking	31.6
	Loudly speaking	204

Table 14. Shedding rate enhancement factor, r_E.

(b)

Age group (year)	Activity level				
	Sleep or nap	Sedentary /passive	Light intensity	Moderate intensity	High intensity
<1	0.63	0.64	1.6	2.9	5.4
1 - <2	0.94	1.0	2.5	4.4	7.9
2 - <3	0.96	1.0	2.5	4.4	8.1
3 - <6	0.90	0.94	2.3	4.4	7.7
6 - <11	0.94	1.0	2.3	4.6	8.7
11 - <16	1.0	1.1	2.7	5.2	10
16 - <21	1.0	1.1	2.5	5.4	10
21 - <31	0.90	0.88	2.5	5.4	10
31 - <41	1.0	0.89	2.5	5.6	10
41 - <51	1.0	1.0	2.7	5.8	11
51 - <61	1.1	1.0	2.7	6.0	11
61 - <71	1.1	1.0	2.5	5.4	9.8
71 - <81	1.1	1.0	2.5	5.2	9.8
≥81	1.1	1.0	2.5	5.2	10
Average	1.0	1.0	2.4	5.0	9

The intrinsic factors E_{p0} and B_0, are the baseline rates of shedding virus and inhaling virus, for infected and susceptible individuals, respectively, who are sedentary and not vocalizing (talking, singing, coughing, sneezing, etc.):

E_{p0}, the quanta shedding rate of an infectious person resting and only orally breathing (no vocalization), which accounts for the amount of virus shedded, the infectivity of each virus shed, and the susceptibility of the person who became infected, for a particular airborne pathogen;

B_0, the average volumetric breathing rate (m^3/h) of a sedentary susceptible person (under the assumption of the same size of all age groups). It is reliably estimated in the literature to be ~ 0.288 m^3/h.

Considering the typical activities of passengers and crew aboard an aircraft, physical activity might range from resting to standing to light exercise (walking the aisle). Vocalization levels are typically above the range in quieter non-aircraft settings and might range from above the speaking level up to the loudly speaking level. The levels will all generally be further enhanced during boarding and deplaning.

Conservative values for r_B and r_E, 2.0 and 1.5 respectively, will be assumed in the following calculations. Note that if any single infectious individual were to be speaking loudly for most of the flight, then these enhancement values could be ~ 10 times higher, and the resulting risk of infection also approximately 10 times higher. It's not unreasonable to expect that on any given flight such an individual might be aboard, and that a pragmatic (not conservative as is this estimate) estimate of risk should account for that finite probability.

Further, recent observations aboard domestic flights suggests that fewer than 10% of passengers and crew are wearing masks, and they are more often surgical masks, which are about 50% effective, rather than N95 masks which are 90-95% effective. Therefore, the penetration efficiency of virus-carrying particles through masks may be taken to be 0.95 for both f_e and f_i., ***inferring that 10% of passengers are wearing masks that are 50% effective***.

Substitution into Eq. (A15) of the above assumed values, as follows:

$r_{ss} = 1$ $r_E = 1.5$; $r_B = 2.0$; $B_0 = 0.288$ m³/h; f_e and $f_i = 0.95$

results in the number of passengers who will probably be infected on any given flight, $PAX_{Flight,Inf}$

$$PAX_{Flight,inf} = N_{PAX}{}^2 \times P_{PAX,ill} \times \%_{Pop,ill,day} \times \%_{fly} \times E_{p0} \times$$

$$\frac{0.288 \times 1.0 \times 1.5 \times 2.0 \times 0.95^2 \times D}{V \times ACH_{tot}} = \%_{Pop,ill,day} \times \%_{fly} \times E_{p0} \times N_{PAX}{}^2 \frac{0.78 \times D}{V \times ACH_{tot}} \qquad (A16)$$

In Eq. A16, the first 3 parameters are determined by the pathogen of interest, while last 4 parameters are determined by the aircraft and the flight parameters.

We can select a typical aircraft and flight parameters as follows:

Boeing 737 cabin with dimensions: L = 30.0 m; W = 3.5 m; H = 2.2 m;

with 189 maximum passengers, and N = 162 typical passengers;

ventilation rate providing ACH_{tot} = 30/h.[16]

The interior volume of the cabin may be estimated from the cross-section drawing below of the cabin interior of a Boeing 737-200 (**Fig. 2**) which shows the nominal 3.5 m width and 2.2 m height. A simple estimate of the volume of air in the cabin could be obtained by assuming a rectangular cross-section of 3.5 m x 2.2 m (7.7 m²) along the 30.0 m length, resulting in V = 231 m³. But a more accurate estimate is obtained by omitting the volume of the overhead compartments, so that the cross-section is 3.5 x 1.58 +1.16 x 0.62 = 6.24 m², resulting in V = 184 m³.
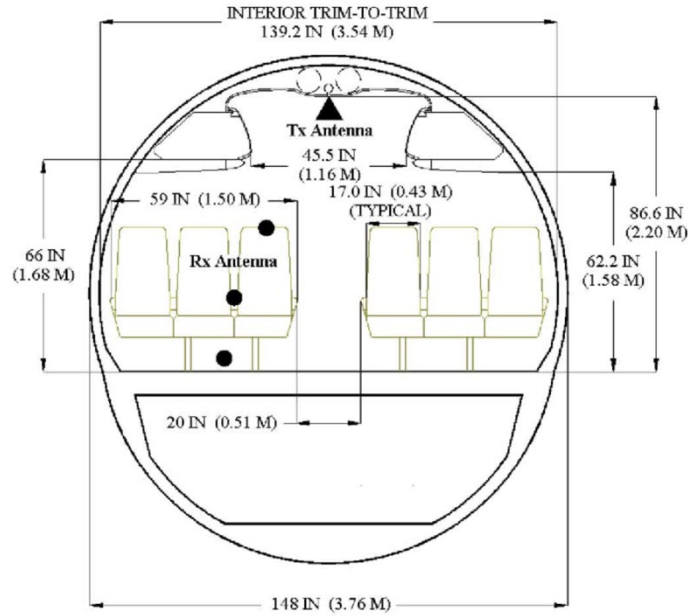
Figure 2. Cabin interior of a Boeing 737-200.[13]

The average US domestic flight time is about D = 2.5 hours.[35]

The average time that a passenger is in the aircraft on the ground includes: 30 minutes boarding (est.); 17 minutes taxi out; nine minutes to taxi in; 20 minutes to deplane (est.) for a total of 76 minutes ~ 1.25 hours on the ground. We'll round this down from 76 minutes to **60 minutes, to be conservative.**[54]

Evaluated for a 2.5-hour flight aboard a Boeing 737, with 30 ACH ventilation, from Eq. (A16):

$$PAX_{Flight,inf} = \%_{Pop,ill,day} \times \%_{fly} \times E_{p0} \times N_{PAX}^2 \frac{0.78 \times D}{V \times ACH_{tot}} =$$

$$\%_{Pop,ill,day} \times \%_{fly} \times E_{p0} \times 162^2 \times \frac{0.78 \times 2.5}{184 \times 30} = 9.27 \times \%_{Pop,ill,day} \times \%_{fly} \times E_{p0} \qquad (A17)$$

In order to evaluate the total number of annual infections transmitted aboard aircraft, we need to consider not just the 162 passengers on an average Boeing 737 flight, but rather the average 106 passengers on the roughly 10,000,000 annual flights. A good assumption is that the pax density on other commercial aircraft is comparable to that on a Boeing 737, and that the ventilation has a comparable 30 ACH.

The average annual number of Passengers on US Airlines is 798,000,000 from **Table 3** of section 2.1.2.1. To prorate the number of passengers who will probably become infected on any given 2.5 hour flight aboard a Boeing 737, it's fair to estimate that all of the 798,000,000 annual passengers all flew aboard a Boeing 737 with 162 passengers aboard, which would require 798,000,000/106 = 7,530,000 flights, $N_{flights,ann}$. This is, of course, a bit lower than the roughly 10,000,000 annual flights reported by the FAA since the average aircraft may be smaller than a 737.

Then the total number of passengers, $PAX_{ann,inf}$, who will probably become infected annually aboard US commercial aircraft is given by:

$$PAX_{ann,inf} = PAX_{Flight,inf} \times N_{flights,ann} = 9.27 \times 7{,}530{,}000 \times \%_{Pop,ill,day} \times \%_{fly} \times E_{p0} =$$

$$69{,}800{,}000 \times \%_{Pop,ill,day} \times \%_{fly} \times E_{p0} \qquad (A18)$$

The total annual number of passengers, $PAX_{ann,deaths}$, who will probably die annually due to transmission of an infectious disease aboard US commercial aircraft is then determined by the mortality rate, M, for the disease of interest:

$$PAX_{ann,deaths} = M \times PAX_{ann,inf} =$$

$$69{,}800{,}000 \times \%_{Pop,ill,day} \times \%_{fly} \times E_{p0} \times M \qquad (A19)$$

Equations A18 and A19 apply to the US annual average infections and deaths across all commercial aircraft, for an arbitrary airborne pathogen, assuming a 2.5 hour cruise period of flight with 30 ACH ventilation.

Rather than using the demographically weighted statistics from the Top-Down Methodology, simpler age-independent infectiousness and mortality rates will be assumed throughout the flying public in the Bottoms-Up Wells-Riley Model. This maintains independence of the input assumptions between the two methodologies.

2.3.1. Residual risk due to <u>Influenza A</u> using a Bottoms-up Wells-Riley formalism

Now we can estimate the annual number of passengers who will probably be infected by inflight transmission of Influenza A, and how many will probably die, by inserting the appropriate values for Influenza A into Equations A18 and A19.
The average number of Annual Symptomatic Influenza A Illnesses in the US from 2010 through 2019 = 28,300,000[10], or 77,500 new cases daily. From section 2.1.2.1, influenza is contagious for 5 days on average.
With an average 5 days of infectiousness, then an average of 5 * 77,500 = 387,500 in the US population are infectious with SARS-CoV-2 on any given day. That amounts to an infectious rate in the population of

$$\%_{Pop,ill,day} = \frac{77{,}500 \times 5}{330{,}000{,}000} = 0.117\%$$

The parameter E_{p0}, that depends on the pathogen, is found equal to 18.4 quanta/h for SARS-CoV-2, and approximately equal to 4 quanta/h for Influenza A, inferred from **Fig. 1** of Peng, et al. work.[39] The ratio of E_{p0} of 18.4/4 ~ 4 implies that the value for P_{indiv} (i.e., AR) should be approximately four times higher for SARS-CoV-2 than for Influenza A. That ratio of AR as provided in 2023 Rafferty is 1.17%/0.5% or about two times higher. Considering the wide range (greater than 10) of possible values for r_B and r_E, this two-fold difference may be interpreted as good agreement, providing some confidence in the accuracy of Eq. (A17).

The annual number of passengers who will probably become infected onboard by Influenza A, from Eq. A18 is

$$PAX_{Flight,inf} = 69,800,000 \times 0.117\% \times 50\% \times 4 = 163,332 \qquad (A20)$$

This is 3x lower than the Top-down estimate from section 2.1.2.1, which is 473,814. This is a fairly good agreement, considering that the two approaches are nearly independent of each other. Possible sources of the higher estimate from the present Wells-Riley formalism include:

- The 3.0 x enhancement of breathing rates due to talking and activity level of the passengers might be higher;
- The value $B_0 = 4$ quanta/h is not well known for Influenza A, and may well be higher.

The annual mortality in the US due to Influenza A is 34,700, so the average mortality rate is 34,7000/28,300,000 = 0.12%
[https://www.cdc.gov/flu/about/burden/index.html]

From Eq. A19, the total annual number of passengers, who will probably die annually due to transmission of Influenza A aboard US commercial aircraft while cruising is

$$PAX_{ann,deaths} = M \times PAX_{ann,inf} = 0.12\% \times 163,332 = 196 \qquad (A21)$$

Repeating the above calculations for the 1-hour time on the ground, with 15 ACH ventilation, another 80% (156) deaths accrue annually due to transmission of Influenza A aboard US commercial aircraft while the aircraft is on the ground with passengers aboard.

Combining the cruise and ground portions of each flight, the total annual number of passengers who will probably die annually due to transmission of Influenza A aboard US commercial aircraft is

$$PAX_{ann,deaths} = 196 + 156 = 352 \qquad (A22)$$

Unlike the Top-down methodology of section 2.1.2.1, the present Wells-Riley formalism makes no assumption regarding secondary infections and deaths in the general population who are infected by those who were infected inflight. In section 2.1.2.1, the annual deaths including those from secondary infections in the general population who were infected from the primary infected passengers was higher, at 599.

In total **352 deaths/year are due to transmission of Influenza A aboard US commercial aircraft.**

2.3.2. Residual risk due to <u>SARS-CoV-2</u> using a Bottoms-up Wells-Riley formalism

Only a few of the variables in the calculations for Risk of Influenza A Infection in the above section need to be modified for the Risk of SARS-CoV-2 Infection: E_{p0}; % of passengers who are infectious; and the mortality rate.

By fitting epidemiological data from 12 well-documented outbreaks of SARS-CoV-2 as presented in Peng (2022), where P_{indiv}, D, V and ACH_{tot} were documented, the best-fit to the data established that $E_{p0} = 18.6$ quanta/h for SARS-CoV-2, which is ~ 4x higher than that for Influenza A.

The COVID-19 mortality rate in the US for the 12 months ending in March 2023, and also for the 20-month period Feb'20 through Sep'21, is about 1.0%.[55]

For the 20-month period Feb'20 through Sep'21, there were approximately 71,100 daily average new cases of COVID-19, and for the 12 months ending in March 2023, there were approximately 65,700 daily average new cases. Therefore, the two periods may both be estimated by assuming 68,400 daily new cases, and 1% mortality rate.

With an average 5 days of infectiousness, then an average of 5 * 68,400 = 342,000 in the US population are infectious with SARS-CoV-2 on any given day. That amounts to an infectious rate in the population of

$$\%_{Pop,ill,day} = \frac{68,400 \times 5}{330,000,000} = 0.104\%$$

And again, the % of passengers who elect to fly while infectious is %fly = 50%. Substituting the above values for COVID-19 into Eq. A18, the total number of passengers, $PAX_{ann,inf}$, who probably became infected with COVID-19 annually while cruising aboard US commercial aircraft during the high-pandemic range of **February 2020 through September 2021, and for the 12 months ending in March 2023,** is

$$PAX_{ann,inf} = 69,800,000 \times 0.104\% \times 50\% \times 4 = 675,106 \qquad (A23)$$

Substituting the 1% mortality for COVID-19 into Eq. A19, the total number of passengers, $PAX_{ann,deaths}$, who probably died due to becoming infected with COVID-19 annually while cruising during the **high-pandemic range of February 2020 through September 2021, and for the 12 months ending in March 2023,** aboard US commercial aircraft is

$$PAX_{ann,deaths} = M \times PAX_{ann,inf} = 1\% \times 675,106 = 6,751 \qquad (A24)$$

As with Influenza A, there are an **additional 80% deaths resulting from the average 60 minutes on the ground with 15 ACH ventilation**, adding 5,400, for a total of **12,151**. As with Influenza A, this is ~2x higher than the Top-down estimate for Secondary deaths from section 2.1.3.1, which is 6,652. Again, this is fairly good agreement, considering that the two approaches are nearly independent of each other, and accounting for the possible sources of the higher estimate from the present Wells-Riley formalism mentioned above relative to Eq. A20.

The results for Infections, Deaths and Economic Burden from both methodologies for both diseases, Influenza A and COVID-19, are summarized in Table 15 below.

Table 15. Infections, Deaths and Economic Burden from both methodologies for both diseases, influenza A and COVID-19.

	Top-Down Epidemiological/Demographic Methodology						Bottoms-Up Wells-Riley Model		
	Analysis Period	Type of Case	Infections	Deaths	Economic Burden ($ B)		Analysis Period	Infections	Deaths
					Total	Medical			
Influenza A	2010 - 2019	Primary	473,814	38	1.6	0.3	4/22 - 3/23, i.e., ongoing	163,332	352
		Secondary	473,814	599				-	-
COVID-19	2/20 - 9/21	Primary	1,058,334	2,068	204	6.1		974,852	12,151
		Secondary	1,058,334	6,652				-	-
Totals			3,064,296	**9,357**	206	6.4		1,138,184	**12,503**

In summary, the annual deaths/year due to transmission of <u>Influenza A</u> aboard US commercial aircraft based on data from 2010 - 2019 is:
- **599** using the "Top-down" methodology based on data from Feb'20 through Sep'21;
- **352** using the "Bottoms-up" Wells-Riley methodology based on data from Mar'22 through Mar'23.

In summary, the annual deaths/year due to transmission of <u>SARS-CoV-2</u> aboard US commercial aircraft is:
- **8,720** using the "Top-down" methodology based on data from Feb'20 through Sep'21;
- **12,151** using the "Bottoms-up" Wells-Riley methodology based on data from Feb'20 through Sep'21, as well as for the 12 months ending in March 2023

Given the nearly independent approaches of the Top-down and Bottoms-up approaches, we might reasonably expect the results between the two to agree within a range no better than ~ 2 – 5x. Furthermore, in order to determine the Risk:Benefit of the application of UV-C to mitigate these disease burdens, or to comprehend the magnitude of the burden, this ~ 2–5x range of uncertainty is not significant. It's therefore reasonable to express a best estimate of these results, approximately as follows.

There is an expected ongoing annual average of ~ 10,000 for the two diseases combined.

Even as the COVID-19 pandemic becomes endemic, with maybe ~ 50,000 deaths/year (comparable to Influenza A) the combined annual deaths/year due to transmission of SARS-CoV-2 and Influenza A aboard US commercial aircraft will still be ~ 2,000 or more. Further, infections and deaths due to inflight transmission of other airborne diseases in the US, e.g., pneumonia, RSV, and others is not negligible.

Of even greater importance than the waning endemic COVID-19, the "next" pandemic could be greatly mitigated by having UV-C operational in advance, as demonstrated in the next section.

3. **Efficacy of UV-C as applied by the Device**

   3.1. **Define the disinfection efficacy in air for ventilation in terms of Air Changes per Hour from peer-reviewed references.**

The standard metric used to quantify air disinfection via ventilation or air filtration is the Air Exchange Rate (AER) measured in air changes per hour (ACH), which is the total volume of air that flows through a room in 1 hour divided by the room volume:

$$ACH\ (h^{-1}) = \frac{Q\ \left(\frac{m^3}{h}\right)}{V\ (m^3)} \tag{A25}$$

where:

Q (m³/h) is the air volume (m³) that flows a room in one hour,
V is the volume (m³) of the room.[49]

For example, if the volume of an aircraft cabin is 100 m³, and the total volume of air that is forced to flow through the cabin by the ventilation system in one hour is 1000 m³, then the AER is 10 ACH.

Traditional air cleaning technology used in aircraft includes the introduction of outside air, and the filtering of recirculated air by the cabin ventilation system. Both the fresh outside air, and the recirculated filtered air contribute to the ACH.

3.2. Equations for disinfection efficacy in air for UV in terms of equivalent Air Changes per Hour, ACH$_{eq}$, as a function of k and D to compare with ACH for ventilation in the aircraft cabin

The standard metric used to quantify an environmental control other than ventilation is equivalent air changes per hour (ACH$_{eq}$ or eACH), which quantifies the ability of an environmental control (e.g., UV) to kill or inactivate an airborne microorganism at the same rate as mechanical ventilation physically removes the airborne microorganism from a space, as measured in ACH. ACH$_{eq}$ is a measure of the UV efficacy that can be obtained using decay model experimental conditions in a well-mixed space. The ACH$_{eq}$ for different microorganisms will vary according to the relative susceptibility of the target pathogen to the wavelength of UV that is applied.[49]

Under ideal conditions in a room where droplet nuclei (exhaled respiratory particles) are released at a single point in time, mechanical room ventilation reduces the number of droplet nuclei in the room in a transient logarithmic fashion when plotted against time. In the absence of mechanisms to introduce new pathogens into an indoor space, and assuming uniform spatial distribution of pathogens throughout the space (i.e., well-mixed air), the concentration of pathogens in air will decay vs. time due to several different mechanisms.[5,19,29]

$$n(t) = n_0\ e^{-R \times t} \tag{A26}$$

The pathogen removal rate, R, is given by

$$R = ACH_{vent} + ACH_{UV} + ACH_{other} + \kappa + \lambda \tag{A27}$$

where:

t = time (h),
n = virus concentration (quanta/m³), where a quantum is defined as the dose of airborne droplet nuclei required to infect a susceptible person,
n_0 = initial virus quanta/m³ at t = 0,
ACH$_{xx}$ = inactivation rate (h⁻¹) from an air disinfection system, such as ventilation, filtration, UV, or other inactivation mechanism,
κ = natural viral inactivation rate = 0.63 h⁻¹ for SARS-CoV-2 in still air at 25 °C [18]
and λ = deposition rate (h⁻¹) onto surfaces due to gravitational settling and surface adsorption.

Studies by Miller's and Kujundzic's groups[27,32] examined the relationship between an upper-room UVGI system, portable air cleaners, and ventilation rates of 0 and 6 ACH and found that, as long as the air was well mixed, the particle removal rates of the three systems were additive.[49]

Note that one air change does not imply that 100 % of the air in the space has been replaced, rather it means that 63 % $(1 - e^{-1})$ of the air in the space has been replaced, assuming a well-mixed space. If the pathogen removal rate (R) is 1 h^{-1}, the airborne viral concentration is reduced by 63 % after one hour and 86 % after two hours. Similarly, it is reduced by 95% and 98% after three and four hours respectively. In this formalism, ACH_{eq} contributes to the total virus removal rate, R, in the same way as the other virus-removal mechanisms, so that UV inactivation may be expressed by an ACH_{eq} value for direct comparison with the other virus-removal system. In this way, any addition to R from the ACH_{eq} of a UV disinfection system contributes to a multilayered infection-control strategy.

Note that the sum of natural decay, κ, and settling, λ, is ~ 1 ACH_{eq} for SARS-CoV-2. If a UV system is designed to enhance the removal of pathogens significantly beyond the rate of natural removal mechanisms, i.e., $ACH_{eq} \gg 1$, then for simplicity, the natural removal mechanisms, κ and λ, may be ignored as components of ACH_{eq} in Eq. (A4). Also ignoring contributions from ACH_{other}, and considering only the air disinfection contributions from ventilation and UV, Eq. (A26) simplifies to

$$n(t) = n_0\, e^{-(ACH_{vent}+ACH_{UV}) \times t} \tag{A28}$$

Therefore, the total equivalent AER in an environment having both traditional ventilation and UV as the only supplemental environmental control is approximately the sum from ventilation and UV:

$$R = ACH_{total} = ACH_{vent} + ACH_{UV} \tag{A29}$$

Since UV is the only air disinfection process other than ventilation (ACH_{vent}) from this point forward in this analysis, we may use the terms ACH_{eq} and ACH_{UV} interchangeably.

For example, an aircraft ventilation system providing 15 - 30 ACH_{vent} of fresh or filtered air may be supplemented by a UV system that provides an additional 30 ACH_{eq} for a total of 45 - 60 ACH_{total} to the space. Thereby, the rate of total reduction of pathogens in the air will be 2 - 3 times as fast with the combined ventilation and UV vs. with ventilation alone. Although some aircraft ventilation is quoted as high as 35 ACH_{vent}, a typical value of 30 ACH_{vent} will be used in most of the calculations herein.
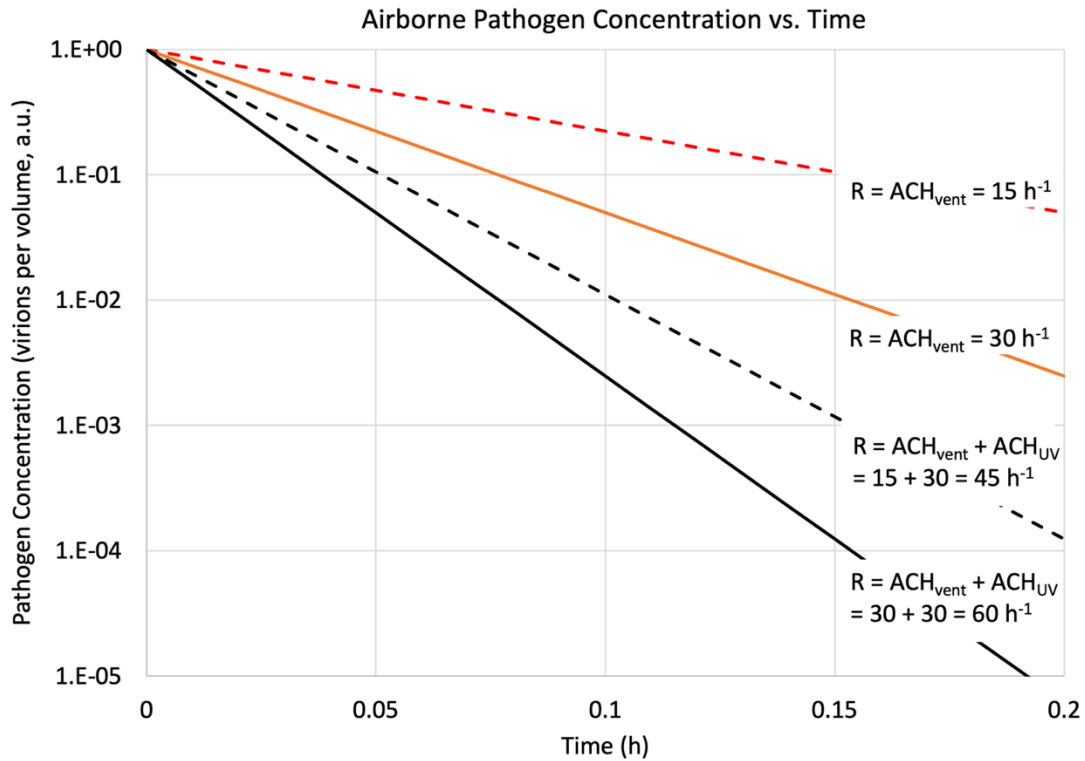
Fig. 3. Pathogen concentration vs. time for ACH_{tot} values of interest for airlines

Pathogen concentration vs. time for ACH values of interest to airlines, plotted from Eq. A25 for various values of R = ACH_{tot}, are shown in **Fig. 3**. The lowest two values, ACH_{vent} = 15 and 30 pertain to the range of values typically found in commercial aircraft. The highest two values represent the addition of a supplemental 30 ACH_{eq} from UV to the two filtered air ventilation rates. In fact, with present technology, 60 − 120 ACH_{eq} may be achieved with UV-C in an aircraft cabin.

Even though the enhancement in ACH due to the UV is only increased by a factor of two to three times, it appears in the exponent of Eq. A28, so that as the pathogen reduction rate is compounded over time the cumulative benefit of the higher ACH_{eq} grows from approximately five times lower concentration after three minutes, approximately 20 times lower at 6 minutes, approximately 100 times lower at nine minutes and approximately 500 times lower at 12 minutes (0.2 hours on the x axis).

Of significant importance, the greatest risk of airborne infection occurs when the pathogen concentration greatly exceeds that required to transmit the disease (e.g., from a super spreader). If the concentration greatly exceeds that required to infect 50% of the occupants, then the reduction in concentration required to reduce the risk of any one occupant being infected may be approximately 100 times greater or more, as will be shown in a later section. Given that this scenario with a very high pathogen concentration and very high level of risk will have an outsized impact on overall risk in airlines than a scenario with lower concentration and lower risk of infection, it is critically important that the baseline ACH of 15-30 from ventilation be supplemented by 2-4 times or more to significantly reduce the likelihood of infections in scenarios with high pathogen concentrations.

When airborne pathogens are introduced into a space at a constant continuous rate R_e by N infectious individuals, the time-dependent pathogen concentration, n(t), is:

$$n(t) = \frac{R_e \times N}{R \times V} + \left(n_0 - \frac{R_e \times N}{R \times V}\right) \times e^{-R \times t} \qquad (A30)$$

assuming well-mixed air and spatial uniformity throughout the space.

where:

        R = pathogen removal rate (h^{-1})
        R_e = emission rate (h^{-1}) of pathogens exhaled per hour per infectious subject,
        N = number of infectious individuals in the space, and
        V = volume of the space (m^3).

There are two distinct methods to quantify the reduction in pathogen concentration due to an air disinfection method in an indoor space.

- One is to quantify the ratio of equilibrium pathogen concentration during a continuous and constant generation of airborne pathogens into the space with and without the subject air disinfection method activated.
- Another is to quantify the transient rate of decay of pathogen concentration following a one-time introduction of pathogens into the space with and without the subject air disinfection method activated.

In equilibrium, at $t = \infty$, for a single infectious individual (N = 1), Eq. A30 simplifies to the equilibrium value of n = n_∞:

$$n_\infty = \frac{R_e}{R \times V} \qquad (A31)$$

The equilibrium pathogen concentration for a given R_e and V with ventilation rate, ACH_{vent}, is:

$$n_{\infty,vent} = \frac{R_e}{ACH_{vent} \times V} \qquad (A32)$$

For comparison, the equilibrium pathogen concentration for a given R_e and V with ventilation rate, ACH_{vent}, supplemented by UV having an inactivation rate ACH_{UV} is:

$$n_{\infty,vent+UV} = \frac{R_e}{(ACH_{vent} + ACH_{UV}) \times V} \qquad (A33)$$

And the ratio of equilibrium pathogen concentrations from Eqs. A29 and A30 is

$$R \equiv \frac{n_{\infty,vent+UV}}{n_{\infty,vent}} = \frac{ACH_{vent}}{ACH_{vent} + ACH_{UV}} = \frac{15}{45} = \frac{1}{3} \qquad (A34)$$

Following the example provided in the previous section, an aircraft ventilation system providing 15 to 30 ACH of fresh or filtered air when supplemented by a UV system that provides an additional 30 ACH_{eq} provides a total 45 to 60 ACH_{eq} to the space.

Therefore, the equilibrium airborne pathogen concentration in Eq. (A34) is reduced by a factor of 2 to 3 with UV-C vs. without it. If the aircraft ventilation system provides only 5-10 ACH, for example when grounded, then the reduction of equilibrium airborne pathogen concentration with and without UV ranges from a factor of 6 to 12 times. If the risk of disease transmission is enhanced due to low ACH_{vent} while a grounded aircraft is occupied, then the supplementation of ACH_{UV} is especially effective in reducing the risk.

It will be quantified later in this document that 30 ACH (for example) of aircraft ventilation reduces the risk of infection to some residual (unmitigated) level, and that the addition of UV in a multi-layered approach makes a significant additional contribution to risk reduction. The benefit of that additional risk reduction afforded by UV disinfection will be quantified in human and financial terms and weighed against the risks due to the incremental UV dose to an individual.

The value for ACH_{eq} (ACH_{UV}) is derived from the application of Eq. A28 for the case when $ACH_{vent} = 0$ such that UV is the only mechanism of pathogen inactivation:

$$n(t) = n_0 \, e^{-ACH_{eq} \times t} \qquad (A35)$$

For UV disinfection of air, the infectious pathogen inactivation rate, ACH_{eq} in Eq. A29, is quantified as $ACH_{eq} = Z \times E$ so that

$$ACH_{eq} \, (h^{-1}) = 3600 \, \left(\frac{s}{h}\right) \times Z \, \left(\frac{m^2}{J}\right) \times E \, (\frac{W}{m^2}) \qquad (A36)$$

where:

Z (m^2/J) is the UV susceptibility constant for the pathogen, sometimes referred to as the UV rate constant, k, (m^2/J)[26]; E is the UV fluence (watts/m^2) assumed to uniform throughout the space; and 1 watt = 1 J/s.

Substituting Eq. A36 into Eq. A35 yields:

$$\frac{n(t)}{n_0} = e^{-3600 \, Z \times E \times t} = e^{-Z \times D} \qquad (A37)$$

where the UV dose is defined in Eq. A37 as D (J/m^2) = 3600 (s/h) x E (J/s-m^2) x t (h).

The dose, D_{90}, at which the initial pathogen concentration, n_0, is reduced by 90% is found by solving Eq. A37 for D_{90}:

$$0.1 = e^{-Z \times D_{90}} \quad \implies \quad D_{90} = \frac{-ln \, ln \, (0.1)}{Z} = \frac{2.30}{Z} \qquad (A38)$$

For example, Z for SARS-CoV in air is 0.377 m^2/J[3,48] so that D_{90} = 6.1 J/m^2. Then, for example, if the uniform UV fluence in the space is 0.01 watts/m^2, then every hour the cumulative UV Dose is 36 J/m^2.

The time, t_{90}, to achieve 90% inactivation of the initial pathogen concentration is defined in Eq. A39:

$$t_{90}(h) = \frac{D_{90} \left(\frac{J}{m^2}\right)}{3600 \times E \left(\frac{W}{m^2}\right)} = \frac{6}{3600 \times 0.01} = \frac{1}{6} \, h \qquad (A39)$$

Equation A39 has been quantified for the case of D_{90} = 6 J/m^2, and E = 0.01 watts/m^2. Resulting in t_{90} being equal to 10 minutes. Therefore, the application of a very low irradiance level of UV-C at 0.01 watts/m^2 inactivates 90% of airborne SARS-CoV-2 virus in only 10 minutes, and 99% in 20 minutes.

3.3. Provide the UV-C susceptibility constant, k, in air for SARS-CoV-2, Influenza, RSV, TB, pneumonia, measles, etc. from peer-reviewed references

Inactivation rates of pathogens subject to 254 nm UV-C have been studied for decades, since 254 nm is the primary wavelength emitted by low-pressure mercury (Hg) lamps, which have been the mainstay light source for disinfection, prior to the recent advent of UV-C LEDs. A database of D_{90} values for hundreds of pathogens in air, water and on surfaces is provided in published manuals and guidelines.[25] A subset, including only viruses and only in air, of Kowalski's dataset is shown below in **Table 16**.

Table 16. Summary of dose data at 254 nm UV-C for 90% inactivation (D_{90}) of viruses in air.[26]

Virus	D_{90} (J/m^2)
Adenovirus	44
Bacteriophage MS2	12
Coliphage T7	8
Coliphage fX-174	3
Coronavirus	6
Coxsackievirus	21
Influenza A	19
Phage phi 6	6
Sindbis virus	22
Vaccinia virus	4
Geometric mean	**10**

A conclusion from **Table 16** is that a typical value for D_{90} for viruses in air at 254 nm is ~ 10 J/m^2. UV-C susceptibility of airborne viruses at wavelengths other than 254 nm has historically been sparse but has been emerging recently from studies using excimer lamps at 222 nm, and UV-C LEDs at a range of UV-C wavelengths above and below 254 nm.[29] The results of one recent study performed in aqueous solution (not airborne) are summarized in **Fig. 4** below.
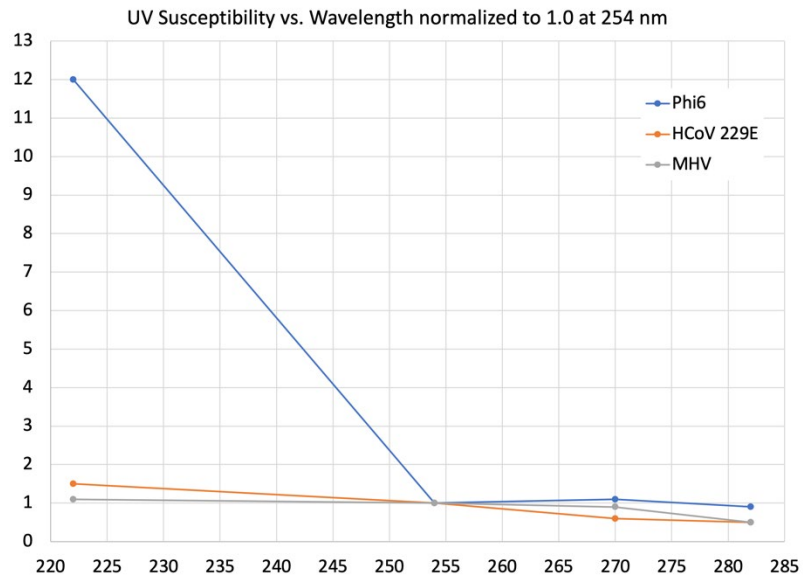
Fig. 4. Susceptibility vs. UV-C Wavelength of three pathogens in aqueous solution.

(The values are relative, normalized to 1.0 at 254 nm.)[29]

From **Fig. 4** it's apparent that there is generally a two-fold decrease in susceptibility from 222 nm to 282 nm, in aqueous solution. The notable exception is the extremely high susceptibility of Phage phi 6 at 222 nm, which is about 12 times higher than that at 254 nm.
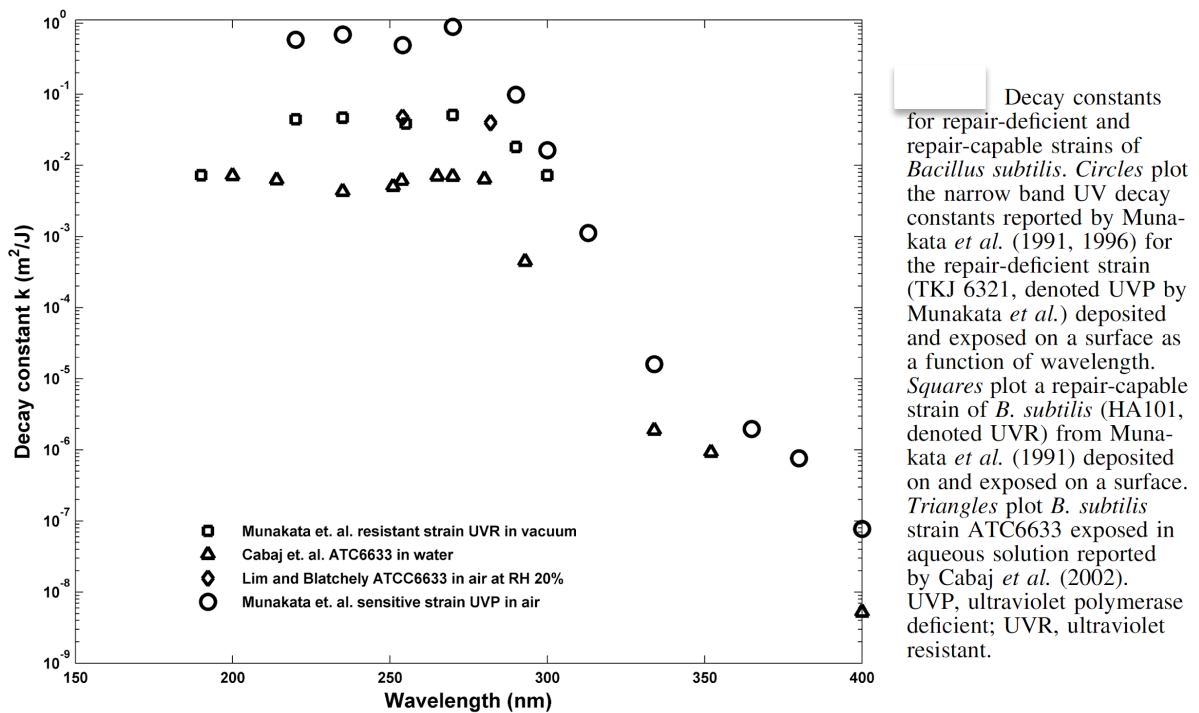
Similar results were reported in 2015 using a tunable UV laser for various pathogens, again in aqueous solution, as shown in **Fig. 5** below.
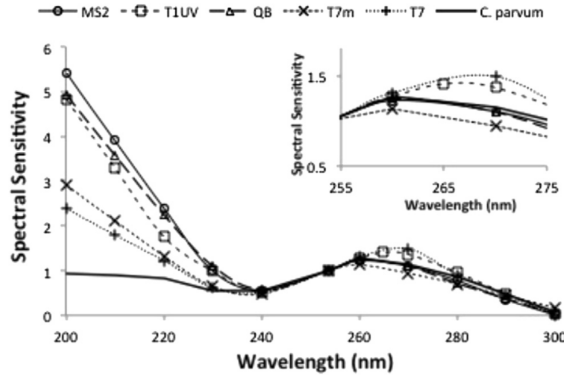
Fig. 5. Relative spectral sensitivity of MS2, T1UV, Q Beta, T7m, and T7 Coliphages and C. *parvum* to UV light from the tunable laser. Note data points at 200 and 300 nm are extrapolated.

Similar results were reported in a 2019 review of four different sources of data for the bacterium, *Bacillus subtilis*, in air, vacuum and water in **Fig. 6** below.[21]

- Y-axis: Decay constant k (m²/J), ranging from 10^{-9} to 10^0
- X-axis: Wavelength (nm), ranging from 150 to 400

Legend:
- □ Munakata et. al. resistant strain UVR in vacuum
- △ Cabaj et. al. ATC6633 in water
- ◇ Lim and Blatchely ATCC6633 in air at RH 20%
- ○ Munakata et. al. sensitive strain UVP in air

Caption text (side panel): Decay constants for repair-deficient and repair-capable strains of *Bacillus subtilis*. *Circles* plot the narrow band UV decay constants reported by Munakata *et al.* (1991, 1996) for the repair-deficient strain (TKJ 6321, denoted UVP by Munakata *et al.*) deposited and exposed on a surface as a function of wavelength. *Squares* plot a repair-capable strain of *B. subtilis* (HA101, denoted UVR) from Munakata *et al.* (1991) deposited on and exposed on a surface. *Triangles* plot *B. subtilis* strain ATC6633 exposed in aqueous solution reported by Cabaj *et al.* (2002). UVP, ultraviolet polymerase deficient; UVR, ultraviolet resistant.

Fig. 6. Pathogen decay constants at 254 nm from four different sources of data for the bacterium, *Bacillus subtilis*, in air, vacuum and water. (Excerpted from Handler. 2019)[21]

The overall conclusion from the 13 different datasets plotted in the three previous figures is that the UV-C susceptibility of several pathogens, including bacteria and viruses, in aqueous and airborne media, tend to peak at around 265 nm, falling off slightly at both shorter and longer wavelengths, then falling off dramatically above about 280 nm, and increasing dramatically (for some pathogens) below 240 nm.

Of relevance to this Appendix, the relatively flat dependence of UV-C susceptibility between 240 and 280 nm infers relative confidence (within about a factor of 2) that susceptibility data from decades of research at 254 nm applies to all wavelengths between 240 and 280 nm.

D_{90} values in Air are listed below in **Table 17** for common pathogens of interest.

Table 17. D_{90} values in air for viruses, bacteria, spores, and fungi of interest in public health, from Ultraviolet germicidal irradiation handbook[26] unless noted otherwise.

Pathogen	Type	D_{90} in Air (J/m²)
SARS-CoV-2	Virus	6[3,48]
Mycobacterium tuberculosis	Bacteria	5
S. aureus (*e.g.*, Methicillin-resistant *S.* aureus, MRSA)	Bacteria	5
Coronavirus (some common colds)	Virus	6[48]
Pathogens responsible for pneumonia: *S. aureus*, *K. pneumoniae*,	Bacteria	6
Escherichia coli	Bacteria	8
Influenza A	Virus	19
Adenovirus	Virus	44
Candida auris	Fungus	~ 100-500
Clostridioides difficile	Bacterial spore	~ 100-500

4.   Explain the unexpectedly high residual risk of airborne infections in aircraft cabins

The results of the calculations herein (i.e., ~10,000 annual deaths due to SARS-CoV-2 and Influenza A transmitted aboard US commercial flights) may be unexpected for the FAA, airline carriers and aircraft manufacturers, perhaps because the detailed calculations, based on statistically significant databases, hadn't been done previously. Statistically significant data, especially for attack rate, hadn't been available until very recently (2023 Rafferty). To provide perspective to these perhaps unexpected results, we need to get beyond the assumption that the 15 to 30 ACH_{vent} on airlines is much higher than in terrestrial settings, and therefore makes the aircraft cabin very safe in comparison.

That assumption breaks down due to the extremely high volume-density of passengers (and crew), e.g., 162 passengers in a volume of 184 m³ = 0.7 people/m³. Compare that with a typical density of 10 people in a crowded conference room (3m x 5m x 8m = 120 m³) of 0.08 people/m³. Due to the 10 times higher volume-density of people in the aircraft cabin vs. the conference room, the aircraft cabin will need 10 times more ventilation to provide comparable clean air to passengers as to people in the conference room. If the conference room has an ACH_{vent} value of six as recommended by the CDC, then the aircraft would need an ACH_{vent} of 60 to be comparably safe as a crowded conference room (where individuals may likely transmit airborne disease).

From Eq. A16, the number of passengers who will probably become infected on any given flight, $PAX_{Flight,Inf}$ is

$$PAX_{Flight,inf} = \%_{Pop,ill,day} \times \%_{fly} \times E_{p0} \times N_{PAX}{}^2 \frac{0.78 \times D}{V \times ACH_{tot}} \qquad (A16)$$

The denominator in Eq. A16 can also be defined as the airflow rate, AF, measured in m³/h or ft³/m (cfm):

$$AF(cfm) \equiv V(m^3) \times \frac{35.3\ ft^3}{m^3} \times \frac{ACH_{vent}(h^{-1})}{60\ (min/h)} = 0.59\ V(m^3) \times ACH_{vent}(h^{-1}) \qquad (A40)$$

So that

$$V(m^3) \times ACH_{vent}(h^{-1}) = 1.70\ AF(cfm)$$

And Eq. A16 can be rewritten as

$$PAX_{Flight,inf} = \%_{Pop,ill,day} \times \%_{fly} \times E_{p0} \times N_{PAX}{}^2 \frac{0.78 \times D}{1.70\ AF(cfm)} =$$

$$\%_{Pop,ill,day} \times \%_{fly} \times E_{p0} \times N_{PAX}{}^2 \times 0.46 \frac{D}{AF(cfm)} \qquad (A41)$$

In Eq. A41, the first 3 parameters are determined by the pathogen of interest, while the last 3 parameters N_{PAX}, AF, and D are determined by the aircraft and the flight parameters.

Those last 3 parameters, which are independent of the choice of pathogen, reveal the relationship for the risk of infection as a function only of the ventilation (or air disinfection) system and the number of occupants:

$$PAX_{Flight,inf} \propto N_{PAX}{}^2 \frac{D}{AF} \propto N_{PAX} \times \frac{N_{PAX}}{AF} \qquad (A42)$$

The scaling relationship of Eq. A42 applies equally to an aircraft cabin as it does to any terrestrial setting (e.g., a classroom or a restaurant).

Eq. A42 reveals the unrecognized challenge for air disinfection inside the aircraft cabin. As asserted by the airline industry, the aircraft ventilation provides a very high 30 ACH_{vent}, which when applied to the volume of the Boeing 737 cabin, provides an impressively high 3345 cfm:

$$AF(cfm) = 0.59\ V(m^3) \times ACH_{vent}(h^{-1}) = 0.59 \times 189 \times 30 = 3257\ cfm$$

Even when the AF for the Boeing 737 is normalized to the number of passengers, it's a remarkably high value:

$$\frac{AF}{N_{PAX}} = \frac{3257}{162} = 20.1\ cfm/PAX$$

This value of 20.1 cfm/PAX compares favorably with the 2019 ASHRAE standard of 15 cfm/person and the recommendations of the WHO (World Health Organization), updated during the COVID-19 pandemic to 21.2 cfm/person for non healthcare facilities, but is far lower than the WHO recommendation of 127 cfm/person for healthcare facilities.[24]

The unrecognized challenge for air disinfection inside the aircraft cabin from Eq. A42 is the additional factor of NPAX further increasing the risk of airborne infection inflight, simply in proportion to the higher probability of having an infectious passenger onboard. Of course, this proportionality of risk to NPAX depends on the assumption that any susceptible passenger may be infected by any infectious passenger regardless of their relative locations inside the cabin, which simply requires that transmission be primarily due to migration of aerosols throughout the cabin, rather than the formerly believed primary transmission by large droplets (the 6-foot rule) or by fomites (surface contamination). This assumption has been firmly supported by several well-documented cases of aerosol transmission of SARS-CoV-2 and Influenza A aboard aircraft.

The degree to which the risk of airborne disease transmission aboard aircraft is due to the excessively high number of passengers relative to the air ventilation of the aircraft cabin is demonstrated in **Table 18** below.

Table 18. Comparison of Air Disinfection parameters in a Boeing 737 cabin vs. Terrestrial settings.

	Setting	Time (hrs)	V (m^3)	N (#)	N/V (#/m3)	ACH (/h)	AF (cfm)	AF/PAX (cfm/person)	$N_{PAX} \times \dfrac{N_{PAX}}{AF}$
737 Aircraft	Boarding & De-planing	1.0	184	162	0.9	15	1628	10	16
	Cruising	2.5				30	3257	20	8
Terrestrial	Restaurant	2	280	20	0.07	3	496	25	0.81
	Conference Room	1	120	10	0.08	4	283	28	0.35
	US Home	4	90	3	0.03	2	106	35	0.08
	Hospital OR	2	72	6	0.08	18	765	127	0.05

Table 18 shows quantitatively why the aircraft cabin carries so much higher risk of airborne disease transmission than any terrestrial setting. Cells highlighted in green indicate favorable quantities, while those in red are extremely unfavorable. The yellow highlight emphasizes the parameter, N_{PAX}^2/AF that is directly proportional to the risk of infection.

The Boeing 737 aircraft cabin (and comparably ventilated and populated cabins) is favorable on the measures of ACH and AF, whereby industry claims assure the public of the safety of cabin air. Indeed, the 30 ACH during cruising exceeds the ACH of every typical terrestrial setting, even the 18 ACH recommended by the WHO during COVID-19 for a hospital operating room. This comparison has been emphasized as evidence of extremely well disinfected air aboard aircraft in several public-facing airline documents such as the 2020 USTRANSCOM report.[45]

However, when the airflow, AF, is normalized to the # of occupants, AF/PAX, the Boeing 737, while comparable, is not as high as any of the terrestrial settings and is ~ 10x lower than the hospital OR. This makes it clear on an intuitive level that the very high ACH in the aircraft cabin is not high enough to overcome the extreme occupancy load in the cabin, relative to typical terrestrial settings. The non-intuitive aspect of the extreme risk of airborne disease transmission aboard aircraft is due to the extra NPAX factor in the right-most column of **Table 18**, N_{PAX}^2/AF, which is the column that compares relative risk of airborne transmission. The aircraft cabin value of N_{PAX}^2/AF is 10–50x higher than the that of a crowded restaurant or conference room, and > 100x higher than that of the hospital OR, for which the USTRANSCOM report claims lower risk in aircraft[45] – an extremely misleading 100x error in its message to the public.

The most egregious aspect of this ~ 10-100x insufficiency in ventilation in the aircraft cabin is that it isn't possible to increase the aircraft cabin ventilation by the necessary ~10x beyond the existing 30 ACH due to energy load, mechanical design, noise and draft discomfort. The ~10x deficit in air disinfection in the aircraft cabin MUST be bridged by a supplemental air disinfection method.

UV-C disinfection is the only technology available that can provide up to 10x supplemental ACH_{eq} safely and economically.

5. **Reduction in risk of infection from the Wells-Riley equation due to various elements in an SMS "Swiss Cheese" model of risk management**

5.1. Extent to which the device as installed effectively mitigates the unmanaged residual risk (i.e., % reduction in risk of infection or death)

As discussed above in the body of this White Paper, Air disinfection by UV irradiance can be quantitatively compared to air disinfection by ventilation by introducing an equivalent ACH (ACH_{eq}) for UV disinfection

$$H_{eq} = 2.30 \times E/D_{90} \tag{A43}$$

where E is the UV irradiance (J/m^2) averaged throughout the volume of the cabin;

D_{90} (J/m^2) is the UV dose required to achieve 90% inactivation of a pathogen in air.

If the irradiance is incident upon occupants, then the Exposure Limit, EL, (also called Threshold Limit Value, TLV) must not be exceeded. For example, D_{90} for SARS-CoV-2 in air is about 6 J/m^2.[48] the irradiance, E, when operated at the allowable EL for 265 nm is 1.2 mW/m^2 = 4.3 J/h-m^2. So, the theoretical ACH_{eq} is

$$ACH_{eq} = 2.30 \; \frac{4.32 \left(\dfrac{J}{h-m^2} \right)}{6 \left(\dfrac{J}{m^2} \right)} = 1.6/h$$

The ACH_{eq} can be enhanced by ~ 5x by tailoring the optical intensity distribution in the space but will generally be limited to ~ 5/h at 265 nm.

The ACH_{eq} can be increased most effectively by utilizing shorter UV-C wavelengths, where the allowed EL rises sharply, especially below 240 nm, as shown in **Figure 8**. New guidelines published by the ACGIH in 2022 are poised to significantly increase the allowed EL below 240 nm, based on decades-old evidence of the greatly reduced penetration depth of UV-C into skin and eyes with decreasing wavelength.

This is the basis of the higher irradiance allowed for 222 nm Kr-Cl excimer lamps relative to today's UV-C LEDs, which are typically limited to > 255 nm. The rapid development of UV-C LEDs indicates a likely availability of cost-effective UV-C LEDs at < 240 nm in < 3 years and < 225 nm in < 10 years.

If the presently available 222 nm excimer lamp emission is used along with the new 2022 ACGIH TLVs which allow 1,279 J/m^2 vs. the 37 J/m^2 allowed with 265 nm LEDs, then the attainable ACH_{eq} with UV irradiated directly into the occupied space, known as DIBEL (Direct Irradiation Below Exposure Limits)[1] will increase from 1.6 ACH_{eq} to 55 ACH_{eq}.

However, the much more efficacious technology available today uses UV-C irradiated into an unoccupied space, for example an unoccupied lavatory or galley or aisle, with reliable and redundant sensors and controls to ensure that the space is unoccupied. Then the irradiance is allowed to greatly exceed the EL, limited only by the output of available UV-C light source and possible long-term degradation of materials under UV-C irradiation. Available UV-C systems today are capable of 30 – 120 ACH_{eq} and will increase by factors of several beyond that in a few years.
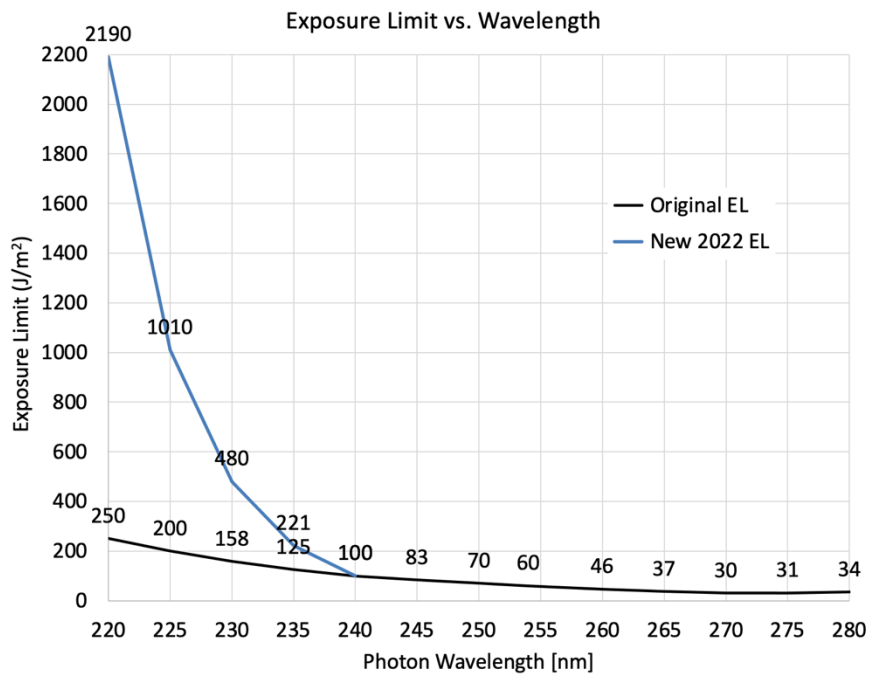
**Fig. 8**. Exposure Limit (J/m2) vs. UV-C wavelength (nm)

When the UV-C irradiation is physically limited to a subset of the space, like the aisle or lavatory, the air in that space may be rapidly disinfected with very high UV-C irradiance, and then that disinfected air (e.g., from the aisle) is beneficially diffused elsewhere by the cabin ventilation, such as to the adjacent occupied seats. In a situation known as well-mixed air, which is typical in any space with high ventilation rates, the air may be roughly assumed to be uniformly disinfected throughout the irradiated volume (e.g., the cabin). This assumption has been validated in numerous Upper-Room UVGI experiments where the intense UV-C irradiates only the space above the heads of occupants, but the entire space is determined to be disinfected by the mixing of the upper room air with the entire room air.[19]

The airflow from ventilation in a typical aircraft cabin is also known to create mixing of the air throughout the cabin (**Fig. 9b**), even though the nominal direction of the airflow might be from the ceiling to the floor (**Fig. 9a**).[51]

In conventional UR-UVGI with mercury lamps, the UV-C has extreme spatial gradients of very high intensity UV-C irradiance in the upper room, which result in diminishing returns of disinfection, effectively wasting a large portion of the UV-C emission. In contrast, the relatively low power and good optical beam control enabled by UV-C LEDs avoids the extreme spatial gradients of very high intensity and the resulting diminishing returns.
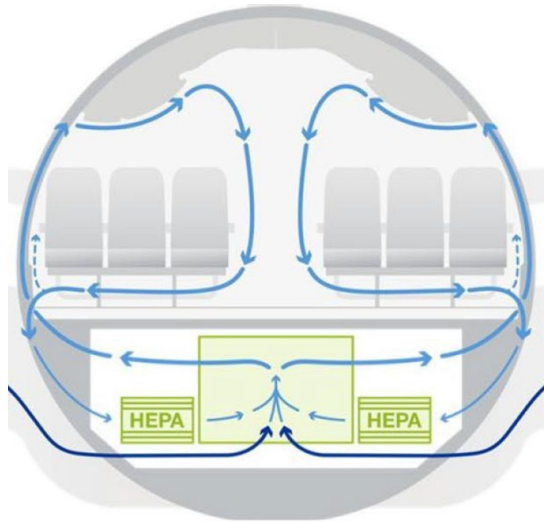
Fig. 9a. Idealized airflow pattern in Boeing 737.
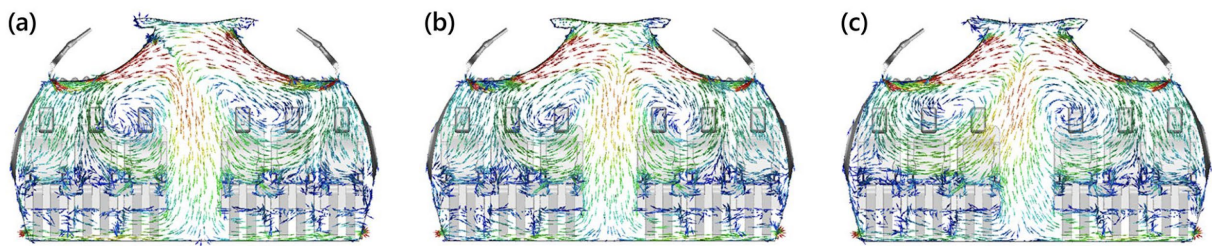
Fig. 9b. Computational Fluid Dynamics Model results for the airflow pattern in Boeing 737 with initial conditions from three different time points to reflect the right-to-left shifts in the counter-rotating cell structure that occur on a periodic basis.

For the case of a UV-C LED Spot Beam (e.g., having a full-width at half-max, FWHM, beam width of 20°) confined to the unoccupied aisle in the cabin, with well-mixed air, and avoiding the diminishing returns of wasted high-intensity zones, the entire emitted UV-C from all of the UV-C LEDs throughout the cabin may be averaged over the entire volume of air in the cabin. In a typical application in a Boeing 737 cabin, having an air volume of about 184 m^3, there may be about 30 UV-C LEDs each emitting about 150 mW (0.15 W) each into Spot beams along the length of the aisle, delivering a total UV-C flux of 4,500 mW. Then the volume-averaged UV-C irradiance in the cabin is 24.5 mW/m^3. In a well-mixed volume of air (e.g., the cabin), a volume-averaged UV-C irradiance of 13-17 mW/m^3 has been shown to result in ACH_{eq} of 16-24/h.[34]

This design rule of equating UV-C power density to expected ACH_{eq} in a well-mixed space, has become a standard guideline for designing UR-UVGI air disinfection systems. We may expect that our delivery of 24.5 mW/m^3 will result in ~ 45 ACH_{eq}.

Thus ACH_{eq} = 30 may be considered to be a baseline example of the expected ACH_{eq} in a commercial aircraft cabin. That baseline may be exceeded by 2x or 4x by increasing the UV-C emitted from each LED, and/or by doubling the number of LEDs in the aisle, so that ACH_{eq} ~ 60 – 120, up to ~ 200 may also be available as options with this technology.

As discussed above in this Appendix, when UV disinfection is added to the aircraft ventilation, the steady state concentration of airborne pathogens is reduced by the factor, R, from Eq. A31, repeated here.

$$R = \frac{ACH_{vent}}{ACH_{vent} + ACH_{UV}} \qquad (A31)$$

Exemplary results of Eq. A31 are presented in **Table 19**. The ACH_{vent} values of 15 and 30 represent a typical range while cruising, and five represents an approximation while on the ground. The ACH_{UV} values are all attainable with present technology, depending on the wavelength of UV and the spacing of the UV emitters throughout the cabin. It indicates that the reduction of residual airborne pathogen concentration left over following removal by the aircraft ventilations system may be further reduced by anywhere from 33% to 89% while cruising, and by up to 96% while grounded.

Table 19. Reduction of Steady-state pathogen concentration vs. combinations of ACH_{vent} and ACH_{UV}.

		ACH_{UV}			
		15	30	60	120
ACH_{vent}	5	0.25	0.14	0.08	0.04
	15	0.50	0.33	0.20	0.11
	30	0.67	0.50	0.33	0.20

The objective of this Section 5.3 is to quantify the extent to which the device as installed effectively mitigates the unmanaged residual risk (i.e., % reduction in risk of infection or death). The formalism outlined in Section 2.3 "Residual risk that is not effectively mitigated by ventilation and masks (i.e., residual risk of infection or death) using a Bottoms-up fundamental Wells-Riley formalism" is taken from Peng, et al. paper,[39] which provides a link to an Excel calculator developed by Prof. Jose L Jimenez & Dr. Zhe Peng, Dept. of Chem. & CIRES, Univ. Colorado-Boulder, along with a team of more than 20 other contributing experts. (Data file available online).[56]

That Excel calculator provides the same results presented here in Section 2.3, and it enables "what if" scenarios by varying any of the input variables found in Eq. A15, repeated here.

$$PAX_{Flight,inf} =$$

$$N_{PAX}{}^2 \times \%_{Pop,ill,day} \times \%_{fly} \times E_{p0} \times B_o \times \frac{r_{ss} \times r_E \times r_B \times f_e \times f_i \times D}{V \times ACH_{tot}} \qquad (A15)$$

Section 2.3 established the baseline scenario resulting in 7,100 annual deaths (during cruising, excluding grounded time) for SARS-CoV-2 for the 12-month period ending in March 2023.

Table 20 below is excerpted from the UC-Boulder Excel calculator, showing only those rows of interest in this study. The yellow highlighted cells are the user inputs that characterize the Boeing 737 cabin, assuming ACH_{vent} = 30, N = 162 passengers, D_{cruise} = 2.5-hour cruising time, 7,530,000 flights/year, 10% mask wearing of 50% effective surgical masks, and the conservative values for r_B and r_E.

The first results column in **Table 20** shows the baseline result of 6,736 annual deaths from transmission of SARS-CoV-2 while cruising. This total of 6,736 is slightly different from the 6,751

calculated herein due to slight non-linearities in the Excel calculator vs. the linear approximation of Eq. A15 of this document. This is the residual risk with all of the mitigation factors in the Swiss Cheese model in place over the period Apr'22 through Mar'23.

Table 20. Results from UC-Boulder Excel calculator for various combinations of UV and mask wearing as infection risk mitigations for COVID-19.

Environmental Parameters for Boeing 737 While Cruising							De-icing done on 3% of flights		
ACH aircraft ventilation (/h)	30	30	30	30	30		5	0	5
UV-C ACH$_{eq}$ (/h)	0	120	0	120	120		0	0	120
ACH$_{tot}$ (/h)	30	150	30	150	150		5	0	125
Masks	actual		Surgical	N95 All	N95 solo				
Duration of event, D (min)	150	150	150	150	150		60	60	60
Number of flights/year	7.53.E+06	7.5.E+06	7.5.E+06	7.5.E+06	7.5.E+06		2.3.E+05	2.3.E+05	2.3.E+05
Parameters related to people and activity									
Total pax, N	162	162	162	162	162		162	162	162
Basic Quanta exhale rate, E (q/h)	18.6	18.6	18.6	18.6	18.6		18.6	18.6	18.6
E enhancement due to activity	3.0	3.0	3.0	3.0	3.0		3.0	3.0	3.0
Exhalation mask efficiency, f$_e$ = f	50%	0%	50%	90%	0%		50%	50%	50%
Inhalation mask efficiency, f$_i$ = f	50%	0%	50%	90%	90%		50%	50%	50%
Fraction of people w/ masks	10%	0%	100%	100%	100%		10%	10%	10%
Parameters related to COVID-19 disease									
Probability of being infective, η$_{inf}$	0.055%	0.055%	0.055%	0.055%	0.055%		0.055%	0.055%	0.055%
Death rate	1.0%	1.0%	1.0%	1.0%	1.0%		1.0%	1.0%	1.0%
# of deaths annually	6,736	1,549	1,870	16	155		984	3,919	50
Reduction in Deaths	-	77%	72%	99.8%	98%				99%

The second results column augments the aircraft ventilation of 30 ACH with 120 ACH$_{eq}$ from the UV-C. As expected, since ACH$_{tot}$ has been increased by 5x above that of the ventilation alone, the # of annual deaths is reduced by 77% (again displaying a slight non-linearity in the formulas used in the Excel calculator).

The third results column augments the aircraft ventilation of 30 ACH with 100% adherence to wearing surgical masks, resulting in a 72% reduction in deaths. Interestingly, this 72% reduction, which requires a reluctant public to comply by 100%, is comparable to the 77% reduction with UV-C that requires no active cooperation from the passengers, imposes no discomfort, and as will be shown later, poses essentially no health risk to crew and passengers.

The fourth results column is the "gold standard" with UV-C and 100% passenger compliance in wearing N95 masks. The resulting 99.8% reduction to only 16 deaths/year provides a realization that we might never achieve 0 deaths/year in the face of deadly airborne diseases.

The fifth results column indicates that even if no other passengers are wearing masks, any given passenger who chooses to wear an N95 mask can reduce their risk of infection and death by 98% if the UV-C system is operating.

The percent reductions in deaths will be the same for the 60-minute ground portion of each flight.

The 6th through 8th columns demonstrate the worst-case scenario for risk of airborne infections aboard the aircraft – when the aircraft is on the ground, being de-iced with little or no ventilation in the cabin, typically at the peak of cold, flu and COVID seasons.
The 6th column assuming that ACH$_{vent}$ = 5 (which is higher than the actual ~ 0 ventilation during de-icing), results in 984 deaths/year due to transmission of SARS-CoV-2 during de-icing. The 7th column assumes the more accurate ACH$_{vent}$ = 0 during de-icing, resulting in 3,919 deaths/year due to transmission of SARS-CoV-2 during those few flights requiring de-icing. This is a tremendous toll from a relatively few flights where de-icing is required. The 8th column indicates that the use of UV-C

during de-icing potentially eliminates 99% of those deaths that are due to the 0 ACH cabin ventilation, reducing the toll to just 50 deaths/year.

While the above **Table 19** pertains to SARS-CoV-2, the % reduction in deaths/year expected from application of UV-C air disinfection is the same for Influenza A, although the absolute values are much lower.

Of course, if ACH_{eq} is < 120, then the % reductions in deaths/year in Table 19 will be lesser. For example, if ACH_{eq} = 30, then the second results column with ventilation = 30 ACH and ACH_{eq} = 30 from the UV-C, the reduction in deaths decreases from 77% to 43%.

The results of **Table 19** above can be visualized in **Figures 10a** and **10b** below, using the pictorial representation of the ICAO Aviation Multi-Layered Disease Defense Strategy (Swiss Cheese Model).
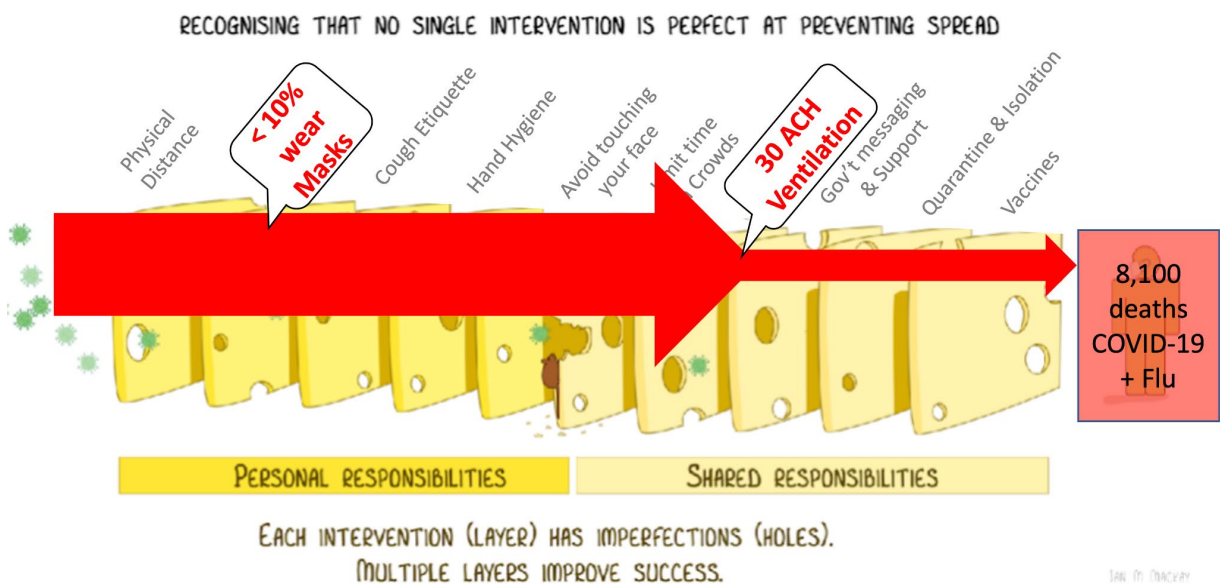
Fig. 10a ICAO Aviation Multi-Layered Disease Defense Strategy.

In Fig. 10a, the broad red arrow from the left indicates an extremely large risk (>> 8,100 deaths) that would accrue without the benefit of the 30 ACH of cabin ventilation. When the broad red arrow passes through the mitigation provided by very-low incidence of mask wearing, the risk is insignificantly abated. But when the broad red arrow encounters the mitigation layer (cheese slice) pertaining to 30 ACH ventilation, the risk is greatly reduced to our present level of unmitigated risk at 8,100 deaths per year due to onboard transmission of airborne diseases (COVID-19 plus Influenza).
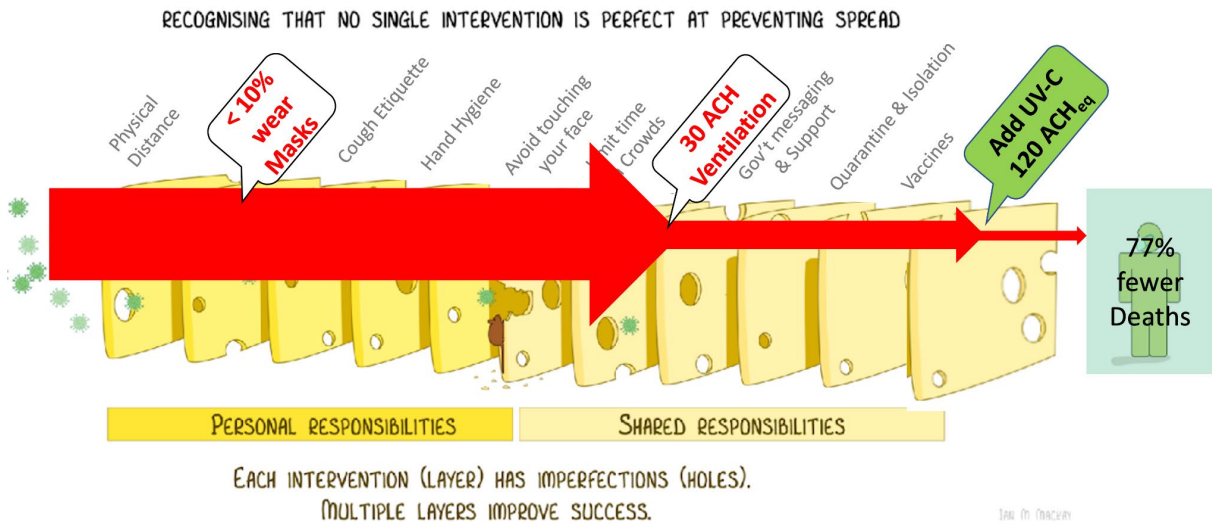
Fig. 10b ICAO Aviation Multi-Layered Disease Defense Strategy (with UV-C air disinfection layer added).

In **Fig. 10b**, the broad red arrow from the left encounters the mitigation layer pertaining to 30 ACH ventilation, reducing the risk to our present level of unmitigated risk at 8,100 deaths per year, and then the contribution of 120 ACH_{eq} from UV-C at the far right further reduces the residual risk by 77%.

Of the estimated 8,000 combined annual deaths/year due to transmission of SARS-CoV-2 and Influenza A aboard US commercial aircraft, approximately 43% - 77% of those deaths may be avoided by supplementing the aircraft ventilation with UV-C providing ACH_{eq} = 30 - 120.

Of the estimated $2.8 B annual US economic burden combined due to transmission Influenza A and $34.3 B due to transmission of SARS-CoV-2 (for 12 months ending March 2023) aboard US commercial aircraft, approximately 43% - 77% of that, or $1.2 – 2.2 B/yr (Influenza A) and $14.8 – 26.5 B/yr (COVID-19) could be saved by supplementing the aircraft ventilation with UV-C providing ACH_{eq} = 30 - 120.

6. Potential safety risks associated with exposure to the radiating device

Repeated exposure to high doses of light of any wavelength of light can pose a risk to humans, particularly to skin and eye tissue. In fact, repeated exposure to high doses of visible or infrared (IR) light, as well as UV light, can pose risks to humans. The allowable Exposure Limit below which harm to eyes and skin is avoided is a strong function of the wavelength of the light. For any given wavelength of light (UV, visible, or IR), it is thus important to define the daily doses below which there is no expectation of photobiological harm from repeated exposure, or exposures below the EL.[1, 47] The low output power, point source optical emission enabling optical beam control, solid-state sensors and controls for UV-C LEDs, and methods for inactivation of pathogens have enabled the development of DIBEL (Direct Irradiation Below Exposure Limits) technology, wherein the UV irradiance is maintained below the allowed EL at all locations in the space that can be occupied.[1] Although DIBEL protocols may be engineered to be essentially risk-free with careful optical design, sensors, and controls, the impact of potential overexposure should nonetheless be considered.[1,26,46,47]

A DIBEL protocol should specify the following:
- wavelength (band or range of wavelengths)
- spatially averaged irradiance in the occupied space
- exposure time, or irradiance schedule over time
- optical distribution (e.g., targeting air volume or surfaces, either the entire space or a subset); and target pathogen(s) and medium.[1]

In the rare event of UV-C overexposure the risk of skin or eye damage may be acute or chronic. Acute damage results from a one-time overexposure that greatly exceeds the allowed EL for an eight-hour period. The damage repairs itself within one to two days and is not cumulative. Those two risks, Erythema and Photokeratitis, are discussed in section 6.2. The chronic risk, that of non-melanoma skin cancer, is discussed in section 6.3, below.

6.2. Erythema and Photokeratitis

The very aspect (phototoxicity) that makes UV-C radiation an effective germicidal agent also is responsible for the unwanted side effects of erythema (reddening of the skin) and photokeratitis ("welder's flash" or "snow-blindness"). Overexposure to this short-wavelength UV radiation can produce these unwanted side effects from a very mild irritation of the skin and eyes to a rather painful case of photokeratitis.

These effects are fortunately transient, as only superficial cells of the eye—the corneal epithelium— and the most superficial layer of the skin—the superficial epidermis— are significantly affected. Normal turnover of these cells soon erases the signs and symptoms of these effects.

Radiant energy in the UV-C band has very shallow penetration depths which account for the very superficial nature of any injury to the skin and eyes from excessive exposure, minimum risk of delayed effects and at the same time the strong absorption by bioaerosols.[46]

6.2.1. Erythema

As the outer (dead tissue) layer of the skin—the stratum corneum—is highly absorbing in the UV-C, only very small traces of incident UV-C penetrate to the germinative (basal) layer of the epidermis.[46]

"The classic studies of Hausser and Vahle showed that with increasing doses of 254 nm radiation above 1 minimal erythema dose (MED), the level of redness hardly increased - even at doses 10-fold above the exposure associated with the just-perceptible redness. This was in sharp contrast to the rapid increase in redness with 313 nm irradiation (UV-B), where severe erythema and blistering occurred at doses only 20 % above those resulting in just perceptible erythema, … This has been interpreted to be related to the penetration depth of the UVR. From these observations, some photodermatologists (…) have argued that UV skin carcinogenesis is not a realistic risk from germicidal (UV-C) lamps, since only a very small amount of radiation from the 254 nm line (that comprises over 90 % of the radiation from a low-pressure mercury discharge lamp) reaches the germinative layer of the epidermis." [22]

In other words, even when the EL is exceeded enough to cause reddening of the skin, a further 10x increase in 254 nm dose hardly increases the level of reddening, indicating that an extreme overdose of 254 nm UV-C well above the EL still produces only minor reddening, with no long-term impact.

6.2.2. Photokeratitis

A radiant exposure of only about 100 J/m^2 at 254 nm will produce photokeratitis and photoconjunctivitis (sometimes referred to as photokeratoconjunctivitis, "welders' flash," "arc eye," or "snowblindness").[2,22,46,47] The surface epithelial cells that are damaged from UV-C exposure are normally sloughed off overnight—certainly within 48 h.[46] This onset of 100 J/m^2 for production of photokeratitis or photoconjunctivitis is ~ 2x higher than the EL = 60 J/m^2 at 254 nm, indicating a significant safety margin built into the EL.

6.3. Non-melanoma skin cancer

CIE report 187 on cancer risks from germicidal lamps has explored in depth the question of the potential for skin cancer (skin carcinogenesis) from ultraviolet C radiation (photocarcinogenesis). This report clearly demonstrates that the risk is exceedingly small.[46] It states "Known side effects of overexposure to UV-C radiation include transient corneal and conjunctival irritation (photo-keratoconjunctivitis) and skin irritation (erythema), which disappear within a 24 – 48 hour period, not currently known to produce lasting biological damage."[22]

The only known long-term incremental risk is that of non-melanoma skin cancer (NMSC) when a person (e.g., crew) is exposed at the maximum allowed Exposure Limit for eight hours per day, five days per year, for 20 years is 0.37% above the risk of an unexposed person.[22]

Annual estimated statistics related to skin cancer in the US are summarized below for NMSC and melanoma.[55,58,59]

NMSC
- 3.6 million cases of Basal cell carcinoma (BCC) and 1.8 million cases of Squamous cell carcinoma (SCC) diagnosed
- The annual cost of treating NMSC is $4.8 billion, so about $900 per case
- One in five Americans will develop skin cancer in their lifetime
- It's thought that about 2,000 people in the US die each year from NMSC

Melanoma
- 186,680 cases diagnosed
- 7,990 deaths
- The annual treatment cost is $3.3 billion

Squamous cell photocarcinogenesis requires the germinative layer of the epidermis to be affected, as that has the long-term "memory" for the skin. The real risk of UV photocarcinogenesis at 254 nm is extremely small, primarily because of the extremely shallow penetration of this wavelength radiation to the basal layer of the epithelium and strong attenuation of the stratum corneum and epidermis are accounted for in the action spectrum for squamous cell carcinogenesis … The penetration to the basal layer of the epidermis becomes an insignificant value at 254 nm.[46,47]

Although the mortality rate from NMSC is extremely low, there is an established correlation (but not causality) between NMSC and later development of melanoma, especially if the NMSC is a squamous cell carcinoma (SCC). So, the burden of deaths and cost of care for NMSC might need to be adjusted for that possibility, although the necessary statistics have not been found for this report.

There were enhanced risks (Hazard Ratios, HR > 1) of other cancers following NMSC (including squamous cell, SCC, and basal cell carcinoma, BCC) as follows:

for all other cancers, HR = 1.40 [95% CI 1.15, 1.71] after BSC and HR = 1.18 [95% CI 0.95, 1.46] after SCC;

for melanoma, HR = 3.28 [95% CI 1.66, 6.51] after BSC and HR = 3.62 [95% CI 1.85, 7.11] after SCC;

for prostate cancer, HR = 1.64 [95% CI 1.10, 2.46] after BSC.

The hazard ratio (HR) is the ratio of the hazard rates corresponding to the conditions characterized by two distinct levels of a treatment variable of interest. The HRs are relative to a baseline of 3584 participants with controls adjusted for age, sex, cigarette smoking history, sun exposure factors and family history of skin cancer. The standardized mortality ratio is the ratio of observed deaths in the study group to expected deaths in the general population.[52]

7. Extent to which the health and safety benefit provided by the UV-C Device outweighs the potential safety risks associated with exposure to the radiating device

7.2. Risk reduction due to UV-C

Of the estimated 8,000 combined annual deaths/year due to transmission of SARS-CoV-2 and Influenza A aboard US commercial aircraft, approximately 43% - 77% of those deaths may be avoided by supplementing the aircraft ventilation with UV-C providing ACHeq = 30 - 120.

Of the estimated $2.8 B annual US economic burden combined due to transmission Influenza A and $34.3 B due to transmission of SARS-CoV-2 (for 12 months ending March 2023) aboard US commercial aircraft, approximately 43% - 77% of that, or $1.2 – 2.2 B/yr (Influenza A) and $14.8 – 26.5 B/yr (COVID-19) could be saved by supplementing the aircraft ventilation with UV-C providing ACHeq = 30 - 120.

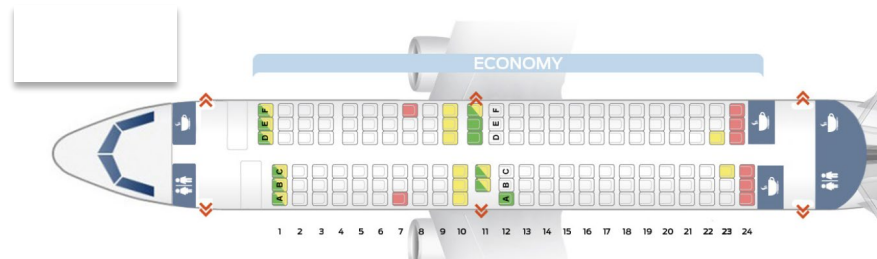### 7.3. Risk associated with exposure to UV-C

According to the Recommended Practice for UV Germicidal Irradiation (UVGI) published by the American National Standards Institute (ANSI) and the Illuminating Engineering Society (IES), ANSI/IES RP-44-21, the current daily safety limit of 254-nm UV-C for 8 hours is 60 J/m², whereas less than ten minutes of summer sun exposure at a UV Index of 10 can deliver the equivalent limiting daily safety dose because of its much more penetrating UV-A and UV-B.

To emphasize this comparison, it must be realized that the UV-C irradiation level in the aircraft cabin is designed to be well below the daily allowed EL pertaining to the wavelength of UV-C applied. For any occupant in the aircraft cabin to experience a daily exposure equal to or exceeding the EL, the sensors and controls of the UV-C disinfection system would have to either be (1) improperly designed, (2) improperly installed, or (3) to have failed during operation. Professional installation, including UV measurements at critical locations throughout the cabin will ensure safety relative to (1) and (2), and the inclusion of triply redundant sensors makes the probability of (3) extremely low. The RP-44-21 statement above is telling us that only in the highly improbable event of an improper installation or
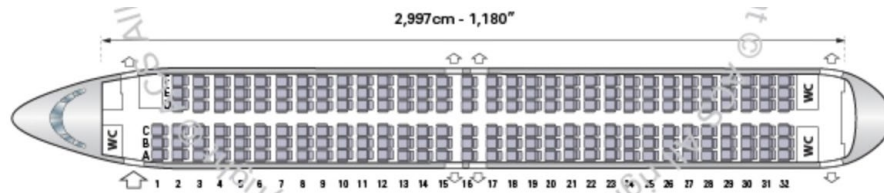
failure of a triply redundant sensor system, will any occupant be at any risk of receiving UV exposure comparable to or exceeding 10 minutes of sun exposure.

The greatest uncertainty in the Risk:Benefit analysis in this report is the quantification of the probability of improper installation of the UV-C system or a failure of the triply-redundant sensors and controls. It's not possible to accurately predict those probabilities even within a factor of 10, whereas every other quantity and statistic in this report is generally known within a factor of about two or less. Thus, the best we can do is to make an order-of-magnitude best estimate of the risk of UV-C overexposure, calculate the risk/benefit ratio, then consider whether the resulting risk/benefit ratio would be significantly affected by modifying the estimated probability of overexposure by one or more orders of magnitude.

A selection of seat maps is shown in **Fig. 11** for various models of Boeing 737, which range from 24 to 37 rows (assume an average 30 rows), with six seats across in most rows. Considering the vertical Spot Beam of UV-C that provides ACH$_{eq}$ of approximately 30 throughout the cabin, each Spot Beam would serve two rows, amounting to 15 Spots along the aisle, plus a Spot Beam for each lavatory (assume two to three laboratories) and one for each Galley area (assuming four galleys), totaling about 22 Spot Beams per aircraft.

https://theflight.info/seat-map-boeing-737-700-southwest-airlines-best-seats-in-plane/

https://www.aircharter.com.br/en/aircraft-guide/group/boeing-usa/boeing-737-400-800-900

https://www.delta.com/us/en/aircraft/boeing/737-900er

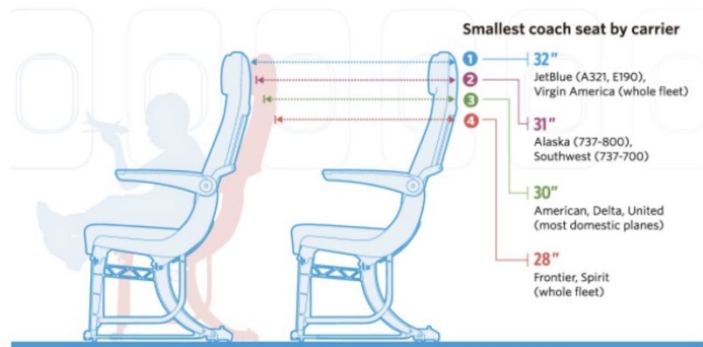**Fig. 11**. Seat maps in typical Boeing 737 aircraft.

Except for the staggered rows of the Southwest layout, each Spot should strategically be placed midway between two adjacent aisles, as shown in **Fig. 12** as circles in the aisle, so as to maximize the distance from the UV-C LED in the ceiling to the armrest on any seat adjacent to the aisle for the geometry of the Spot Beam.

71
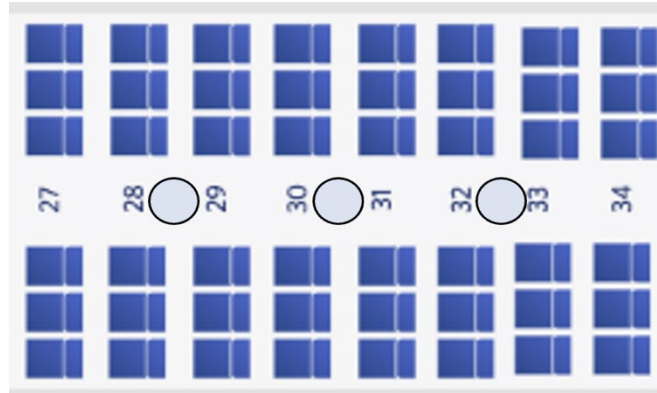
Fig. 12. Spot Beam layout for B737 aircraft.
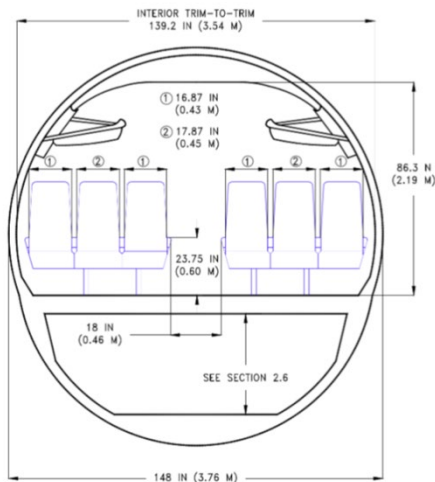
Fig. 13. Cross section of B737[17]   **Fig. 14.** Seat spacing in B737[61]

As shown in **Fig. 13**, the aisle width is 0.6 m, if the UV-C LED in the Spot Beam were mounted directly adjacent to a row, then the lateral distance from the LED to the armrest is 0.3 m and the diameter of the Spot Beam at the height of the armrest would be limited to less than 0.6 m.

In contrast, if the LED is midway along the 0.76 m separation of rows along the aisle, as shown in **Fig. 14**, then the lateral distance between the UV-C LED and the armrest is sqrt $(0.3^2 + 0.38^2)$ = 0.48 m, so that the diameter of the Spot beam may be expanded from 0.6 m to 0.96 m. This relaxed spacing allows for a greater geometric margin of safety between the armrest and the edge of the beam, as well as allowing for a greater UV flux within the beam. Thereby, both safety and efficacy (ACH$_{eq}$) may be enhanced.

The exposure at the outer edge of the armrest is less than half the EL, and the skin or eye of a passenger would have to extend beyond the outer edge of the armrest by greater than four inches for eight hours or more to receive an exposure equal to the EL. However, the sensors and controls are designed to turn the Spot Beam off if an occupant's arm extends beyond the outer edge of the armrest, so that the above scenario where an occupant receives the EL in eight hours actually requires a failure of the sensor/control system.

So, quantifying the probability of an occupant receiving an exposure equal to or exceeding the EL is reduced to estimating the probability that the sensor/control system of the UV-C Puck fails to detect an occupant beyond the outer edge of the armrest.

As a very conservative first estimate, we can assume that 0.01% of all Pucks have a defective sensor/control system which allows for an occupant whose arm extends beyond the armrest by four inches for eight hours to receive a dose equal to the EL.

$$P_{def} \equiv Probability\ of\ a\ defective\ sensor/control\ in\ any\ Puck\ is\ approximately\ 0.01\%$$

In this example, each Puck serves two rows, and a total of 12 passengers, and the four passengers seated in the aisle seats are the only ones at risk of overexposure, thus one third of the passengers served by each Puck are at risk from a defective Puck. Therefore, the risk that a passenger is located adjacent to a defective Puck is 0.003% per passenger, or 1 in 30,000 passengers. However, to receive an overexposure, the probability that a passenger keeps bare skin or eye extended at least four inches beyond the edge of the armrest for eight hours must also be estimated. A conservatively high estimate of such might be about 1% of passengers.

$$P_{extend} \equiv Probability\ a\ PAX\ extends\ eye\ or\ skin\ 4"\ beyond\ armrest\ for\ 8\ hours \sim 1\%$$

Then the probability that a passenger receives a dose equal to or exceeding the EL is

$$P_{>EL} \equiv Probability\ that\ a\ PAX\ exceeds\ EL = \frac{1}{3} \times P_{def} \times P_{extended} \sim 0.00003\%$$

7.4. Quantitatively compare the risk vs. benefit of the UV-C application

7.4.1. Comparison of Risk-Benefit for Acute UV-C over-exposure

From section 3.2.2, the total number of passengers who probably became infected with COVID-19 annually while cruising aboard US commercial aircraft over the past 12 months is 710,000, which is ~ 0.1% of the ~ 800,000,000 annual passengers.

The annual number of passengers who will probably be infected by Influenza A, from Eq. A18 is 3,350,000, which is ~ 0.4% of the ~ 800,000,000 annual passengers, in total approximately 0.5% for the two diseases combined.

In this analysis, the risk of UV-C overexposure is 0.00003% and the risk of contracting disease is 0.5% so that the Benefit:Risk is 15,000:1.

Table 20. Probability of passengers receiving a one-time UV exposure above the EL.

UV-C Risk	P-def	Probability of a defective sensor/control		0.01%
	P-extended	Probability of skin or eye extended 4" beyond edge of armrest		1.00%
	f-aisle	Fraction of passengers in an aisle seat		33%
	P- >EL	Probability that any given passenger exceeds the EL	= P-def x P-extended x f-aisle	3.3E-07
	PAX-Ann	Total Passengers		800,000,000
	PAX-Ann->EL	Total PAX receiving 1-time UV-C dose exceeding EL	= PAX-Ann x P- >EL	267

The 0.00003% risk of acute (one-time) overexposure may (or may not) result in a 1 to 2-day skin or eye irritation, with no long-term effects or risks, compared to the 15,000 x greater risk at 0.5% of contracting COVID-19 or Influenza A that persists for several days to weeks, and has a finite risk of hospitalization or death.

7.4.2. Compare Risk-Benefit for Chronic UV-C over-exposure:

The only known long-term health risk due to chronic, occupational overexposure of UV-C is for Non-Melanoma Skin Cancer (NMSC), which is quantified in the following excerpt from the CIE Technical Report 187.[22]

> *"Using the best available information, a lifetime exposure risk was calculated (see Appendix B) which showed that an accumulated daily exposure to 254 nm radiation at the ACGIH / ICNIRP threshold limit value (TLV) (i.e., 6 mJ·cm^{-2} (3 mJ·cm^{-2} effective), received over eight h) for five days a week, over 20 years, would increase the risk of non-melanoma skin cancer by a factor of about 0.37 %."*

Such long-term exposure is only feasible for the flight attendants (assuming UV-C is not installed in the cockpit). As in the calculations above for acute overexposure, a chronic overexposure can only occur if a UV-C Puck is improperly installed, or the sensor/control system is defective. Improper installation should be avoided by measuring the UV-C output distribution upon installation. A conservatively high probability of a defective sensor/control system in a Puck was estimated above to be 0.01%. If a flight attendant is seated adjacent to a defective Puck on a given flight, then an acute overexposure is a possibility as analyzed above.

However, for a chronic overexposure to occur, that same flight attendant would have to be seated adjacent to a defective Puck (0.01% probability on each flight) AND have skin or eye extended at least four inches beyond the outer edge of the armrest (1% probability) constantly for nearly every flight for 20 years. **This is inconceivable.**

There seems to be virtually no possibility of any individual aboard an aircraft receiving a long-term chronic dose at or above the EL for eight hours per day, five days per week, for 20 years.

There seems to be virtually no scenario for any occupant aboard an aircraft equipped with a UV-C designed below the EL to receive a chronic, occupational dose of UV-C sufficient to increase the risk of non-Melanoma Skin Cancer.

A very unlikely scenario that could result in chronic, occupational overexposure would require that a given flight attendant would be seated in the same seat on the same aircraft in which a defective Puck were allowed to operate without detection and correction of the defect for 20 years, AND have skin or an eye extended at least four inches beyond the outer edge of the armrest (1% probability) constantly for nearly every flight for 20 years. In that extremely unlikely event, a flight attendant with a 20-year flying career would have a 1% x 0.01% = 0.0001% probability of chronic overexposure (1 in

1,000,000 flight attendants who are employed at any given time). The number of flight attendants in the US is about 100,000, of which only 19% have more than 11 years of tenure.

From these statistics, a conservatively high estimate of the number of flight attendants presently on the job who will have at least a 20-year career is about 20,000 or less. Given the above estimate in a very unlikely scenario that any given flight attendant could have a 1 in 1,000,000 chance of experiencing a chronic, occupational (20-year) overexposure, then there is only about a 2% chance (20,000/1,000,000) of even one flight attendant employed today might receive a chronic overexposure over the next 20 years. That 1/50th of a single flight attendant who accumulates a chronic overexposure 20 plus years from now would then have a 0.37% increased likelihood of having an NMSC.

The lifetime risk of contracting NMSC for any American is 20%.[58] Then the incremental risk of contracting NMSC from the UV-C overexposure for that 1/50th of a flight attendant is 1/50 x 20% x 0.37% or 0.0016%.

In a very unlikely scenario that could result in chronic, occupational overexposure to flight attendants, the risk of even one flight attendant contracting NMSC over a 20-year period from UV-C overexposure aboard the aircraft is 0.0016%. That 0.0016% of an NMSC case is highly treatable, at a cost of about $900 per treatment, or <<< $1 total economic burden, with virtually no probability of even one death.

Conclusion to Risk-Benefit analysis.

By installing UV-C air disinfection aboard all US commercial aircraft, we can expect to avoid about half of the estimated 8,000 annual deaths in the US due to transmission of Influenza A and COVID-19 aboard aircraft, or ~ 10 avoided deaths per day.

The risk incurred in order to avoid about 4,000 annual deaths is the remote (conservatively estimated) risk of 267 passengers receiving a one-time acute overexposure resulting in one to two days of skin or eye irritation, with no long-term, chronic health risk.

The conservatively underestimated benefit of saving ~ 10 lives every day must be weighed against the conservatively overestimated risk of ~ 1 passenger per day having 1-2 days of skin or eye irritation. Whereas the estimated benefit is based on statistically sound data, and not susceptible to large errors, the estimated risk of UV-C overexposure has been conservatively overestimated, perhaps by 100 times or more. Therefore, it may be that only ~ 1 person per year might experience 1-2 days of skin or eye irritation in order to save ~ 4,000 lives.

The risk-benefit of economic burden results in >> 100% return on investment (ROI) annually, every year following a one-time investment of ~ $1B to install UV-C in every US commercial aircraft. The average cost of ~ 80,000 lives saved over a 20-year period by UV-C air disinfection aboard aircraft is only ~ $10,000.

Every day that we delay the installation of UV-C air disinfection in the US commercial aircraft fleet, ~ 10 people die unnecessarily.

8. Evidence of aerosol transmission on aircraft

Extensive evidence of inflight transmission of 11 different airborne diseases.[41] The two of interest in this document, SARS-CoV-2 and H1N1 (a subtype of Influenza A) are shown in **Tables 21a** and **21b** below.

Table 21a. Summary of contact tracing data for inflight transmission of SARS-CoV-2.

SARS-CoV-2 Study (First Author and year (investigation #) [reference]	# passengers to be traced	# of passengers traced	# index cases	# 2ndry cases	2ndry cases within 2 rows	# of people on board	Evidence Level
Bae, 2020 (1) [103]	287	287	6	1	0	299	High
Bae, 2020 (2) [103]	202	202	3	1	-	205	High
Blomquist, 2021 (1) [105]	425	79	55	5	4	2368	High
Bohmer, 2020 (2) [106]	-	-	1	0	-	-	High
Burke, 2020 (1) [102]	13	13	1	0	-	-	High
Chen 2020 (1) [107]	330	330	11	1	1	342	High
Choi, 2020 (2) [108]	294	0	2	2	-	294	High
Draper, 2020 (1) [109]	389	326	14	0	-	-	High
Eichler, 2021 (1) [101]	148	148	1	2	2	149	High
Eichler, 2021 (2) [101]	-	-	2	1	1	94	High
Eldin, 2020 (2) [115]	-	-	1	0	-	-	High
Khanh, 2020 (1) [111]	216	184	1	15	11	217	High
Murphy, 2020 (1) [3]	60	48	1	13	-	61	High
Speake, 2020 (1) [10]	241	-	11	11	8	241	High
Totals for High Evidence Levels	**2605**	**1617**	**110**	**52**	**27**	**4270**	
Bernard Stoecklin, 2020 (1) [104]	13	-	1	0	-	234	Med
Eldin, 2020 (1) [115]	-	-	1	1	-	-	Med
Hoehl, 2020 (1) [110]	95	95	7	2	2	102	Med
Nye, 2021 (1) [117]	-	-	1	3	3	-	Med
Nye, 2021 (2) [117]	-	-	2	2	2	-	Med
Nye, 2021 (3) [117]	-	-	3	1	1	-	Med
Nye, 2021 (4) [117]	-	-	6	1	0	-	Med
Nye, 2021 (5) [117]	-	-	40	3	-	-	Med
Nye, 2021 (6) [117]	-	-	5	3	3	-	Med
Bohmer, 2020 (1) [106]	-	-	1	0	-	-	Low
Nir-Paz, 2020 (1) [116]	9	9	2	0	-	11	Low
Pavli, 2020 (1) [112]	-	981	21	5	4	2334	Low
Qian, 2020 (1) [113]	-	-	1	10	-	-	Low
Schwartz, 2020 (1) [114]	25	25	1	0	-	350	Low
Swadi, 2020 (1) [1]	84	84	2	4	4	86	Low

Table 21a lists 14 separate flights where inflight transmission of SARS-CoV-2 has been traced with a High Evidence Level, totaling 52 secondary cases, only 27 (52%) of which were within the conventionally assumed 2 rows of infectious range, **suggesting that at least 48% of the cases were transmitted by aerosols.** Note that the term "secondary or 2ndry" case in the Rafferty reference is

defined in the present document to be a "primary" case. i.e., a person who is infected while onboard the flight.

Table 21b. Summary of contact tracing data for inflight transmission of H1N1 and Influenza A

H1N1 & Influenza A Study (First Author and year (investigation #) [reference]	# passengers to be traced	# of passengers traced	# index cases	# 2ndry cases	2ndry cases within 2 rows	# of people on board	Evidence Level
Baker, 2010 (1) [12]	112	102	12	4	4	379	High
Han, 2009 (1) [92]	114	114	1	0	-	115	High
Han, 2009 (2) [92]	110	110	1	1	0	111	High
Han, 2009 (3) [92]	110	110	2	7	1	112	High
Moser, 1979 (1) [96] (Influenza A)	54	53	1	38	-	54	High
Ooi, 2010 (1) [88]	596	23	1	5	2	596	High
Pang, 2011 (2) [93]	1846	1846	1	8	-	1854	High
Pang, 2011, (1) [93]	1283	1283	1	20	-	1303	High
Young, 2014 & Shankar, 2014 (1) [87, 91]	278	232	6	6	1	278	High
Totals for High Evidence Levels	**4503**	**3873**	**26**	**89**	**8**	**4802**	
Foxwell, 2011 (1) [95]	445	145	6	8	8	445	Med
Foxwell, 2011 (2) [95]	293	131	1	1	1	293	Med
Kim, 2010 (1) [89]	337	199	1	1	0	338	Med
Neatherlin, 2013 (1) [90]	225	146	1	8	3	226	Med
Neatherlin, 2013 (2) [90]	167	133	1	4	3	168	Low
Zhang, 2013 (1) [94]	274	168	1	9	-	274	Low

Table 21b lists 9 separate flights where inflight transmission of H1N1 or Influenza A has been traced with a High Evidence Level, totaling 89 secondary cases, only 8 (9%) of which were within the conventionally assumed 2 rows of infectious range, **suggesting that at least 91% of the cases were transmitted by aerosols.**

9. Return on Investment for UV-C in aircraft cabins

ROI for U.S. air carriers' installation cost for the AeroClenz UV-C system. The AeroClenz UV-C system is intended to significantly improve flight safety rather than increase revenue. However, like other safety equipment, it may have a secondary revenue enhancement effect as it improves the public's confidence in flying safety. Passengers' fear of contracting COVID-19 decreased passenger revenue for U.S. air carriers from $145.44 billion in 2019 to $49.89 billion in 2020 and $86.67 billion in 2021. (https://www.statista.com/statistics/197677/passenger-revenues-in-us-airline-industry-since-2004/) The difference between 2019 and the average of 2020 and 2021 passenger revenue is $77.16 billion. The estimated cost to U.S. air carriers for fleet-wide installation of the AeroClenz UV-C system is only ~ $1 per passenger ticket for one year. So if only 1% of passengers had their confidence improved enough to fly it would cover the entire installation cost. If 20% of passengers had their confidence improved enough to fly, then passenger revenue would have increased by $14.66 billion over the

installation cost. The lifespan of an AeroClenz UV-C system installation is estimated to be 20 yrs – and it is likely that a pandemic as disruptive as COVID-19 will occur during this time.

10. References

1. Allen G, Benner K, Bahnfleth W. Inactivation of Pathogens in Air Using Ultraviolet Direct Irradiation Below Exposure Limits. J Res Natl Inst Stand Technol. 2022; 126
2. Barnard IRM, Eadie E, Wood K. Further evidence that far-UVC for disinfection is unlikely to cause erythema or pre-mutagenic DNA lesions in skin. Photodermatol Photoimmunol Photomed. 2020; 36(6):476–7
3. Bartsch SM, Ferguson MC, McKinnell JA, O'Shea KJ, Wedlock PT, Siegmund SS, et al. The Potential Health Care Costs And Resource Use Associated With COVID-19 In The United States. Health Aff (Millwood). 2020; 39(6):927–35
4. Beggs CB, Avital EJ. Upper-room ultraviolet air disinfection might help to reduce COVID-19 transmission in buildings: a feasibility study. PeerJ. 2020; 8:e10196
5. Biggerstaff M, Cauchemez S, Reed C, Gambhir M, Finelli L. Estimates of the reproduction number for seasonal, pandemic, and zoonotic influenza: a systematic review of the literature. BMC Infect Dis. 2014; 14(1):480
6. Buonanno G, Morawska L, Stabile L. Quantitative assessment of the risk of airborne transmission of SARS-CoV-2 infection: Prospective and retrospective applications. Environ Int. 2020; 145:106112
7. Bureau of Transportation Statistics. Preliminary Estimated Full Year 2019 and December 2019 U.S. Airline Traffic Data. 2020 Retrieved 17 April 2023 from https://www.bts.gov/newsroom/preliminary-estimated-full-year-2019-and-december-2019-us-airline-traffic-data
8. Centers for Disease Control and Prevention. Ending Isolation and Precautions for People with COVID-19: Interim Guidance. 2022 Retrieved 17 April 2023 from https://www.cdc.gov/coronavirus/2019-ncov/hcp/duration-isolation.html
9. Centers for Disease Control and Prevention. Estimated COVID-19 Burden. 2022 Retrieved 17 April 2023 from https://www.cdc.gov/coronavirus/2019-ncov/cases-updates/burden.html
10. Centers for Disease Control and Prevention. Estimated Flu-Related Illnesses, Medical visits, Hospitalizations, and Deaths in the United States — 2019–2020 Flu Season. 2023 Retrieved 17 April 2023 from https://www.cdc.gov/flu/about/burden/2019-2020.html
11. Centers for Disease Control and Prevention. Key Facts About Influenza. 2023 Retrieved 17 April 2023 from https://www.cdc.gov/flu/about/keyfacts.htm
12. Centers for Disease Control and Prevention. National, Regional, and State Level Outpatient Illness and Viral Surveillance. Fluview Interact. . 2023 Retrieved 17 April 2023 from https://gis.cdc.gov/grasp/fluview/fluportaldashboard.html
13. Chiu S, Chuang J, Michelson DG. Characterization of UWB Channel Impulse Responses Within the Passenger Cabin of a Boeing 737-200 Aircraft. IEEE Trans Antennas Propag. 2010; 58(3):935–45
14. Civil Aviation Authority Strategy & Policy Department. CAA Passenger Survey Report 2017. Civil Aviation Authority; 2018.
15. de Courville C, Cadarette SM, Wissinger E, Alvarez FP. The economic burden of influenza among adults aged 18 to 64: A systematic literature review. Influenza Other Respir Viruses. 2022; 16(3):376–85
16. Cutler DM, Summers LH. The COVID-19 Pandemic and the $16 Trillion Virus. Jama. 2020; 324(15):1495–6
17. December 2007 31. Boeing 737 Aircraft Profile. Flight Glob. Retrieved 5 May 2023 from https://www.flightglobal.com/boeing-737-aircraft-profile/76702.article
18. van Doremalen N, Bushmaker T, Morris DH, Holbrook MG, Gamble A, Williamson BN, et al.

Aerosol and Surface Stability of SARS-CoV-2 as Compared with SARS-CoV-1. N Engl J Med. 2020; 382(16):1564–7

19. First MW, Nardell EA, Chaisson W, Riley RL. Part I: Basic principles. In: Guidelines for the application of upper-room ultraviolet germicidal irradiation for preventing transmission of airborne contagion. Transactions-American Society of Heating Refrigerating and Air Conditioning Engineers 105; 1999:869–76.

20. Gammaitoni L, Nucci MC. Using a mathematical model to evaluate the efficacy of TB control measures. Emerg Infect Dis. 1997; 3(3):335–42

21. Handler FA. Predicting Inactivation of Bacillus subtilis Spores Exposed to Broadband and Solar Ultraviolet Light. Environ Eng Sci. 2019; 36(6):667–80

22. Internationale Beleuchtungskommission, editor. UV-C photocarcinogenesis risks from germicidal lamps: technical report. Vienna: CIE Central Bureau; 2010.

23. Johansson MA, Quandelacy TM, Kada S, Prasad PV, Steele M, Brooks JT, et al. SARS-CoV-2 Transmission From People Without COVID-19 Symptoms. JAMA Netw Open. 2021; 4(1):e2035057–e2035057

24. Kennedy HE. Chapter 62. Ultraviolet Air and Surface Treatment. In: 2019 ASHRAE Handbook—HVAC Applications. Atlanta: American Society of Heating, Refrigerating and Air-conditioning Engineers. ASHRAE; 2019:62.1-62.17.

25. Kinahan SM, Silcott DB, Silcott BE, Silcott RM, Silcott PJ, Silcott BJ, et al. Aerosol tracer testing in Boeing 767 and 777 aircraft to simulate exposure potential of infectious aerosol such as SARS-CoV-2. PLOS ONE. 2021; 16(12):e0246916

26. Kowalski W. Ultraviolet Germicidal Irradiation Handbook: UVGI for Air and Surface Disinfection. Berlin, Heidelberg: Springer; 2009.

27. Kujundzic E, Matalkah F, Howard CJ, Hernandez M, Miller SL. UV Air Cleaners and Upper-Room Air Ultraviolet Germicidal Irradiation for Controlling Airborne Bacteria and Fungal Spores. J Occup Environ Hyg. 2006; 3(10):536–46

28. Lydia S. U.S. Air Travel Remains Down as Employed Adults Fly Less. 2022 Retrieved 17 April 2023 from https://news.gallup.com/poll/388484/air-travel-remains-down-employed-adults-fly-%20less.aspx

29. Ma B, Linden YS, Gundy PM, Gerba CP, Sobsey MD, Linden KG. Inactivation of Coronaviruses and Phage Phi6 from Irradiation across UVC Wavelengths. Environ Sci Technol Lett. 2021; 8(5):425–30

30. Martin SB, Bahnfleth WP, Dunn C, Freihaut J. The U.S. General Services Administration requires that UVC be included in cooling coil air-handling units for all new facilities and alteration projects to maintain coil cleanliness and improve air quality. ASHRAE J. 2008

31. Mathieu E et al. United States: Coronavirus Pandemic Country Profile. 2023 Retrieved 17 April 2023 from https://ourworldindata.org/coronavirus/country/united-states

32. Miller SL, Hernandez M, Kujundzic E, Howard C. Evaluating Portable Air Cleaner Removal Efficiencies for Bioaerosols.

33. Molinari N-AM, Ortega-Sanchez IR, Messonnier ML, Thompson WW, Wortley PM, Weintraub E, et al. The annual impact of seasonal influenza in the US: Measuring disease burden and costs. Vaccine. 2007; 25(27):5086–96

34. Mphaphlele M, Dharmadhikari AS, Jensen PA, Rudnick SN, van Reenen TH, Pagano MA, et al. Institutional Tuberculosis Transmission. Controlled Trial of Upper Room Ultraviolet Air Disinfection: A Basis for New Dosing Guidelines. Am J Respir Crit Care Med. 2015; 192(4):477–84

35. National Research Council. The Airliner Cabin Environment and the Health of Passengers and Crew. National Academy Press; 2002.

36. Our World in Data. Daily new confirmed COVID-19 cases. COVID-19 Data Explor. . 2023 Retrieved 17 April 2023 from https://ourworldindata.org/covid-cases

37. Parliamentary Office of Science and Technology. Statistical information on air passenger numbers and characteristics. London, UK: 2000.

38. Pawlyk O. It's Almost Impossible to Get COVID-19 on an Airplane, New Military Study Suggests.

Military.com. . 2020 Retrieved 5 May 2023 from https://www.military.com/daily-news/2020/10/15/its-almost-impossible-get-covid-19-airplane-new-military-study-suggests.html

39. Peng Z, Rojas ALP, Kropff E, Bahnfleth W, Buonanno G, Dancer SJ, et al. Practical Indicators for Risk of Airborne Transmission in Shared Indoor Environments and Their Application to COVID-19 Outbreaks. Environ Sci Technol. 2022; 56(2):1125–37

40. Putri WCWS, Muscatello DJ, Stockwell MS, Newall AT. Economic burden of seasonal influenza in the United States. Vaccine. 2018; 36(27):3960–6

41. Rafferty AC, Bofkin K, Hughes W, Souter S, Hosegood I, Hall RN, et al. Does 2x2 airplane passenger contact tracing for infectious respiratory pathogens work? A systematic review of the evidence. PLOS ONE. 2023; 18(2):e0264294

42. Richards F, Kodjamanova P, Chen X, Li N, Atanasov P, Bennetts L, et al. Economic Burden of COVID-19: A Systematic Review. Clin Outcomes Res. 2022; 14:293–307

43. Riley RL, Nardell EA. Clearing the Air: The Theory and Application of Ultraviolet Air Disinfection. Am Rev Respir Dis. 1989; 139(5):1286–94

44. Rothman T. The Cost of Influenza Disease Burden in U.S. Population. Int J Econ Manag Sci. 2017; 6:443

45. Silcott D, Kinahan SM, Santarpia JL, Silcott B. TRANSCOM/AMC Commercial Aircraft Cabin Aerosol Dispersion Tests. Nebraska: National Strategic Research Institute; 2020.

46. Sliney D. Balancing the Risk of Eye Irritation from UV-C with Infection from Bioaerosols. Photochem Photobiol. 2013; 89(4):770–6

47. Sliney DH, Stuck BE. A Need to Revise Human Exposure Limits for Ultraviolet UV-C Radiation†. Photochem Photobiol. 2021; 97(3):485–92

48. Walker CM, Ko G. Effect of Ultraviolet Germicidal Irradiation on Viral Aerosols. Environ Sci Technol. 2007; 41(15):5460–5

49. Whalen JJ. Environmental control for tuberculosis: basic upper-room ultraviolet germicidal irradiation guidelines for healthcare settings. 2020

50. World Bank. Population, Total for United States [POPTOTUSA647NWDB]. World Dev. Indic. . 2023 Retrieved 17 April 2023 from https://fred.stlouisfed.org/series/POPTOTUSA647NWDB

51. Zee M, Davis AC, Clark AD, Wu T, Jones SP, Waite LL, et al. Computational fluid dynamics modeling of cough transport in an aircraft cabin. Sci Rep. 2021; 11(1):23329

52. Principles of Epidemiology | Lesson 3 - Section 3. 2021 Retrieved 8 May 2023 from https://www.cdc.gov/csels/dsepd/ss1978/lesson3/section3.html

53. Air Traffic By The Numbers | Federal Aviation Administration. Retrieved 5 May 2023 from https://www.faa.gov/air_traffic/by_the_numbers

54. ASPM Taxi Times: Standard Report - ASPMHelp. Retrieved 5 May 2023 from https://aspm.faa.gov/aspmhelp/index/ASPM_Taxi_Times__Standard_Report.html

55. Basal & Squamous Cell Skin Cancer Statistics. Retrieved 5 May 2023 from https://www.cancer.org/cancer/types/basal-and-squamous-cell-skin-cancer/about/key-statistics.html

56. COVID-19_Aerosol_Transmission_Estimator. Google Docs. Retrieved 5 May 2023 from https://docs.google.com/spreadsheets/d/16K1OQkLD4BjgBdO8ePj6ytf-RpPMlJ6aXFg3PrIQBbQ/edit?usp=embed_facebook

57. Shrinking Airline Seats From Smaller Pitch and Less Width. Retrieved 5 May 2023 from https://econlife.com/2017/06/tbt-shrinking-airline-seats/

58. Skin cancer. Retrieved 5 May 2023 from https://www.aad.org/media/stats-skin-cancer

59. Skin Cancer Facts & Statistics. Skin Cancer Found. Retrieved 5 May 2023 from https://www.skincancer.org/skin-cancer-information/skin-cancer-facts/

60. TLV/BEI Guidelines. ACGIH. Retrieved 1 May 2023 from https://www.acgih.org/science/tlv-bei-guidelines/

61. United States COVID - Coronavirus Statistics - Worldometer. Retrieved 5 May 2023 from https://www.worldometers.info/coronavirus/country/us/